DISSERTATION

IMPROVEMENT IN DYE SENSITIZED SOLAR CELL EFFICIENCY THROUGH FUNCTIONALIZATION OF REDOX MEDIATORS AND PASSIVATION OF THE PHOTOANODE USING A HOME-BUILT ATOMIC LAYER DEPOSITION SYSTEM

Submitted by

Joshua D. Thomas

Department of Chemistry

In partial fulfillment of the requirements

For the Degree of Doctor of Philosophy

Colorado State University

Fort Collins, Colorado

Fall 2017

Doctoral Committee:

Advisor: Amy L. Prieto

Ellen R. Fisher
Carmen S. Menoni
Walajabad S. Sampath

ABSTRACT

IMPROVEMENT IN DYE SENSITIZED SOLAR CELL EFFICIENCY THROUGH FUNCTIONALIZATION OF REDOX MEDIATORS AND PASSIVATION OF THE PHOTOANODE USING A HOME-BUILT ATOMIC LAYER DEPOSITION SYSTEM

The efficiency of dye sensitized solar cells (DSSCs) is driven based on the contributions of a vast array of kinetic and thermodynamic processes which must all function in sync with one another. The redox mediator factors into a majority of these processes and thus its proper function is vital to adequate function of the DSSC as a whole. The function of the redox mediator can be altered in two ways: changing the identity of the redox couple used and modifying one of the components which the redox couple is interacting with. Herein, both methods have been performed to optimize the properties and processes involved in efficient DSSC function.

Several cobalt bipyridine coordination complex type mediators have been synthesized and differentiated through the modification of the ligand structure. The purpose of the modification was to generate complexes with more positive redox potentials to increase the open circuit voltage of the cells. Subsequently, attempts were made to further modify the ethyl ester substituted ligands which yielded the highest redox potential in order to provide higher stability for the resulting mediator. While the outcome of the synthesis was unsuccessful at this point, promising results have been shown.

Further, an apparatus was constructed in order to cheaply perform atomic layer deposition of aluminum oxide on the surface of the mesoporous titanium dioxide photoanodes for DSSCs. Atomic layer deposition has been shown to reduce the rate of recombination with the oxidized mediator. In this case, improvement in the open circuit voltage of the cell was shown. However, the overall improved performance of the DSSCs shown in the literature could not be replicated. It is hoped that

more high resolution analytical techniques could be used to elucidate the deficiencies still present in the use of this technique.

ACKNOWLEDGEMENTS

I have been fortunate in more ways than anyone has a right to be in order to reach this point in my academic career. I've been able to surround myself with fantastic people, friends, family, colleagues, classmates, partners, teachers, students, and mentors. I've learned to be a scientist and electrochemist from some of the very best at both of those things. I unfortunately did not get to finish my graduate career with one of those mentors who taught me so much of what I know now. But I will always be thankful to C. Michael Elliott for that time that I had learning from him. Who I am today as a scientist and a person is in no small part because of his influence.

After Mike passed away during the summer of my 4th year in graduate school, it happened so suddenly that I didn't know what would happen right away. But almost as soon as it happened, Amy L. Prieto contacted me and volunteered to take me into her group and gave me that new chance. She took it upon herself to learn everything she could about the work that I had been doing so that I could finish this work instead of starting over from scratch. This thesis could not exist with her support.

And what remained constant from when I was born until now has always been the love and support of my parents. No matter what I have wanted to do in life, they were immediately interested in it too whether it was track and field, chemistry, or saving the environment. They didn't always know what I was talking about but listening to me to about it anyway with a smile on their faces probably made it better.

TABLE OF CONTENTS

CHAPTER 1: AN INTRODUCTION TO DYE SENSITIZED SOLAR CELLS

1.1 Justification for dye sensitized solar cells

In order to be successful in the current political and economic climate, it is unlikely that any individual photovoltaic technology will answer the demands for every possible application. For companies interested in commercializing different photovoltaic technologies, as they become more efficient and commercially viable, it will become important to find a niche in which they fit the best. Dye sensitized solar cells (DSSCs) are unlikely to surpass conventional silicon technologies in terms of efficiency as a photovoltaic or be used in enormous solar fields for large scale energy collection due to concerns about their long term stability, lower light absorption, or liquid based electrolyte which must be properly contained. However, DSSCs have both current and potential advantages that should allow this technology to fit into an entirely different niche of necessary photovoltaic technology. Due to their low materials and processing costs, dye sensitized solar cells may find their ideal application in consumer goods. It has also been shown in the literature that the efficiency of DSSCs is higher when illuminated by lower intensity light which may suggest utilization in indoor applications.[1] Finally, since DSSCs can be prepared with reasonably low annealing temperatures and a thin mesoporous photoanode it has been shown that flexible substrates can be utilized for particular applications where flexibility and freedom of movement is a prerequisite.[2, 3]

DSSCs were not heavily studied until the previously described work by Grätzel and O'Regan where a mesoporous network of TiO_2 nanoparticles was used to vastly increase the surface area of the photoanode surface.[4] Their DSSC utilizing that mesoporous network achieved an efficiency of 10.1 % using a modified ruthenium tris-bipyridine complex known as N3 (shown in figure 1.1), a redox mediator composed of the couple iodide/tri-iodide (I^-/I_3^-), and a platinized glass cathode. Work was performed on DSSCs prior to this discovery, however the amount of dye which could be adsorbed on the surface of a

flat semi-conductor film was not enough to absorb a sufficient amount of visible light and aggregated dye that was not directly bound to the semi-conductor surface could not inject electrons in the same way adsorbed dye could.[5]

Typically a DSSC can be broken down into 3 primary components: a photoanode, a cathode, and an electrolyte which shuttles charge between the two. The basic composition can be seen in figure 1.1 using example components from Grätzel and O'Regan's seminal paper from which nearly all modern DSSC research stems.[4] The photoanode consists of a mesoporous film made of an n-type high band gap semi-conductor, most commonly titanium dioxide (TiO_2), which is deposited on a transparent conducting oxide coated glass substrate and sensitized with one or multiple dyes which allow the anode to absorb a high percentage of the light in the visible spectrum. In figure 1.1, the dye shown is a ruthenium tris-bipyridyl complex commonly known as 'N3'. The cathode historically has consisted of tiny islands of platinum deposited onto a conductive glass substrate such as fluorine doped tin oxide coated glass, though other materials have been and continue to be studied. The electrolyte is commonly solvated by acetonitrile, though other solvents are being increasingly considered. It contains a redox mediator which shuttles charge between the sensitizer and the cathode, a salt acting as a supporting electrolyte, and typically some additives such as the ubiquitous 4-*tert*butylpyridine which will

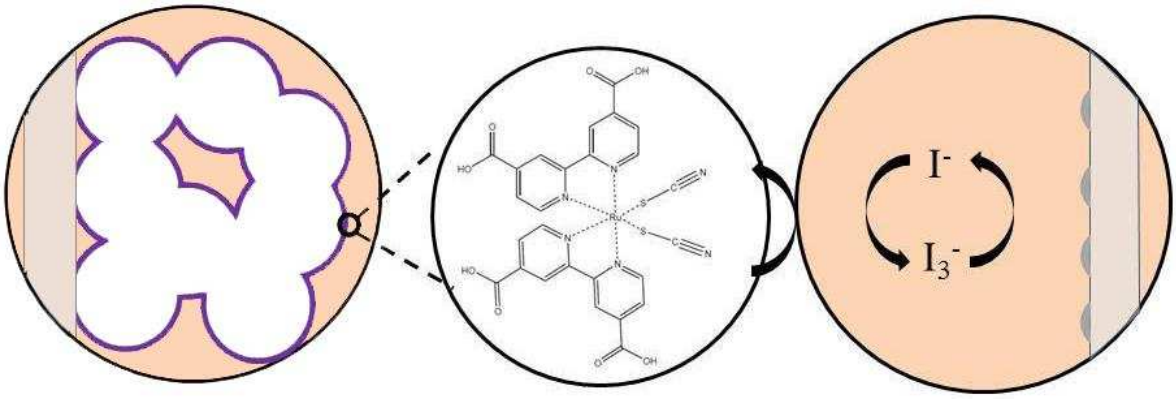

Figure 1.1: Schematic is representative of the DSSC developed by Gratzel and O'Regan in 1991 using a mesoporous TiO_2 film sensitized with the ruthenium sensitizer, N3, the iodide/tri-iodide redox couple, and a platinized film counter electrode.

be discussed in great detail further on. Iodide/tri-iodide (I^-/I_3^-) is the well characterized literature example for the redox couple, while it has been shown by this group that lithium salts typically function as the best supporting electrolytes.[6] Research over the previous 25 years has only yielded modest improvements in DSSC efficiency relative to the original work published by Grätzel and O'Regan in Nature in 1991.[4] This could partially be attributed to the impressive efficiency achieved in that work, however another reason is the complexity involved in balancing the multitude and variety of processes occurring simultaneously in a functioning DSSC.

1.2 Function of a dye sensitized solar cell

Since then, a vast amount of work has been performed to develop alternative components to those used by O'Regan and Grätzel in an attempt to improve both the efficiency and the cost of these devices. Ultimately, improvement upon those initial studies through rational design requires a fundamental understanding of the underlying kinetic and thermodynamic processes occurring during function of a DSSC. Figure 1.2 and table 1.1 summarize the processes competing during the course of normal DSSC function. In figure 1.2, those processes in a functional DSSC that are kinetically favorable appear in green while processes that are ideally kinetically unfavorable appear in red. Though all of these processes occur simultaneously in a functioning cell, it can be helpful to consider the path of a single electron.

Following excitation of an electron from the ground state of the sensitizer by visible light (represented by 'a') the electron is quickly injected into the conduction band of the semi-conductor as shown by process 'b'. The electron migrates through the semi-conductor and then is transferred to the transparent conducting oxide (TCO) serving as a back contact which is shown in figure 1.2 as process 'c'. After travelling through the circuit to the cathode, the electron reduces the oxidized form of the redox mediator (process 'd') and the mediator begins its migration through the electrolyte back to the photoanode.[7] The reduced form of the mediator has a redox potential which is more negative than the

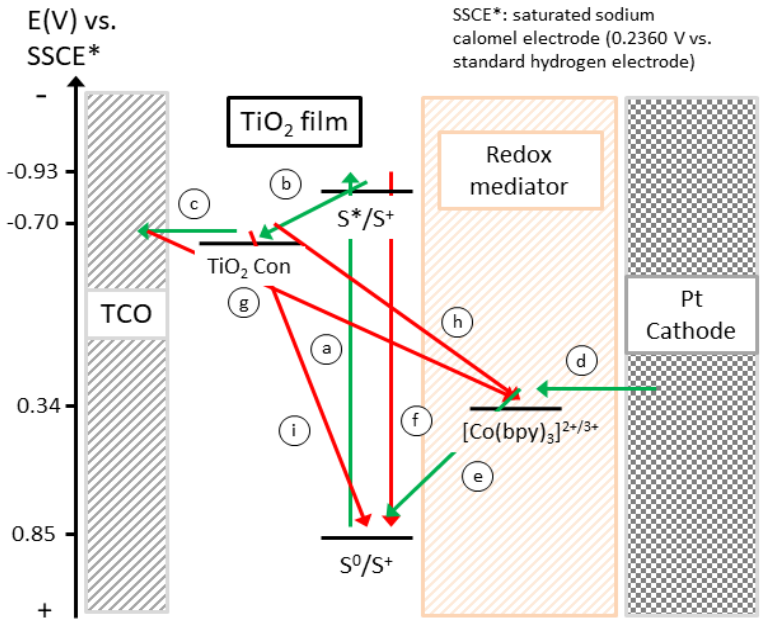

Figure 1.2: Energy diagram representing processes which occur in a normally functioning DSSC using TiO_2 sensitized with the N3 dye and deposited on a fluorine doped tin oxide substrate, cobalt (II/III) tris-2,2'-bipyridine as the redox mediator, and a platinized counter electrode. Processes where the electron is flowing forward are represented in green while recombination type processes are shown in red. Processes are labelled with letters from 'a'-'i' which are further described in the text and in table 1.1.

ground state of the dye so it is thermodynamically favorable to reduce the previously oxidized form of the dye expressed as process 'e', returning the electron to its original position.[8] Depending on the specific components of the cell and their interactions, there can be also be a variety of undesirable side processes which work to trap the electron and decrease the efficiency of the cell.

Certain processes such as relaxation of the excited electron in the sensitizer back into the ground state (process 'f') are commonly slower than competing processes such as charge injection to the conduction band of the semi-conductor. Thus, it is not commonly considered past the initial choice of sensitizer. Another process which no longer degrades efficiency to a great extent is process 'g' which can be described as recombination of the electron in the TCO with the oxidized mediator.[9] Modern DSSCs typically apply a thin blocking layer composed of the same semi-conductor (TiO_2) which passivates the TCO surface to the mediator. Other recombination processes which have a stronger ability to erode the cell's efficiency are the transfer of the electron from the semi-conductor back to the oxidized

Table 1.1: Description of the processes displayed in figure 2 along with estimated time scales the processes occur during. The example cell here utilizes a TiO_2 photoanode, N3 dye, $Co(bpy)^{2+/3+}$ mediator, and gold cathode. Values were reported in the literature and are referenced within. Due to exceptionally high charge transfer resistance (50,000 $\Omega \cdot cm^2$) there is no appreciable charge transfer between $Co(bpy)^{2+/3+}$ and the TCO.

Process	Description	Time scale (s)	Ref
a.	Dye excitation	N/A	N/A
b.	Charge injection	10^{-11}	[1]
c.	Charge migration to TCO	10^{-3}	[1]
d.	Mediator regeneration	10^{-4}	[24]
e.	Dye regeneration	10^{-5}	[8]
f.	Dye relaxation	10^{-8}	[1]
g.	Mediator recombination from TCO	N/A	[9]
h.	Mediator recombination from TiO_2	10^{-2}	[8]
i.	Dye recombination from TiO_2	10^{-4}	[1]

mediator or to the oxidized ground state of the dye (processes 'h' and 'I' respectively). Both of these processes can be controlled, directly or indirectly, by the identity of the redox mediator used. There are also other factors not directly related to electron transfer which can help or hinder the function of the DSSC and will be discussed later.

From a mathematical standpoint, the efficiency of any photovoltaic cell can be calculated from the open circuit voltage (V_{oc}), short circuit current (I_{sc}), fill factor (FF), and power of the incident light (P_{in}) as shown in equation 1.1 where efficiency is represented by the Greek symbol 'η'. For a DSSC, the V_{oc} is determined by the difference in potential between the quasi-fermi level of the photoanode and the potential of the redox mediator. The I_{sc} can be limited by non-ideal behavior of any of the processes

$$\eta = \frac{I_{sc}V_{oc}FF}{P_{in}}$$

Equation 1.1: Power conversion efficiency equation

$$FF = \frac{V_{mp}I_{mp}}{V_{oc}I_{sc}}$$

Equation 1.2: Determination of the fill factor

shown in figure 1.2 and described above as well as incomplete absorption of light, an insufficient quantity of adsorbed dye, and slow redox mediator diffusion. The fill factor (FF) can be calculated from equation 1.2 and is a representation of the ratio between the product of the voltage (V_{mp}) and current (I_{mp}) at the maximum power point versus the product of the V_{oc} and I_{sc}. Another way to explain it would be as an ideality factor comparing the ideal power based on the open circuit voltage and short circuit current and the maximum power actually attained. The fill factor is generally not targeted when trying to improve efficiency because it tends to be difficult to predictably alter. It is more common for studies to target improvements based on either the short circuit current or the open circuit voltage with the understanding that the fill factor is likely to be effected by any change in components as well. Of the components in a DSSC, all are vital to its proper function however the electrolyte and specifically the redox mediator are involved in a majority of the processes determining efficiency. So focus on the rational and controlled modification of the redox mediator is likely to result in a better understanding of how to improve the overall efficiency of the DSSC cell.

Herein, synthetic modification of the redox mediator has been used in an attempt to achieve multiple goals. Further optimization of the redox potential of the mediator has been performed by the synthesis of multiple cobalt bipyridine based complexes with increasing positive redox potentials. Efforts were also made to improve the stability of these complexes through synthetic modification of the ligand system and increased use of the chelating effect. Other work that was performed here explicitly focuses on both understanding and optimizing the interactions between the redox mediator and the semi-conductor serving as a photoanode. Cobalt coordination complexes have been shown to have many advantages as a redox mediator but fast electron recombination from the photoanode is a glaring weakness in DSSCS. Atomic layer deposition of non-conducting oxides onto the photoanode has previously been shown to serve as an effective means for curbing recombination but is also excessively

expensive. A system has been designed here which shows promise as a means to perform the same tasks at significantly lower costs.

1.3 Influence of the redox mediator on DSSCs

It has been suggested that future improvements of dye sensitized solar cells will come from targeted improvement of the V_{oc} of the DSSC as opposed to the I_{sc}.[10] This is anticipated because the most commonly used mediator system (I^-/I_3^-) has a redox potential which is around 700 mV more negative of the ground state of many commonly used sensitizers.[11] While a certain amount of overpotential is necessary to drive the efficient regeneration of the dye by the redox mediator; that potential difference is suggested to have a wide range (between 150 mV and 400 mV) depending on the identity of the dye and redox mediator.[12] This suggests that research into alternative mediator systems whose redox potential is significantly more positive then the I^-/I_3^- redox couple may lead to an increased V_{oc} for the cell. Prior research has shown, as would be expected, that several processes will be affected by any change to a component like the redox mediator, which could reduce the V_{oc} or the efficiency in other ways.[12-14] Despite the complexity of having so many coupled processes, recent literature has demonstrated that it is possible to yield modern high efficiency DSSCs that utilize cobalt coordination complexes as alternative redox mediators to I^-/I_3^- in order to improve the V_{oc} of the cells.

The use of cobalt coordination complexes as a mediator system for DSSCs was first reported by Nusbaumer and co-workers with the complex cobalt(II/III)-bis[2,6-bis(1'butylbenzimidazol-2'-yl)pyridine] abbreviated as $Co(dbbip)^{2+/3+}$.[15] Cobalt (II/III) tris-2,2'-bipyridine or $Co(bpy)^{2+/3+}$ has since become the mediator of choice not just relative to other cobalt coordination complexes but in some of the highest efficiency DSSCs of any liquid electrolyte based cell.[16, 17] Both of these complexes exhibit reduction potentials which are positive of the I^-/I_3^- system. This ideally should lead to higher open circuit voltages. That is not always observed to be the case due to the other intricacies involved in full function of DSSCs. For instance, higher rates of recombination are suggested to drive the potential of the quasi-fermi level

in the TiO_2 more positive leading to a lower observed V_{oc}. Several methods have been developed in order to reduce the higher rate of recombination while still allowing for the more positive potential and will be discussed extensively further on. Several other advantages, besides the redox potential, encourage the use of these complexes over iodide/tri-iodide such as low absorption of visible light, non-corrosive behavior towards other cell components, and it is estimated that the required overpotential in order to efficiently regenerate the oxidized ground state of the dye is lower than that of the traditional I^-/I_3^- redox mediator.[18]

Unfortunately, there are also other disadvantages to using $Co(bpy)^{2+/3+}$ that have made it more challenging to reach efficiencies which can exceed that of DSSCs using the I^-/I_3^- system. Its identity as a coordination complex means that $Co(bpy)^{2+/3+}$ has a much larger radius compared to the iodide system no matter what other adjustments can be made. This leads to slower diffusion, which has previously been shown to limit the steady state current exhibited by the cell due to decreased mass transport.[14] This is especially true within the pores of the mesoporous film, which further slow the diffusion of the oxidized complex in and the reduced complex out. In order to somewhat alleviate the mass transport issues, thinner films are used and the pore sizes can be calibrated with post-deposition treatment using titanium (IV) chloride.[19] It has also been shown that the recombination kinetics for the $Co(bpy)^{2+/3+}$ system lead to higher rates of charge transfer back to the oxidized mediator which is then exacerbated by the slow diffusion through the porous layer.[12] Finally, while $Co(bpy)^{2+/3+}$ has been shown to not be corrosive to other components in the DSSC, its own long term stability has been called into question.[20] In order to improve the long-term stability of these mediators, the composition of the electrolyte must be optimized. Alternatively, synthetic modification of the ligand system could exhibit a variety of effects on the complex, including improved stability which will be discussed later.

One of the greatest advantages of coordination complexes instead of the molecular I^-/I_3^- system as the redox mediator is that fine-tuning of the redox potential is possible through synthetic alteration

of the ligands attached to the metal center.[20, 21] This was first shown by Sapp and co-workers who synthesized a series of cobalt complexes with functionalized bipyridine ligands utilizing both electron donating and withdrawing functional groups at multiple positions along the pyridine rings of $Co(bpy)^{2+/3+}$.[13] Not only was it shown that the potential was somewhat controllable through the use of that functionalization, but it was also shown that recombination with the photoanode could be reduced by the use of bulky electron donating groups on the 4,4' positions of the bipyridine. Those electron donating groups ultimately drove the reduction potential of the complex more negative instead of more positive but cobalt(II/III) tris(4,4'-di-tert-butyl-2,2'-bipyridine) or $Co(dtb)^{2+/3+}$ was still studied periodically as a mediator system due to the improvement in the obtained current of the cell due to reduced recombination rates.[8, 22] However, there is still incentive to look towards driving the redox potential of the mediator more positive in order to improve the open circuit voltage as a means to improve the efficiency of the cell. It has been shown that using the same 4,4' positions but utilizing electron withdrawing substituents leads to a shift in the redox potential which is more positive.[13, 23] The lack of stability of these complexes tends to be exacerbated relative other cobalt coordination complexes. It is expected that the electron withdrawing substitutions make the bipyridine ligands more labile and prone to substitution with other constituents in the solution. In the case of DSSCs, the most likely competing ligands are going to be the solvent acetonitrile, and the common additive *tert*-butylpyridine. Previous studies into varying both position and identity of the synthetic modifications made to the bipyridine ligands of Cobalt (II/III) tris-2,2'-bipyridine based coordination complexes have shown that they can be used to separately tune the redox potential of the couple.[13, 23] But until this study it has been unclear what their combined effect might be. Specifically, this dissertation poses the question "Can the positive shift in potential provided by electron-withdrawing groups substituted in the 4,4' positions be magnified by attaching those functional groups at the 5,5' positions instead?" Herein I show the synthesis and characterization of five cobalt coordination complexes with unsubstituted,

dimethyl substituted, and di-ethyl ester substituted bipyridines with substitutions placed at either the 4,4' or 5,5' positions for each bipyridine.[24] The synthesized complexes are shown in figure 1.3. The selection of these complexes allows for evaluation of the presence of both electron-withdrawing moieties and electron-donating moieties at each pair of positions. It was found that the addition of electron-withdrawing groups led to a positive shift in the redox potential of the complex while the opposite was shown given the presence of electron-donating substitutions. Interestingly, it was also shown that there was a positive shift in potential for both complexes using substitutions at the 5,5' positions relative to 4,4' substitutions. Other properties such as molar absorptivity coefficient, charge transfer resistance on potential cathode materials, diffusion coefficient, and stability of the complexes in DSSC-like conditions were also evaluated. It was found that as expected, stability of the complexes was reduced in complexes using electron-withdrawing substituents and there is no evidence to suggest a

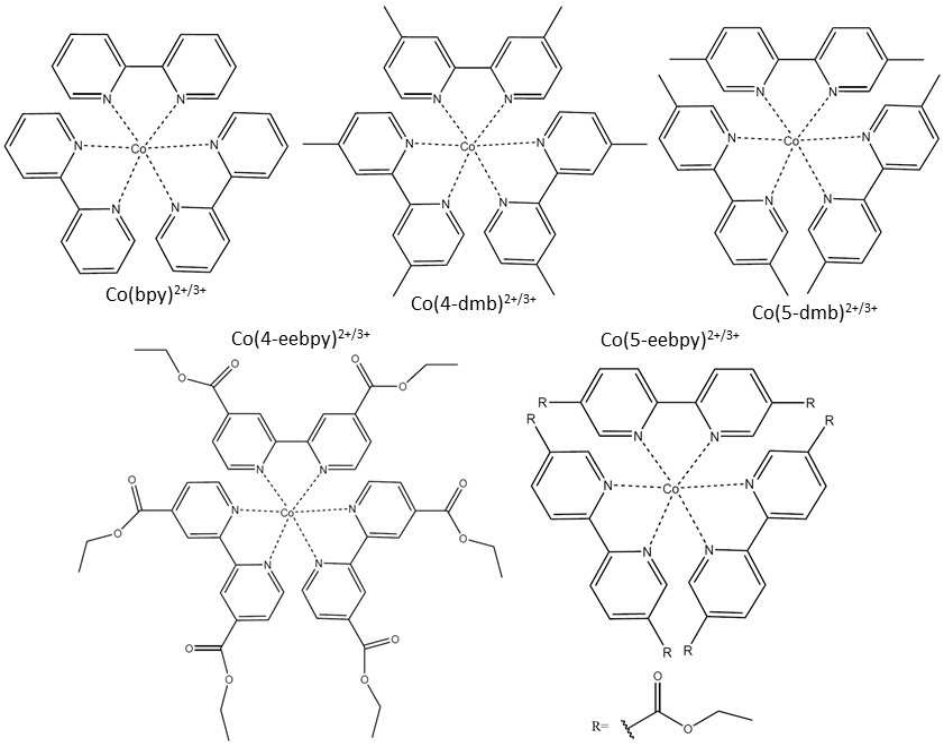

Figure 1.3: Complexes synthesized and characterized to examine effect of substitution identity and substitution position for cobalt based (II/III) redox mediator complexes.

significant improvement or further decline in the stability based on the position of the substituent. As stability concerns would leave our most positively shifted complex unusable in actual DSSCs, further synthetic functionalization would be necessary to improve the stability of the complex.

1.4 Addressing flaws in current redox mediators

Stability for these cobalt based coordination complexes has been questioned for some time now though it has not been considered a significant problem until recently because the efficiencies of cells utilizing them as redox mediators were not high enough to warrant concerns about long term stability. DSSCs with these alternative redox couples have begun to reach efficiencies exceeding 13 %, renewing interest in synthetically tuning these complexes not just for their redox potentials but also in order to improve stability. Generally, the most commonly suggested mechanism for decomposition is that ligand replacement is possible over long times depending on the other components in the DSSC. In the case of the ruthenium based sensitizers, such as N3, thiocyanate is one of the constituent ligands and is known to be labile enough on ruthenium to be able to influence the stability of cobalt based mediators.[1] *Tert*-butylpyridine is a common additive to DSSCs which has been shown to help improve the open circuit voltage of the cell by adsorbing somewhat to the mesoporous TiO_2 surface. However, it can also compete with the ligands already attached to the cobalt, especially in the case of bipyridines with more electron withdrawing substituents. Even the solvent, especially due to its high effective concentration can compete with the ligands for coordination sites. Acetonitrile is sufficiently coordinating to cause trouble over longer periods of time.

It has been suggested by multiple groups that stability of these coordination complexes can be improved through the use of the chelating effect while using ligands with increased denticity.[23] There have already been some examples in the literature. These include using a pair of tri-dentate ligands such as cobalt (II/III) bis-terpyridine and a cobalt complex with a pyrrole substituted onto the bipyridines at the 6 position in order to encourage formation of the bis-species.[21, 25] There have also recently been

multiple examples of hexadentate ligands being used to make cobalt based redox mediators for DSSCs but the ligands were made to be electron donating in nature.[26, 27] Using ligands which are likely to be more electron donating in nature relative to the unsubstituted $Co(bpy)^{2+/3+}$ system, the ligands will coordinate more strongly to the metal center in the first place. In order to utilize the more positively shifted potential of $Co(5\text{-eebpy})^{2+/3+}$, a synthesis was attempted employing 1,3,5-benzenetrimethanol as a linker to generate a hexadentate, hemi-cage ligand for the Co(II/III) redox mediator. The ligand as proposed is shown in figure 1.4. Unfortunately, attempts to form the ligand faced complications in the final synthetic step. There is evidence by mass spectrometry that the ligand was created in very low yield such that it could not be isolated from partially reacted side products. Improvements to the synthetic method have been proposed and we are optimistic that the complex can be completed. A similar complex was prepared by Freitag and co-workers which showed only small differences in diffusion coefficient but greatly improved stability over 120 hours of light exposure.[26]

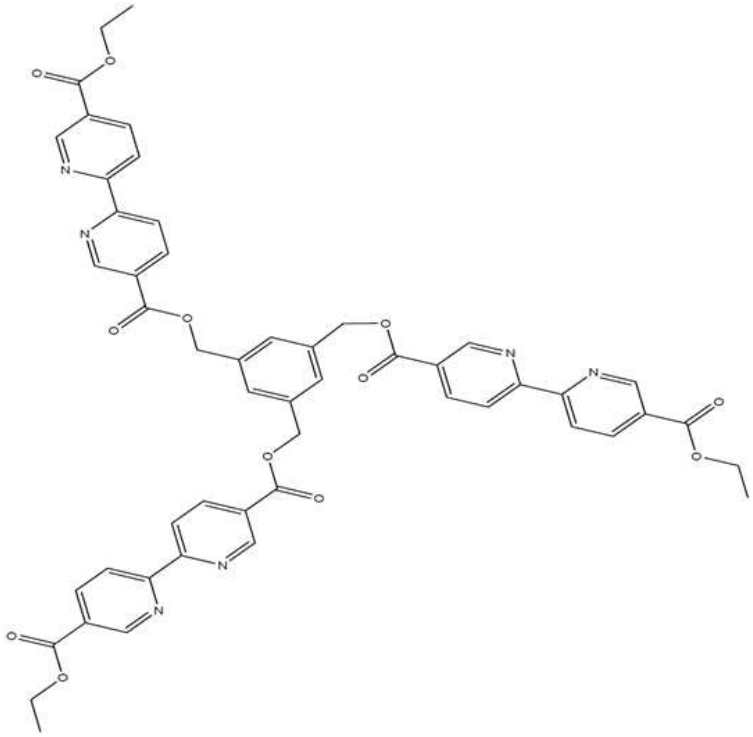

Figure 1.4: Hexadentate ligand used to generate stable cobalt (II/III) mediator with high positive redox potential. Ethyl ester substituted bipyridine moieties are joined by a 1,3,5-benzenetrimethanol linker.

1.5 Reduction in recombination rates through modification of the photoanode surface

As has been previously mentioned, dye sensitized solar cell function is predicated on a complex balance of processes, both negative and positive, which must be optimized in order to maximize efficiency. One key negative process that is still a concern for higher efficiency DSSCs is recombination of the injected electron with the redox mediator coming from the TiO_2 conduction band during the process of electron migration (which corresponds to process 'h'). For the historically used iodide/tri-iodide mediator system, recombination of the electron with the oxidized form of the mediator involves a complex multi-step mechanism which is still not entirely understood and makes the recombination rate very slow relative to its ability to diffuse across the electrolyte.[28] This severely limits recombination and was a key factor in the early success shown by Grätzel.[4, 29] The $Co(bpy)^{2+/3+}$ system was chosen as a newer potential mediator due to the suggestion that high reorganization energy stemming from the transition between cobalt (II) and cobalt (III) would limit recombination rates in a similar way.[30, 31] However despite that advantage, recombination rates are typically much higher using the coordination complex mediator instead of the I^-/I_3^- system.[32]

There have been two methods which are commonly embraced in an effort to minimize the recombination rate exhibited by the $Co(bpy)^{2+/3+}$ system. The synthetic modification of the bipyridine ligand system and the addition of other small molecules which adsorb to the anode surface have both been utilized in a number of studies to reduce charge transfer between the mediator and anode surface. Reducing the recombination rate was one of the motivations for the work performed by Sapp and co-workers to substitute bulky alkyl groups onto the 4,4' positions of the bipyridine ligands of $Co(bpy)^{2+/3+}$.[13] It was shown that the addition of those bulky groups limited the recombination rate by sterically separating the mediator and the TiO_2. The opposite approach has been taken by the use of bulky organic dyes which block off more of the TiO_2 surface then ruthenium based sensitizers as well as

through the use of additives like chenodeoxycholic acid which can agglomerate on the TiO_2 surface, accomplishing the same goal.[8, 33]

Another method that has been suggested as a means to lower the rate of recombination is the deposition of an ultra-thin layer of a non-conductive oxide such as aluminum oxide (Al_2O_3) onto the surface of the mesoporous photoanode. In order to deposit a sufficiently thin layer, several deposition methods have been utilized. Sol-gel type procedures led to some improvement of the open circuit voltage but the layer was considered too imprecise to integrate with the complex mesoporous film sufficiently.[34] Atomic layer deposition (ALD) on the other hand is extremely precise. As opposed to chemical vapor deposition, ALD uses alternating pulses of pre-cursor gases in order to provide monolayer level precision to the deposition process. In the case of the deposition of aluminum oxide, trimethylaluminum is typically used in combination with water vapor. The reaction is self-limiting in the sense that each pre-cursor type can only react with sites on the mesoporous film which have been terminated with the other pre-cursor, not with itself. It has been shown that the rate of the reaction is maximized at relatively low temperatures (~126 °C) which could be important to the use of flexible (plastic) substrates for making DSSCs for particular commercial applications.[35]

Hamman and co-workers observed improvement of the efficiency of DSSCs using a ferrocene based mediator system through the addition of one cycle of Al_2O_3 deposited by ALD; while Liberatore and co-workers observed similar improvements using $Co(dtb)^{2+/3+}$ as the redox mediator.[31, 34] Interestingly, with an individual monolayer (one cycle of both pre-cursor pulses) improvement in both the open circuit voltage and the short circuit current was observed. As continued cycles of ALD deposited more Al_2O_3, the efficiency began to decline relative to the samples with only single cycle of the pre-cursors. The hypothesis is that a single cycle allows for reaction mainly at surface trap sites on the TiO_2 surface which are suggested to accelerate the rate of recombination between TiO_2 and the oxidized mediator.[36] By filling those trap sites, the short circuit current will increase due to reduced

recombination while the quasi-fermi level in the TiO_2 increases allowing for an increase in the open circuit voltage. Due to the low deposition temperature used for ALD of Al_2O_3, there has been at least one study attempting to deposit the layer onto dyed films.[37] The purpose of the film in that study was to inhibit desorption of dye from the film surface but it may also allow for multiple cycles to minimize recombination without limiting charge injection.

Atomic layer deposition (ALD) offers an incredible amount of precision, predicated on alternating pulses of self-limiting pre-cursors. The cost of the apparatus performing the deposition typically exceeds $100,000 which clashes with the core idea of DSSCs as an affordable alternative to other photovoltaic technologies.[38] Instead, since only a single monolayer of Al_2O_3 need be deposited, it is possible an ALD apparatus could be built which could perform the desired experiments at a cost much less than that of the purchased system. Previously, Elam and co-workers assembled an ALD reactor for the deposition of Al_2O_3.[39] An alternative home-built system has been constructed here based in some ways off of the design of that system and it has been shown that it is capable of depositing Al_2O_3 onto our mesoporous TiO_2 films. The deposited films were characterized by x-ray diffraction, x-ray photoelectron spectroscopy, and through testing of assembled DSSCs. However, given the available analytical techniques, we were unable to determine if an individual monolayer could be precisely deposited. It has been shown that after performing just 1 cycle on the apparatus, aluminum oxide could be detected using angle resolved x-ray photoelectron spectroscopy (XPS). But it was unclear based on these results if the deposition provided the necessary precision for DSSC improvement. It was then hypothesized that the presence of the monolayer could be indirectly observed by matching the results observed in the literature.[22] The improvement in observed open circuit voltage was evident and consistent, but not as significant an improvement as was observed in the literature. Sample to sample consistency could be one potential cause for the lack of reproducibility relative to the literature. If this

work was to be resumed, the high-resolution transmission electron microscope may allow for a more quantitative evaluation of the deposited material and better trouble-shooting of the home-built system.

1.6 Alternative redox mediators and the future of DSSCs

Recently, research has expanded to study other options for redox mediator systems which may take advantage of some of the benefits inherent in both the commonly studied molecular I^-/I_3^- system and $Co(bpy)^{2+/3+}$ systems. Organic molecular systems such as 2,2,6,6-Tetramethyl-1-piperidinyloxy radical ($TEMPO^{0/+}$) have begun to see utilization as potential redox mediators.[1, 40, 41] Table 1.2 shows a comparison of some relevant factors of several well-studied mediator systems with the more recent $TEMPO^{0/+}$ system. The examples chosen for table 1.2 were all among the highest efficiency examples for the given mediator system.[17, 33, 42-44] $TEMPO^{0/+}$ exhibits a redox potential which is more positive then both the I^-/I_3^- system and $Co(bpy)^{2+/3+}$ systems while being much smaller than the coordination complex

Table 1.2: Commonly used mediators in the literature and relevant properties to dye sensitized solar cells. Diffusion coefficients are reported in the literature at low concentrations. There may be some variability in solution viscosity however. Redox potentials were re-calculated from literature vs. saturated sodium calomel reference electrodes. Synthetic tunability of the mediators is valuable for future optimization of the properties of the cell.

Mediator species	Diffusion coefficient at low concentrations (cm^2/s)	Potential (V vs. SCCE)	Synthetic tunability (Is it possible? Are there examples?)	Top efficiency	Ref
Iodide/tri-iodide (I^-/I_3^-)	1-2 x 10^{-5}	0.15	Not tunable	12.0 %	[40]
Ferrocene/ ferrocenium (Fc/Fc+)	2.6 x 10^{-5}	0.38	Somewhat tunable, hasn't been used in DSSC applications	7.5 %	[31]
$Co(bpy)^{2+/3+}$	2-4 x 10^{-6}	0.34	Tunability has been shown frequently in DSSC applications	13.0 %	[17]
$TEMPO^{0/+}$	1.1 x 10^{-5}	0.56	Tunability has been shown in DSSC applications	5.4 %	[41]
$Co(phen)^{2+/3+}$	7 x 10^{-7}	0.38	Tunability has been shown in DSSC applications	14.3 %	[42]

based systems like $Co(bpy)^{2+/3+}$. This means that diffusion coefficients and thus limitations based on mass transport are likely to be diminished using the $TEMPO^{0/+}$ system. It was also shown that with some organic dyes like LEG-1 (a relatively new triphenylamine based dye) a relatively low driving force of 0.2 eV is required in order to achieve greater than 80 % regeneration efficiency.[41, 45] For cobalt complexes, desired potentials for efficient regeneration of similar dyes is close to double at 0.4 eV which theoretically limits the V_{oc}.[18] However, like the coordination complex based systems, it has been shown that these organic molecular systems can still allow for tuning of the properties of the mediator using synthetic functionalization.[46] The common active feature of these systems is the nitroxide moiety around which other structural functionalization can be added. The oxidized and reduced forms of this nitroxide radical are shown in figure 1.5. Like with any of the other potential mediator systems, there are significant downsides to these new organic mediator systems which must be addressed.

Due to the reactivity of the nitroxide radical and its small size, recombination processes seem to occur at a higher rate than other mediator systems; the smaller size of the system means that some of the strategies designed to minimize rates of recombination for $Co(bpy)^{2+/3+}$ don't function as effectively. The use of bulky sterically hindering sensitizers on the surface of the TiO_2 have been shown to be not as effective at preventing recombination with $TEMPO^{0/+}$ as has been shown for $Co(bpy)^{2+/3+}$.[41] Atomic layer

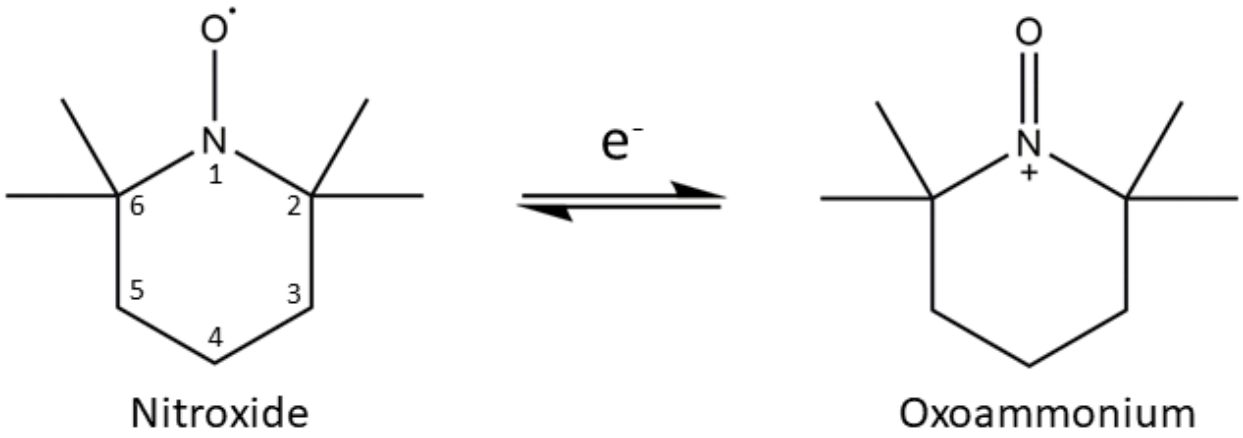

Figure 1.5: Both oxidized and reduced forms of the $TEMPO^{0/+}$ mediator. The positions on the nitroxide are labelled in order to more easily consider possible synthetic substitutions.

deposition of an ultra-thin layer of a non-conducting oxide such as Al_2O_3 however, may prove to be an effective means for reducing the recombination rate because it does not rely on steric interactions to block the oxidized form of the mediator from the surface of the photoanode. Covering up or removing some of the surface trap sites from the TiO_2 surface which are suspected to promote recombination is an alternative method for reducing the rate of recombination.

Stability of the mediator is also seen as a weakness in earlier studies due to the presence of the nitroxide radical.[40] It has been suggested specifically that the oxidized form of the mediator is less stable in solution. Synthetic modification of the mediator may allow for long term stability of the oxidized species and a decrease in the recombination rate based on the substitutions used. The redox potential of the couple being more positive than other options for mediator systems allows for any substitutions either electron donating or withdrawing in nature in order to stabilize the radical.

Due to the complex nature of dye sensitized solar cells as a technology, research is typically compartmentalized such that each component is individually optimized in the presence of standardized components from the literature such as the iodide/tri-iodide mediator system. This is one of the reasons why there is relatively little research for optimization of the interactions between the $Co(bpy)^{2+/3+}$ mediator system and its constituents parts such as alternative cathode materials. Professor C. Michael Elliott has suggested that this approach will not be enough for DSSCs to reach their full potential.[47] He suggested an alternative paradigm where careful consideration of the pairings of sensitizers and mediators could lead to quicker optimization of the overall system. Given the ability to make small changes to coordination complexes and organic molecular mediator systems synthetically allows for extensive libraries of redox mediators to match with the large assortment of dyes. Ultimately, for the grouping of dye and mediator, the desire is to have a small difference in potential between the ground state of the dye and the redox potential of the mediator while maintaining a high rate for electron transfer from mediator to dye. Large libraries of even just currently reported dyes and

mediators could be tested instead of relying on optimizing the components individually and may lead to a jump in efficiency which brings DSSCs up to levels nearing more conventional technologies.

REFERENCES FOR CHAPTER 1

1. Hagfeldt, A.; Boschloo, G.; Sun, L.; Kloo, L.; Pettersson, H., Dye-Sensitized Solar Cells. *Chemical Reviews* **2010,** *110* (11), 6595-6663.

2. Weerasinghe, H. C.; Huang, F.; Cheng, Y.-B., Fabrication of flexible dye sensitized solar cells on plastic substrates. *Nano Energy* **2013,** *2* (2), 174-189.

3. Baker, J.; McGettrick, J. D.; Gethin, D. T.; Watson, T. M., Impedance Characteristics of Transparent GNP-Pt Ink Catalysts for Flexible Dye Sensitized Solar Cells. *Journal of The Electrochemical Society* **2015,** *162* (8), H564-H569.

4. O'Regan, B.; Gratzel, M., A low-cost, high-efficiency solar cell based on dye-sensitized colloidal TiO2 films. *Nature* **1991,** *353* (6346), 737-740.

5. Shimura, M.; Shakushiro, K.; Shimura, Y., Photo-electrochemical solar cells with a SnO2-liquid junction sensitized with highly concentrated dyes. *Journal of Applied Electrochemistry* **1986,** *16* (5), 683-692.

6. Xue, D.; Ashbrook, L. N.; Gaddie, R. S.; Michael Elliott, C., Tris(4,4′-di-t-butyl-2,2′-bipyridine)cobalt: Cation Effects on the Voltammetry at ITO and on Mediator Performance in Dye Sensitized Solar Cells. *Journal of The Electrochemical Society* **2013,** *160* (6), H355-H359.

7. Tsao, H. N.; Burschka, J.; Yi, C.; Kessler, F.; Nazeeruddin, M. K.; Gratzel, M., Influence of the interfacial charge-transfer resistance at the counter electrode in dye-sensitized solar cells employing cobalt redox shuttles. *Energy & Environmental Science* **2011,** *4* (12), 4921-4924.

8. Feldt, S. M.; Gibson, E. A.; Gabrielsson, E.; Sun, L.; Boschloo, G.; Hagfeldt, A., Design of Organic Dyes and Cobalt Polypyridine Redox Mediators for High-Efficiency Dye-Sensitized Solar Cells. *Journal of the American Chemical Society* **2010,** *132* (46), 16714-16724.

9. Kavan, L.; Yum, J.-H.; Nazeeruddin, M. K.; Grätzel, M., Graphene Nanoplatelet Cathode for Co(III)/(II) Mediated Dye-Sensitized Solar Cells. *ACS Nano* **2011,** *5* (11), 9171-9178.

10. Hamann, T. W.; Jensen, R. A.; Martinson, A. B. F.; Van Ryswyk, H.; Hupp, J. T., Advancing beyond current generation dye-sensitized solar cells. *Energy & Environmental Science* **2008,** *1* (1), 66-78.

11. Grätzel, M., Conversion of sunlight to electric power by nanocrystalline dye-sensitized solar cells. *Journal of Photochemistry and Photobiology A: Chemistry* **2004,** *164* (1–3), 3-14.

12. Feldt, S. M.; Lohse, P. W.; Kessler, F.; Nazeeruddin, M. K.; Gratzel, M.; Boschloo, G.; Hagfeldt, A., Regeneration and recombination kinetics in cobalt polypyridine based dye-sensitized solar cells, explained using Marcus theory. *Physical Chemistry Chemical Physics* **2013,** *15* (19), 7087-7097.

13. Sapp, S. A.; Elliott, C. M.; Contado, C.; Caramori, S.; Bignozzi, C. A., Substituted Polypyridine Complexes of Cobalt(II/III) as Efficient Electron-Transfer Mediators in Dye-Sensitized Solar Cells. *Journal of the American Chemical Society* **2002,** *124* (37), 11215-11222.

14. Nelson, J. J.; Amick, T. J.; Elliott, C. M., Mass Transport of Polypyridyl Cobalt Complexes in Dye-Sensitized Solar Cells with Mesoporous TiO2 Photoanodes. *The Journal of Physical Chemistry C* **2008,** *112* (46), 18255-18263.

15. Nusbaumer, H.; Moser, J.-E.; Zakeeruddin, S. M.; Nazeeruddin, M. K.; Grätzel, M., CoII(dbbip)22+ Complex Rivals Tri-iodide/Iodide Redox Mediator in Dye-Sensitized Photovoltaic Cells. *The Journal of Physical Chemistry B* **2001,** *105* (43), 10461-10464.

16. Yella, A.; Lee, H.-W.; Tsao, H. N.; Yi, C.; Chandiran, A. K.; Nazeeruddin, M. K.; Diau, E. W.-G.; Yeh, C.-Y.; Zakeeruddin, S. M.; Grätzel, M., Porphyrin-Sensitized Solar Cells with Cobalt (II/III)–Based Redox Electrolyte Exceed 12 Percent Efficiency. *Science* **2011,** *334* (6056), 629.

17. Mathew, S.; Yella, A.; Gao, P.; Humphry-Baker, R.; CurchodBasile, F. E.; Ashari-Astani, N.; Tavernelli, I.; Rothlisberger, U.; NazeeruddinMd, K.; Grätzel, M., Dye-sensitized solar cells with 13% efficiency achieved through the molecular engineering of porphyrin sensitizers. *Nat Chem* **2014,** *6* (3), 242-247.

18. Feldt, S. M.; Wang, G.; Boschloo, G.; Hagfeldt, A., Effects of Driving Forces for Recombination and Regeneration on the Photovoltaic Performance of Dye-Sensitized Solar Cells using Cobalt Polypyridine Redox Couples. *The Journal of Physical Chemistry C* **2011,** *115* (43), 21500-21507.

19. Tsao, H. N.; Comte, P.; Yi, C.; Grätzel, M., Avoiding Diffusion Limitations in Cobalt(III/II)-Tris(2,2'-Bipyridine)-Based Dye-Sensitized Solar Cells by Tuning the Mesoporous TiO2 Film Properties. *ChemPhysChem* **2012,** *13* (12), 2976-2981.

20. Bella, F.; Galliano, S.; Gerbaldi, C.; Viscardi, G., Cobalt-Based Electrolytes for Dye-Sensitized Solar Cells: Recent Advances towards Stable Devices. *Energies* **2016,** *9* (5).

21. Yum, J. H.; Baranoff, E.; Kessler, F.; Moehl, T.; Ahmad, S.; Bessho, T.; Marchioro, A.; Ghadiri, E.; Moser, J. E.; Yi, C.; Nazeeruddin, M. K.; Gratzel, M., A cobalt complex redox shuttle for dye-sensitized solar cells with high open-circuit potentials. *Nat Commun* **2012,** *3*, 631.

22. Ondersma, J. W.; Hamann, T. W., Impedance Investigation of Dye-Sensitized Solar Cells Employing Outer-Sphere Redox Shuttles. *The Journal of Physical Chemistry C* **2010,** *114* (1), 638-645.

23. Kirner, J. T.; Elliott, C. M., Are High-Potential Cobalt Tris(bipyridyl) Complexes Sufficiently Stable to Be Efficient Mediators in Dye-Sensitized Solar Cells? Synthesis, Characterization, and Stability Tests. *The Journal of Physical Chemistry C* **2015,** *119* (31), 17502-17514.

24. Thomas, J. D., Prieto, Amy L., Elliott, C. Michael, Utilization of 5,5' disubstituted tris-bipyridine cobalt complexes as high potential dye sensitized solar cell electrolyte mediators. *Journal of The Electrochemical Society* **In preparation**.

25. Aribia, K. B.; Moehl, T.; Zakeeruddin, S. M.; Gratzel, M., Tridentate cobalt complexes as alternative redox couples for high-efficiency dye-sensitized solar cells. *Chemical Science* **2013,** *4* (1), 454-459.

26. Freitag, M.; Yang, W.; Fredin, L. A.; D'Amario, L.; Karlsson, K. M.; Hagfeldt, A.; Boschloo, G., Supramolecular Hemicage Cobalt Mediators for Dye-Sensitized Solar Cells. *ChemPhysChem* **2016,** *17* (23), 3845-3852.

27. Kashif, M. K.; Nippe, M.; Duffy, N. W.; Forsyth, C. M.; Chang, C. J.; Long, J. R.; Spiccia, L.; Bach, U., Stable Dye-Sensitized Solar Cell Electrolytes Based on Cobalt(II)/(III) Complexes of a Hexadentate Pyridyl Ligand. *Angewandte Chemie International Edition* **2013,** *52* (21), 5527-5531.

28. Boschloo, G.; Hagfeldt, A., Characteristics of the Iodide/Triiodide Redox Mediator in Dye-Sensitized Solar Cells. *Accounts of Chemical Research* **2009,** *42* (11), 1819-1826.

29. Papageorgiou, N.; Maier, W. F.; Grätzel, M., An Iodine/Triiodide Reduction Electrocatalyst for Aqueous and Organic Media. *Journal of The Electrochemical Society* **1997,** *144* (3), 876-884.

30. Mosconi, E.; Yum, J.-H.; Kessler, F.; Gómez García, C. J.; Zuccaccia, C.; Cinti, A.; Nazeeruddin, M. K.; Grätzel, M.; De Angelis, F., Cobalt Electrolyte/Dye Interactions in Dye-Sensitized Solar Cells: A Combined Computational and Experimental Study. *Journal of the American Chemical Society* **2012,** *134* (47), 19438-19453.

31. Hamann, T. W.; Farha, O. K.; Hupp, J. T., Outer-Sphere Redox Couples as Shuttles in Dye-Sensitized Solar Cells. Performance Enhancement Based on Photoelectrode Modification via Atomic Layer Deposition. *The Journal of Physical Chemistry C* **2008,** *112* (49), 19756-19764.

32. Klahr, B. M.; Hamann, T. W., Performance Enhancement and Limitations of Cobalt Bipyridyl Redox Shuttles in Dye-Sensitized Solar Cells. *The Journal of Physical Chemistry C* **2009,** *113* (31), 14040-14045.

33. Daeneke, T.; Kwon, T.-H.; Holmes, A. B.; Duffy, N. W.; Bach, U.; Spiccia, L., High-efficiency dye-sensitized solar cells with ferrocene-based electrolytes. *Nat Chem* **2011,** *3* (3), 211-215.

34. Liberatore, M.; Burtone, L.; Brown, T. M.; Reale, A.; Carlo, A. D.; Decker, F.; Caramori, S.; Bignozzi, C. A., On the effect of Al2O3 blocking layer on the performance of dye solar cells with cobalt based electrolytes. *Applied Physics Letters* **2009,** *94* (17), 173113.

35. Lin, C.; Tsai, F.-Y.; Lee, M.-H.; Lee, C.-H.; Tien, T.-C.; Wang, L.-P.; Tsai, S.-Y., Enhanced performance of dye-sensitized solar cells by an Al2O3 charge-recombination barrier formed by low-temperature atomic layer deposition. *Journal of Materials Chemistry* **2009,** *19* (19), 2999-3003.

36. Ondersma, J. W.; Hamann, T. W., Measurements and Modeling of Recombination from Nanoparticle TiO2 Electrodes. *Journal of the American Chemical Society* **2011,** *133* (21), 8264-8271.

37. Son, H.-J.; Prasittichai, C.; Mondloch, J. E.; Luo, L.; Wu, J.; Kim, D. W.; Farha, O. K.; Hupp, J. T., Dye Stabilization and Enhanced Photoelectrode Wettability in Water-Based Dye-Sensitized Solar Cells through Post-assembly Atomic Layer Deposition of TiO2. *Journal of the American Chemical Society* **2013,** *135* (31), 11529-11532.

38. Lubitz, M.; Medina, P. A.; Antic, A.; Rosin, J. T.; Fahlman, B. D., Cost-Effective Systems for Atomic Layer Deposition. *Journal of Chemical Education* **2014,** *91* (7), 1022-1027.

39. Elam, J. W.; Groner, M. D.; George, S. M., Viscous flow reactor with quartz crystal microbalance for thin film growth by atomic layer deposition. *Review of Scientific Instruments* **2002,** *73* (8), 2981-2987.

40. Zhang, Z.; Chen, P.; Murakami, T. N.; Zakeeruddin, S. M.; Grätzel, M., The 2,2,6,6-Tetramethyl-1-piperidinyloxy Radical: An Efficient, Iodine- Free Redox Mediator for Dye-Sensitized Solar Cells. *Advanced Functional Materials* **2008,** *18* (2), 341-346.

41. Yang, W.; Vlachopoulos, N.; Hao, Y.; Hagfeldt, A.; Boschloo, G., Efficient dye regeneration at low driving force achieved in triphenylamine dye LEG4 and TEMPO redox mediator based dye-sensitized solar cells. *Physical Chemistry Chemical Physics* **2015,** *17* (24), 15868-15875.

42. Yu, Q.; Wang, Y.; Yi, Z.; Zu, N.; Zhang, J.; Zhang, M.; Wang, P., High-Efficiency Dye-Sensitized Solar Cells: The Influence of Lithium Ions on Exciton Dissociation, Charge Recombination, and Surface States. *ACS Nano* **2010,** *4* (10), 6032-6038.

43. Lin, R. Y.-Y.; Chuang, T.-M.; Wu, F.-L.; Chen, P.-Y.; Chu, T.-C.; Ni, J.-S.; Fan, M.-S.; Lo, Y.-H.; Ho, K.-C.; Lin, J. T., Anthracene/Phenothiazine π-Conjugated Sensitizers for Dye-Sensitized Solar Cells using Redox Mediator in Organic and Water-based Solvents. *ChemSusChem* **2015,** *8* (1), 105-113.

44. Kakiage, K.; Aoyama, Y.; Yano, T.; Oya, K.; Fujisawa, J.-i.; Hanaya, M., Highly-efficient dye-sensitized solar cells with collaborative sensitization by silyl-anchor and carboxy-anchor dyes. *Chemical Communications* **2015,** *51* (88), 15894-15897.

45. Gabrielsson, E.; Ellis, H.; Feldt, S.; Tian, H.; Boschloo, G.; Hagfeldt, A.; Sun, L., Convergent/Divergent Synthesis of a Linker-Varied Series of Dyes for Dye-Sensitized Solar Cells Based on the D35 Donor. *Advanced Energy Materials* **2013,** *3* (12), 1647-1656.

46. Kato, F.; Kikuchi, A.; Okuyama, T.; Oyaizu, K.; Nishide, H., Nitroxide Radicals as Highly Reactive Redox Mediators in Dye-Sensitized Solar Cells. *Angewandte Chemie International Edition* **2012,** *51* (40), 10177-10180.

47. Elliott, C. M., Dye-sensitized solar cells: Out with both baby and bathwater. *Nat Chem* **2011,** *3* (3), 188-9.

CHAPTER 2: UTILIZATION OF 5,5' DISUBSTITUTED TRIS-BIPYRIDINE COBALT COMPLEXES AS HIGH POTENTIAL DYE SENSITIZED SOLAR CELL ELECTROLYTE MEDIATORS

2.1 Overview

Herein, it will be shown that substituted cobalt tris-2,2'-bipyridine coordination complexes where substitutions are located at the 5,5' positions instead of the normally utilized 4,4' positions have encouraging properties which may be useful as a redox mediator for liquid electrolyte based dye sensitized solar cells. It was found that the redox potential of the Co(II/III) couple was more positive when substitutions were placed on the 5,5' positions in the cases of both electron-donating and electron-withdrawing substituents. The redox potential of the complex with ethyl ester groups substituted at the 5,5' positions of the bipyridines (Co(5-eebpy)) was observed to be as high as +0.67 V vs. SCCE. The charge transfer resistance between the cathode and the complexes was found to vary widely depending on the position and identity of the substituents suggesting different charge transfer mechanisms depending on the substitution. While the diffusion coefficients in acetonitrile solutions were found to not change much depending on the position of substituents. It was interesting to note that in the more viscous γ-butyrolactone, the complexes utilizing 5,5' substitutions had noticeably faster diffusion coefficients. No evidence was found to suggest that substitutions at the 5,5' positions lead to improved or diminished stability. However, it is clear that when using electron withdrawing groups to drive the complexes potential more positive, the stability of these complexes is still an issue.[1]

2.2 Introduction

It is generally understood that as a third generation photovoltaic technology, dye sensitized solar cells (DSSC), have the ability to yield commercially relevant conversion efficiencies at lower materials costs then traditional photovoltaic technologies.[2] As of the writing of this chapter, high efficiencies for DSSCs with liquid electrolytes are reported around 14 % through the use of organic, high

extinction coefficient sensitizers with cobalt coordination complex based mediators utilizing phenanthroline or bipyridine ligands.[3, 4] These efficiencies are achieved through a balance of several electron transfer and diffusional processes which can be affected through both device engineering and synthetic considerations.[5] Synthetic modification of the redox mediator can alter the attainable open circuit voltage, the kinetics of several important processes, and exacerbate or mitigate mass transfer limitations, all of which affects the efficiency.

In early high efficiency DSSCs, iodide/ tri-iodide (I^-/I_3^-) was used as a mediator redox couple due to its slow kinetics for electron recombination with the titanium dioxide photoanode and fast electron transfer to the commonly used ruthenium based N3 dye.[6-8] However, the redox potential of the couple is fixed several hundred millivolts negative of the dye ground state which restricts the attainable open circuit voltage. Cobalt based coordination complexes began to be used by the Grätzel group and the Elliott group around 2001 due to their more positive redox potentials, lower extinction coefficients, and synthetic tunability in relation to the I^-/I_3^- couple.[9, 10] These complexes tend to be non-volatile and non-corrosive to the other components of the cell; including the cathode and sealing materials. The use of coordination complexes like cobalt (II/III) tris-2,2' bipyridine is advantageous in both commercial applications and fundamental research due to the ability to tune certain properties of the DSSC by functionalization of the ligands around the metal center. As shown by Sapp and co-workers, substitution of different functional groups allows for manipulation of the redox potential which cannot be accomplished with a molecular species like the iodide/ tri-iodide couple.[10] Prior publications have also shown that substitutions with bulky alkyl groups (such as *tert*-butyl) at the 4,4' positions of the bipyridine ligand limit the rate of back electron transfer between mediator and photoanode.[11, 12] This substitution of functional groups with electron donating character has the unintended consequence of shifting the redox potential of the complex more negative compared to the unsubstituted complex. Choosing substitutions which are more electron withdrawing shows the opposite effect and leads to a

more positive redox potential when compared to the unsubstituted complex which can serve to increase the attainable open circuit voltage.[1]

The work performed shows that a combination of position and identity of functional group substitutions on 2,2' bipyridine ligands for cobalt (II/III) coordination complexes affects a number of processes vital to DSSC function including redox potential of the assembled cobalt coordination complexes, shown in figure 2.1. To effectively evaluate the newly synthesized complexes, the previously described processes were individually considered and the effects these synthetic changes have were evaluated. Electrochemical potential was evaluated using multiple common cathode materials (gold and glassy carbon) and as expected, the potential was driven more positive by the presence of the ethyl ester substituents.[10] Absorption coefficients were evaluated using UV-Vis spectroscopy and as expected absorption mimicked previously studied cobalt 2,2-bipyridine based complexes in that absorption of visible light is minimal. Impedance spectroscopy was used to compare the rate of charge transfer between differently substituted complexes and commonly used cathode materials. The ester substituents yielded very high resistance to charge transfer on gold cathodes but surprisingly low

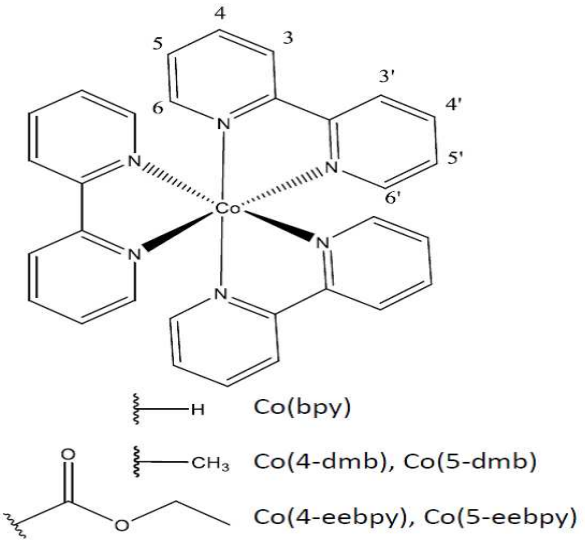

Figure 2.1: Structure of the unsubstituted cobalt tris-2,2'-bipyrdine and substituents utilized to demonstrate the effect of electron donating and withdrawing character on the assembled complexes. Position numbers represent relevant positions around the bipyridine. The 4,4' and 5,5' positions are utilized in this manuscript.

resistance on glassy carbon cathodes. Modeling of this impedance data also allowed for characterization of diffusional properties of these complexes in both acetonitrile and γ-butyrolactone. Diffusional properties of the synthesized complexes were concurrently assessed through the use of potential step chronoamperometry utilizing thin layer cells. It was found that as expected, the diffusion coefficient increased as the size of the substituent increased. This increase was accentuated in more viscous solvents such as γ-butyrolactone as opposed to acetonitrile. Stability concerns have been raised previously for high potential cobalt coordination complex based mediators and thus assembled complexes have been qualitatively evaluated based on electrochemical reversibility and aging studies while in the presence of commonly used DSSC solvents and additives.[1] While it was confirmed that using more electron withdrawing substituents leads to higher instability, no significant difference was discovered between the stability of complexes with the same substituents at different positions.

2.3 Experimental section

Materials used

The following chemicals were used as received, solvents were ACS grade unless otherwise noted: absolute ethanol (Pharmco-aaper), ethyl ether (EMD Millipore), acetonitrile (Sigma Aldrich), dichloromethane (Fisher Scientific), chloroform (Fisher Scientific), methanol (Fisher Scientific), gamma-butyrolactone (Sigma-Aldrich, ReagentPlus), sulfuric acid (Acros, reagent grade), 70 % nitric acid (EMD, reagent grade), potassium permanganate (Fisher Scientific, ACS grade), cobalt (II) perchlorate hexahydrate (G. Frederick Smith Chemical Company), 2,2' dipyridal (Sigma-Aldrich, 99.5 %), lithium triflate (Sigma-Aldrich, 96 %), 4-*tert*-butylpyridine (Sigma-Aldrich, 99 %), nitrosonium tetrafluoroborate (Sigma-Aldrich, 95 %), and lithium perchlorate (Sigma-Aldrich, reagent grade). *Tert*-butylammonium hexafluorophosphate (TCI America) was recrystallized twice from methanol before use.

Synthesis of 4,4'-diethyl ester-2,2'-bipyridine

4,4' dimethyl-2,2'-bipyridine (4-dmb) was previously synthesized using reported methods.[13] The overall synthetic methodology was also based off of work done by Gamba et al.[14] After characterization by ^{1}H-NMR and melting point determination to ensure purity, 3.50 g of 4-dmb was added to a solution of 1.0 M potassium permanganate in 250 mL of distilled water. The solution was refluxed for 2 hours and during that time transitioned in color from dark pink/purple, to brown, and finally to black. The solution was then allowed to cool to room temperature. The black solid manganese dioxide byproduct was filtered, leaving the supernatant clear and colorless. The solution was chilled in an ice bath and slowly acidified using concentrated nitric acid until a white solid was precipitated. The solid was collected by filtration and was dried overnight in a vacuum oven at 80 °C.

The resulting 4,4' dicarboxyl-2,2'-bipyridine (4-dcb) was characterized by ^{1}H-NMR and melting point determination. Following characterization, 2.00 g of 4-dcb was suspended in 75 mL of absolute ethanol. After the addition of ~6 mL of concentrated sulfuric acid, the solution was refluxed for 36 hours. During that time the suspended 4-dcb dissolved into solution as the reaction proceeded. The solution was allowed to cool to room temperature and any remaining solid was filtered out (the remaining solid is attributed to a minor impurity of partially carboxylated starting material which could not be fully esterified). The solution volume was reduced by rotary evaporation until the product began to precipitate. Approximately 100 mL of cold distilled water was added and a flocculent white solid was precipitated out. The solid was collected by filtration and dried in the vacuum oven. The product, 4,4'-diethyl ester-2,2'-bipyridine (4-eebpy), was recrystallized out of ethanol before characterization by ^{1}H-NMR, mass spectrometry, and melting point determination.

Synthesis of 5,5'-diethyl ester-2,2'-bipyridine

Beginning from 5,5' dimethyl-2,2'-bipyridine (5-dmb), which was also prepared using previously reported methods, 5,5'-diethyl ester-2,2'-bipyridine (5-eebpy) was prepared using the same

methodology above.[13, 14] Characterization was carried out between each synthetic step and that characterization as well as percent yields are reported in the supplementary information.

Assembly of Co(II) complexes

Cobalt (II) tris-2,2'-bipyridine (Co(bpy)), cobalt (II) tris-4,4'-dimethyl-2,2'-bipyridine (Co(4-dmb)), and cobalt (II) tris-5,5'-dimethyl-2,2'-bipyridine (Co(5-dmb)) were all prepared using the same procedure.[10] For simplicity, only the assembly of the complex utilizing 5,5'-dimethyl-2,2-bipyridine is described here. All assembled complexes were characterized by ^{1}H-NMR and elemental analysis.

A small excess of 5,5'-dimethyl-2,2'-bipyridine (~3.1 equivalents) was dissolved at high concentration in refluxing methanol (for 1.00 g ~40 mL was appropriate). 1.0 equivalent of cobalt (II) perchlorate hexahydrate (0.662 g) was added and the mixture was allowed to continue refluxing for 2 hours in order to ensure complete reaction. In the first 20 minutes of the reaction, the solution transitions from bright red, corresponding to the cobalt perchlorate, to a bronze/orange color for the dissolved product. The solution was allowed to come to room temperature and the volume of ethanol was reduced by rotary evaporation until precipitate just begins to form (in this case to approximately 15 mL). To the remaining volume of solution, enough cold ethyl ether was added to triple the volume of solution which caused the cobalt (II) tris-5,5'-dimethyl-2,2'-bipyridine (Co(5-dmb)) to precipitate out of solution as a pale yellow solid. The solid could then be collected by filtration and dried in a vacuum oven at room temperature.

The synthesis of cobalt (II) tris-5,5'-diethyl ester-2,2'-bipyridine (Co(5-eebpy)) and cobalt (II) tris-4,4'-diethyl ester-2,2'-bipyridine (Co(4-eebpy) were also performed in analogous fashion to each other. For simplicity, only the assembly of Co(5-eebpy) is shown here. Approximately 3.1 equivalents of the 5-eebpy ligand (0.6146 g) was dissolved into ~40 mL of refluxing methanol. Following that addition, 1 equivalent of cobalt (II) perchlorate (0.2416 g) was added and the solution allowed to reflux for 2 hours to ensure complete formation of the complex. Within 10 minutes of the addition of the cobalt (II)

perchlorate, the assembled complex begins to precipitate out of solution as a gold/orange solid. The solid is filtered from the methanol and dried in the vacuum oven at 60 °C. A small amount of the complex remains behind in solution and can be extracted in a similar fashion to the unsubstituted bipyridine complex. Yield and characterization data for all complexes is provided in the supplementary information.

Oxidation of cobalt complexes

For the impedance experiments, it was necessary to oxidize some of the cobalt (II) complexes to their cobalt (III) analogues prior to running samples. Having both halves of the redox couple in solution in appreciable amounts minimizes the effect of the experiment on the bulk concentration of either redox species. The oxidation was performed through the addition of an excess of nitrosonium tetrafluoroborate ($NOBF_4$) to a solution of the complex in dichloromethane. The oxidations were performed with ~100 mg of the complex in 10 mL of solvent. After stirring for ~20 minutes, water was added to quench any remaining $NOBF_4$. At this point, different purification procedures were used to recover each set of complexes (unsubstituted and dimethyl substituted vs. di-ethyl ester substituted). For the unsubstituted and dimethyl substituted complexes, the water was removed by separatory funnel and the dichloromethane was reduced in volume by half. Approximately 20 mL of cold ethyl ether was added and the cobalt (III) complex crashes out of solution. The solid can then be filtered and dried in the vacuum oven. For the di-ethyl ester substituted complexes, after the volume of the dichloromethane was reduced, ethanol was added due to lower solubility of those complexes compared to ethyl ether. At that point the di-ethyl ester substituted complexes could be filtered and dried as before.

Complex and ligand characterization data

Ligands were characterized using melting point determination on a Mel-Temp II melting point apparatus from Laboratory Devices Inc., ^{1}H-NMR spectroscopy was performed on an Agilent Innova 300

MHz spectrometer, and mass spectrometry was performed on an Agilent G6220A TOF LC/MS using ESI/APCI ionization mode and positive ion mode. Cobalt (II) complexes were characterized using ^{1}H-NMR spectroscopy and elemental analysis was performed by Galbraith Laboratories using combustion analysis. Characterization data and percent yields for ligands and cobalt (II) complexes are provided in the supplementary information. UV-Vis spectroscopy was performed on an Agilent 8453 UV-Visible spectroscopy system. The mediator complexes were dissolved in dichloromethane to a concentration of 10 mM to determine the absorption coefficient of the complexes in the visible region that could correspond with likely sensitizers.

Cyclic voltammetry

Cyclic voltammetry was performed on a CH Instruments model 750D bi-potentiostat using a 3 electrode set-up and a saturated sodium calomel reference electrode (0.2360 V vs. NHE). Platinum wire was used as an auxiliary electrode while gold (surface area (SA)= 0.0079 cm^2) and glassy carbon (SA= 0.283 cm^2) working electrodes were used. Working electrodes were polished before and between uses on a felt pad saturated with a slurry of 0.3 µm alumina powder and water. Experiments were performed in 20 mL scintillation vials with ~ 5 mL of solution. Solutions were all kept at 10 mM concentration of the cobalt (II) mediator complex in acetonitrile for the unsubstituted and dimethyl substituted complexes and dichloromethane for the di-ethyl ester substituted complexes. *Tert*-butylammonium hexafluorophosphate was used as a supporting electrolyte at a concentration of 0.100 M in solution. Potentials were scanned between -0.2 V and 1.2 V vs. SCCE for 3 cycles for each experiment. Scan rates varied between 50 mV/s and 200 mV/s.

Impedance spectroscopy

Impedance spectroscopy was performed on a CH Instruments model 750D bi-potentiostat using common electrode materials and a 1 Mil (25.1 µm) spacer of non-adhesive Kapton® tape. Gold and glassy carbon electrodes were used as representative cathode materials in a two electrode symmetrical

cell. The gold film electrodes were prepared by thermal evaporation with a layer 60 μm of chromium used as a whetting layer followed by 200 μm of gold onto fluorine doped tin oxide glass. The glassy carbon electrodes were characterized before use using cyclic voltammetry and x-ray photoelectron spectroscopy (XPS). The $E_{1/2}$ of the ferrocene/ferrocenium redox couple at 100 mM in acetonitrile with 200 mM lithium perchlorate was found to be 0.44 V vs SCCE on the glassy carbon electrode which matches well with the literature.[15] The high resolution plots and atomic percent information for carbon and oxygen species in the XPS are included in the supplementary information. No other elements were detected. The geometric area of the cell is (0.44 cm^2) which was set by a hole punched in the Kapton® film separator. Concentrations of the unsubstituted and di-ethyl ester substituted mediator complexes were set to match typical concentrations used in DSSC sandwich cells (0.135 M for the Co^{2+} complex and 0.015 M for the Co^{3+} complex). The concentration of the cobalt (II) di-methyl substituted complexes was set to 0.06 M due to low solubility for the 4,4' di-methyl substituted complex in acetonitrile. Experiments were performed in acetonitrile and gamma-butyrolactone to evaluate differences in behavior between more and less coordinating solvents respectively. Lithium trifluoromethanesulfonate (LiTrif) was used as a supporting electrolyte at a concentration of 0.200 M. Frequencies were scanned between 0.1 Hz and $5x10^5$ Hz with a potential perturbation of 10 mV. Impedance spectra were fitted using the CH Instruments impedance simulator software using the model circuit included in the supplementary information.

Potential-step chronoamperometry

Potential step chronoamperometry was performed in order to determine diffusion coefficients for the mediator complexes in bulk solution for both acetonitrile and gamma-butyrolactone. For these experiments, the unsubstituted and di-ethyl ester cobalt (II) complexes were dissolved to a concentration of 0.135 M with 0.20 M supporting electrolyte in the form of lithium trifluoromethanesulfonate. As with the impedance experiments, a concentration of 0.06 M was used

for the di-methyl substituted complexes due to decreased solubility of the complex using 4-dmb in acetonitrile. Experiments were performed on symmetrical cells consisting of either gold or glassy carbon electrodes with a geometric area of 0.44 cm^2 fixed by a Kapton® film mask used to separate the working and auxiliary electrodes. The Kapton® film was determined to be 25 µm thick by micrometer which sets the distance (d) between working and counter electrodes. The potential was stepped to + 0.50 V vs. the auxiliary electrode in the 2 electrode symmetrical cell set-up. The potential step was held for 10 seconds to ensure an adequate number of data points in the mass transfer limited region.

2.4 Results and discussion

Several key metrics have been identified that can be used to pre-emptively evaluate the utility of new coordination complexes for use as dye sensitized solar cell mediators. By synthetically tuning the ligands of the coordination complex, many of these metrics can be controlled. The addition of electron withdrawing groups to the bipyridine ligands drives the absorption to higher wavelengths; however the magnitude of absorption is still small for all complexes tested. The reduction potentials of the complexes on possible cathode materials were found to become significantly more positive with the addition of electron withdrawing groups. Altering the position on which those groups are found from 4,4' to 5,5'drives the potential more positive as well regardless of the character of the functional group. The charge transfer resistances of the complexes varied depending on the identity and position of the substitutions with larger substitutions generally leading to higher resistance. However, some interesting variances were discovered between the behaviors of the complexes on gold versus glassy carbon. The diffusion coefficients of the complexes were slower, as expected, in the more viscous γ-butyrolactone compared to acetonitrile. That higher viscosity also accentuated the differences observed in the diffusion coefficients, which lead to faster diffusion of the 5,5' substituted complexes versus the 4,4' substituted complexes. The stability of the complexes which is expected to occur by ligand dissociation of the bipyridines has been shown to be worse for the substitutions with more electron withdrawing

character. The position of the substituents doesn't appear to make any substantial difference in this effect.

Absorption coefficient

One of the characteristics that make cobalt coordination complexes utilizing bipyridine type ligands desirable for use in DSSCs is their low absorption of visible light compared to the commonly used iodide/tri-iodide couple. Ideally, the redox mediator used in a DSSC will absorb no visible light allowing for no competition with the sensitizer for photons. Though the complexes examined here do absorb some visible light, they respond as expected. The absorption spectra of both cobalt (II) and cobalt (III) complexes as well as their calculated absorption coefficients are reported in the supplementary information as figures 2.S4, 2.S5, and table 2.S5 respectively. The highest absorption peak for most of these complexes occurs in the UV region below 400 nm and corresponds to absorption within the ligands themselves. A shoulder is observed coming off of this high absorption peak which corresponds to a metal to ligand charge transfer event with much lower intensity then the absorption stemming from the ligands. The addition of electron withdrawing groups however leads to a red-shift of the peak absorption as seen most strongly with the Co(4-eebpy) complex. However, even with the Co(4-eebpy) complex the absorption attributed to the compound decreases sharply after its peak at 434 nm. A red shift can also be observed as the Co(II) complexes transition to Co(III) complexes but the variation is not significant enough to increase the competition between mediator and most possible sensitizers. Many of the commonly used sensitizers for DSSCs absorb light with wavelengths above 450 nm.[2] Absorption coefficients were calculated at a wavelength of 450 nm and are reported in Table 2.S5. All of the coefficients reported are below 300 $mol^{-1}cm^{-1}L$, so it is expected that no competition between the sensitizer and the complexes will take place. Assuming a path length of ~60 μm through the portion of a typical DSSC sandwich cell containing redox mediator, even the most red-shifted complex, Co(4-eebpy), allows more than 63 % of the light to be transmitted completely through the cell at common

DSSC concentrations. Since DSSCs are most commonly illuminated through the photoanode however, only mediator within the pores of the photoanode would compete for visible light absorption. This would allow the transmittance through that layer (estimated around 12 μm) to likely exceed 90 %.

Reduction potentials

It has been shown by Sapp and co-workers that a methyl substituent added 'meta' to the nitrogen (5-dmb) will yield a more positive redox potential for cobalt (II/III) tris-2,2' bipyridine based complexes compared with 4,4' (para) substituted analog.[10] It has also been shown more recently that the addition of electron withdrawing moieties drives the potential of cobalt (II/III) tris-2,2'-bipyridine based complexes more positive compared to the unsubstituted complex.[1] However, until now the combined effect of these two approaches has not been explored.

In order to accurately describe the reduction potential of the complexes, it was important for the electrochemistry performed to be reversible and reproducible. Solvent choice was a concern for both di-ethyl ester substituted complexes after it was observed that cyclic voltammograms (CVs) performed in acetonitrile were not as reproducible on gold working electrodes as can be seen in figure 2.S6. In less-coordinating solvents such as dichloromethane, reproducibility was more consistent over multiple cycles. This behavior was not observed for the other complexes or when electrochemistry was performed on glassy carbon electrodes. Estimated peak currents and redox potential did not change considerably between solvents, so it was decided in order to allow for clarity with the trends to report cyclic voltammetry (figures 2.2 and 2.3 and table 2.1) for the ethyl ester substituted complexes as performed in dichloromethane. While it is not entirely clear what the cause of this phenomenon is, hypotheses will be discussed later as it pertains to the stability of the complexes.

The comparison of cyclic voltammograms found in figures 2.2 and 2.3 revealed several peak groupings according to the substituent present on the ligands of the complexes. The redox potential of the 4,4' and 5,5' dimethyl substituted complexes, due to the substituent's electron donating nature, are

shifted approximately 130 and 90 mV more negative in potential respectively, compared to the unsubstituted complex. The two complexes synthesized with ester substitutions on the bipyridines exhibit redox potentials shifted ~300 mV positive of the unsubstituted and dimethyl substituted cobalt tris-2,2'-bipyridine based complexes. For both of the substituent types, the potential of the 5,5' substituted analogue is shifted more positively in potential. The evidence shows that using substitutions on the 5,5' positions drives the redox potential more positive regardless of the electron withdrawing or electron donating character of the substitution.

Experimental values of $E_{1/2}$ for both gold and glassy carbon working electrodes are reported versus a saturated sodium calomel electrode reference (+0.232 V vs. NHE) in table 2.1. There is a much larger difference observed in $E_{1/2}$ between the ethyl ester substituents compared to the methyl substituents on both electrodes. However, this larger shift is obscured by the larger peak separation (ΔE_p) exhibited by the 4,4' di-ethyl ester substituted complex. One likely cause of the large peak separation is the presence of the ethyl ester substituents in the 4,4' positions acting as a steric barrier to

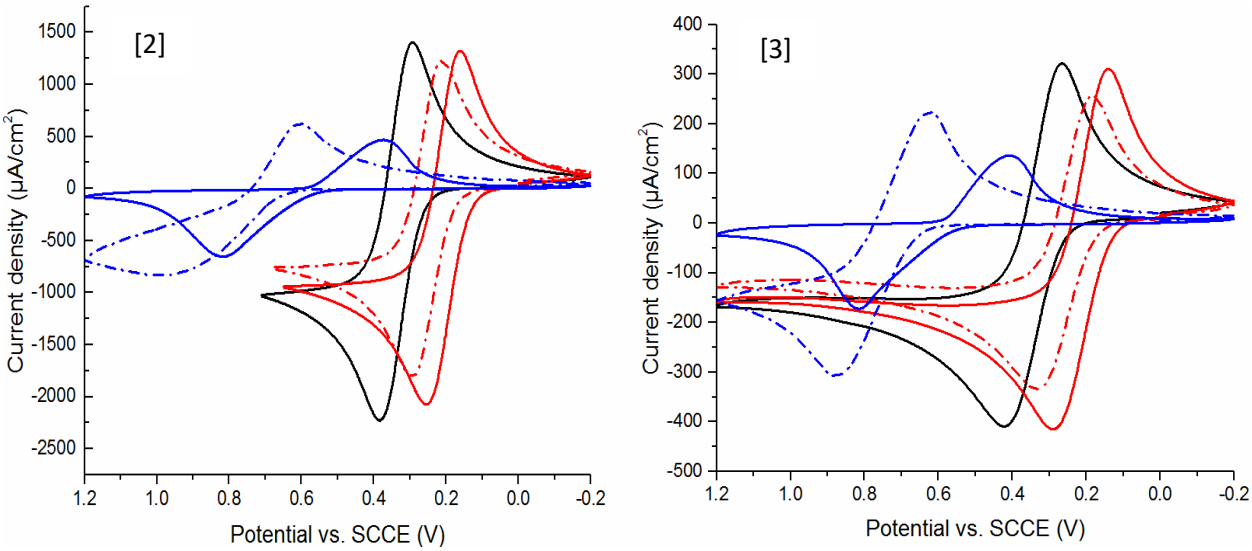

Figures 2.2 and 2.3: Cyclic voltammogram of synthesized cobalt bipyridine complexes using 10 mM Co2+ species and 100 mM TBAPF6 in acetonitrile for Co(bpy) (—), Co(4-dmb) (—), and Co(5-dmb) (----), and dichloromethane for Co(4-eebpy) (—), and Co(5-eebpy) (----). The working electrode in figure 2.2 was gold while figure 2.3 was glassy carbon with a platinum wire counter electrode, and a SCCE auxiliary electrode. All potentials are vs. SCCE and the scan rate was 50 mV/s.

the charge transfer event. This hypothesis is supported by the the 5,5' di-ethyl ester substituted complex exhibiting the next largest peak separation, shown in table 2.1. The di-methyl substituents do not provide a sufficient barrier, independent of their position, to negatively affect the ΔE_p as shown by the fact that both Co(4-dmb) and Co(5-dmb) exhibit similar ΔE_p values compared to the unsubstituted complex. Resistance to charge transfer will be discussed further as it pertains to impedance fitting below and also provides an indication of the blocking effect of these substituents.

A mediator's interaction with the sensitizer of a functioning DSSC for the purposes of dye regeneration is also an important consideration when deciding on a DSSC mediator. While it has been shown that a mediator with a more positive redox potential can increase the open circuit voltage (V_{oc}) of a DSSC, efficiency of the cell can still suffer without sufficient driving force for effective regeneration of the sensitizer. The effect of different amounts of driving force on dye regeneration has previously been studied for a number of cobalt complexes using bipyridine and phenanthroline based ligands and several dyes.[11] It was found by Feldt et al. that Marcus theory can be applied to this interaction such that depending on the concentration of the mediator, a minimum driving force of between 0.25 and 0.4 eV is required for highly efficient dye regeneration. This means that some commonly used dyes in the literature may no longer serve as appropriate choices for pairing with the high potential mediator, Co(5-eebpy). The commonly used dyes N3 ($E_{1/2}$=0.85 V vs. SCCE) and N749 ($E_{1/2}$=0.66 V vs. SCCE) would leave

Table 2.1: $E_{1/2}$ and ΔE_p were determined by cyclic voltammetry with 10 mM Co^{2+} species and 100 mM $TBAPF_6$ in acetonitrile for Co(bpy), Co(4-dmb), and Co(5-dmb) and dichloromethane for Co(4-eebpy) and Co(5-eebpy). A 50 mV/s scan rate was used.

Complex	Gold (V vs. SCCE)		Glassy Carbon (V vs. SCCE)	
	$E_{1/2}$	ΔE_p	$E_{1/2}$	ΔE_p
Co (II/III) bpy	0.34	0.10	0.35	0.16
Co (II/III) 4-dmb	0.21	0.09	0.22	0.14
Co (II/III) 5-dmb	0.25	0.08	0.26	0.14
Co (II/III) 4-eebpy	0.59	0.39	0.60	0.35
Co (II/III) 5-eebpy	0.75	0.27	0.72	0.27

little in the way of overpotential to promote fast dye regeneration.[6, 16, 17] Organic sensitizers with more positive ground state redox potentials such as L0 ($E_{1/2}$=1.14 V vs. SCCE) and Y123 ($E_{1/2}$=1.33 V vs. SCCE) may prove to be more effective choices.[11, 18-20] The interaction of specific sensitizers with these possible high potential mediators may be examined in more depth in future work.

Charge transfer kinetics

Interaction of the redox mediator with the electrode surface of the cathode is a key consideration when choosing the redox mediator and an appropriate material for the cathode. In the ideal case, the regeneration of the mediator at the cathode surface would be instantaneous. A proportional metric to the rate of mediator regeneration is the resistance to charge transfer between the complex and the cathode material. The resistance to charge transfer (R_{ct}) can be measured through impedance spectroscopy and is a commonly used method in the evaluation of the compatibility of a mediator complex with a cathode material in a DSSC.[7, 21, 22] Here, the R_{ct} was found on both gold and glassy carbon electrodes using a symmetric cell method and two solvents, acetonitrile and γ-butyrolactone. A model impedance spectrum is shown in figure 2.4. The first semi-circle, at high

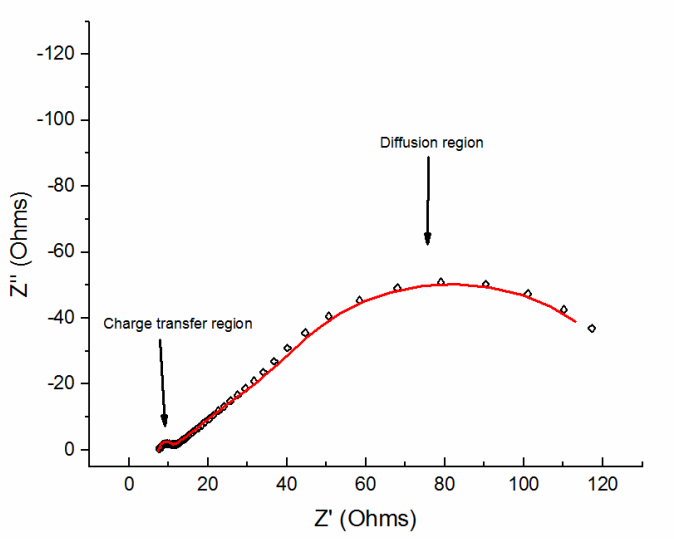

Figure 2.4: Example impedance spectrum with labels indicating which semi-circle is attributed to the charge transfer and which is attributed to diffusion. The black diamonds represent the experimental data while the fit is shown in red. This impedance spectrum was found using Co(5-eebpy) on gold electrodes with conditions explained in the experimental section.

frequencies, was attributed to the charge transfer reaction while the second was attributed to the diffusion between both symmetrical electrodes. All of the impedance data was modeled using the circuit in figure 2.S3 though the diffusion and will be discussed later. While platinized electrodes are commonly used as cathode materials in DSSCs, this group has previously shown that the electrochemistry of cobalt bipyridine based coordination complexes is less reversible on platinized electrodes compared to gold or glassy carbon.[10]

The R_{ct} for the 5 complexes in both acetonitrile and γ-butyrolactone are shown in table 2.2. The unsubstituted complex consistently exhibits the lowest resistance values regardless of solvent or cathode material. The Co(5-dmb) complex displays very similar R_{ct} values given all variations as well. The addition of substituents to the 4,4' positions increases R_{ct} in the case of both the methyl substituents and the ester substituents when performing experiments on the gold working electrode. Interestingly, the observed charge transfer resistance attributed to the 4,4' ethyl ester complex on gold in both solvents was anomalously high. In acetonitrile, it was hypothesized that some displacement of the ligands on the Co(4-eebpy) complex could occur with the somewhat coordinating acetonitrile and that free 4-eebpy ligand may be able to interact with the surface of the gold in an analogous fashion to *tert*-butylpyridine as described by this group in a prior publication.[23] However, this hypothesis is not entirely supported by the similarly high resistance to charge transfer in the less coordinating γ-butyrolactone where complex degradation is not expected to be as severe. Thus, it is unclear at this point what is causing the increased R_{ct} for experiments performed in γ-butyrolactone.

There is an intriguing decrease in the R_{ct} of complexes with substitutions in the 5,5' position instead of the 4,4' positions on a gold cathode. The Co(5-eebpy) complex exhibits a smaller value of R_{ct} (1.62 $\Omega \cdot cm^2$ in ACN) then even the Co(4-dmb) complex (3.24 $\Omega \cdot cm^2$ in ACN) despite the differences in the substituents size. For Co(4-dmb) and Co(5-dmb), with the only difference being the position of the substitution, there is a fivefold improvement in the R_{ct} in both ACN and GBL for Co(5-dmb). However,

the trends observed on the glassy carbon did not match those observed for gold for all of the complexes.

When experiments were performed on the glassy carbon electrodes, the behavior of the complexes substituted with methyl groups was similar to what was observed on gold. When methyl groups were at the 4,4' positions, observed values of R_{ct} were higher than those calculated for the 5,5' substituted complexes. This trend was reversed when dealing with the complexes whose bipyridines had ethyl ester functional groups substituted onto them. As can be seen on table 2.2, while the R_{ct} of Co(4-eebpy) was found to be 13.18 $\Omega \cdot cm^2$ in ACN, Co(5-eebpy) exhibited a higher R_{ct} of 19.51 $\Omega \cdot cm^2$ in ACN. At this point, it is hypothesized that a difference in the mechanism of charge transfer is responsible for the unexpected discrepancy. If the electron transfer between Co(4-eebpy) and the glassy carbon electrode occurs via an inner sphere charge transfer mechanism, it's likely that the resistance to charge transfer would be lower. If this was the mechanism for both ethyl ester substituted complexes, the transfer would more easily occur using the Co(4-eebpy) complex which can more easily adsorb to the glassy carbon surface with the esters substituted at the 4,4' positions as can be seen in figure 2.1. These results suggest that more importance be placed on compatibility testing of potential mediator complexes with numerous cathode materials.

Table 2.2: R_{ct} was determined by fitting of impedance spectroscopy according to figure 2.S3. Spectroscopy was performed on multiple electrodes and in multiple solvents. Concentrations used were analogous to concentrations used in DSSCs except for those used in with the dimethyl substituted complexes which were much lower. All experimental conditions are reported above.

Complex	R_{ct} on gold (Ω·cm)		R_{ct} on glassy carbon (Ω·cm)	
	ACN	GBL	ACN	GBL
Co (II/III) bpy	0.51	1.61	7.79	14.9
Co (II/III) 4-dmb	3.24	10.7	14.9	19.8
Co (II/III) 5-dmb	0.61	2.17	7.78	17.6
Co (II/III) 4-eebpy	113	138	13.1	21.6
Co (II/III) 5-eebpy	1.62	2.95	19.5	72.8

Diffusion coefficients

One of the factors limiting cobalt coordination complex use in DSSCs when compared to iodide/tri-iodide is the diffusion coefficient of the species in solution. In low concentrations with acetonitrile as a solvent, the diffusion coefficient for the iodide/tri-iodide redox couple in bulk solution has been reported to be 1.8 x 10^{-5} cm^2/s.[24] However, cobalt bipyridine and terpyridine coordination complexes are regularly reported in the literature with diffusion coefficients in acetonitrile which are close to half that under similar conditions.[25, 26] The effect of this limitation has previously been reported for similar coordination complexes in different solvents.[24] Device engineering can minimize the thickness and maximize the pore size of the photoanode film reducing its effect on the diffusion coefficient, however there is still an inherent limitation place on the steady state current stemming from the rate of diffusion of the mediator through bulk solution.[27] Even with this limitation, some of the most efficient examples of functioning DSSCs use the unsubstituted cobalt (II/III) tris-2,2'-bipyridine as a redox mediator.[3, 19]

Here, it has been observed that synthetic functionalization of the complex's ligands will lead to some decrease in the diffusion coefficient through bulk solution. We also report some evidence that by altering the position of the synthetic functionalization from 'para' to 'meta' relative to the nitrogen on the bipyridine ligands the effect of that steric bulk can be reduced. This evidence is clearer when utilizing more viscous solvents compared to the traditionally used acetonitrile.

Diffusion coefficients were evaluated using two methods: modelling of electrochemical impedance spectroscopy (D_l) and through the use of thin layer cells with potential step

$$n = \frac{L}{D^{1/2}}$$

Equation 2.1: Fitting parameters for open finite diffusion circuit element for impedance spectroscopy.

$$D_t = \frac{L^2}{4\pi\tau}$$

Equation 2.2: Equation to determine diffusion coefficient from chronoamperometry time constant.

chronoamperometry (D_c). For the fitting of impedance spectroscopy, the second semi-circle at lower frequencies observed in the representative spectra shown in figure 2.4 can be fitted with an open finite diffusion element as part of the model circuit shown in figure 2.S3. For experimental techniques, the diffusion distance (L) between working and auxiliary electrodes was fixed at 25.1 µm by a Kapton® film spacer. The open finite diffusion element in the model circuit provides a value represented by the equation 2.1 where (n) is the value provided by the model. It can be normalized using (L) to obtain the units cm^2/s. For chronoamperometry experiments, as seen in figure 2.5, a time constant (τ) can be obtained at the point where the concentration depletion region exceeds the spacing in the cell and the current transitions from Cottrell semi-infinite diffusion behavior to current determined by mass transfer limitations. Using equation 2.2, the diffusion coefficient can be calculated with the previously described time constant and the depth of the Kapton film spacer (L).[28] Diffusion coefficients for all complexes in acetonitrile and γ-butyrolactone are reported in table 2.3.

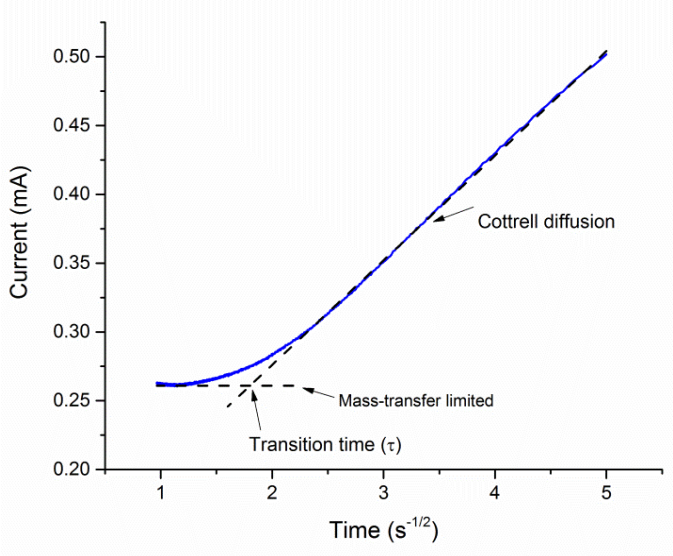

Figure 2.5: Chronoamperometry plot of electrolyte solution containing 0.15 M $Co(5\text{-eebpy})_3(ClO_4)_2$ complex in ACN with 0.2 M lithium triflate between 2 gold film electrodes. A 0.50 V potential step was used. At early times current was controlled by Cottrell semi-infinite diffusion while at late times current becomes controlled by mass transfer limitations. The time constant (τ) found where these processes transition from one to the other can be used to determine the diffusion coefficient of the electroactive species in solution.

Results show that as expected, the observed diffusion coefficients are slower when the bulkier ethyl ester substituents are used. On the other hand, the diffusion coefficients for Co(bpy), Co(4-dmb), and Co(5-dmb) are identical within experimental error. Under similar solution conditions to what would be used in a functioning DSSC, Co(bpy) was found to have a diffusion coefficient of 2.5 x 10^{-6} cm^2/s in acetonitrile; while Co(4-dmb) (2.2 x 10^{-6} cm^2/s) and Co(5-dmb) (2.4 x 10^{-6} cm^2/s) were found to be within the average error of close to 0.7 x 10^{-6} cm^2/s. The larger complexes, Co(4-eebpy) and Co(5-eebpy) were observed to have noticeably lower diffusion coefficients relative to the others but were very similar to each other in acetonitrile.

The difference between complexes substituted with more bulky vs. less bulky functional groups was made more apparent by impedance spectroscopy compared to chronoamperometry. However, a clear divergence of diffusion coefficients took place when the solvent was changed to γ-butyrolactone. Due to the low viscosity of acetonitrile, the relative size of the complexes had a smaller effect on the observed diffusion coefficient.

When impedance spectroscopy was performed in the more viscous γ-butyrolactone, a significant difference was observed relative to the diffusion coefficients of Co(4-dmb) and Co(bpy). While both Co(bpy) and Co(5-dmb) were observed to have diffusion coefficients of 6.5 x 10^{-7} cm^2/s, the

Table 2.3: Diffusion coefficients for all complexes are reported from chronoamperometry data (D_c) and from impedance model fitting (D_I) in both acetonitrile and γ-butyrolactone. Values are reported with error as standard deviation.

Complex	Acetonitrile (x 10^{-6} cm^2/s)		γ-butyrolactone (x 10^{-7} cm^2/s)	
	Diffusion (D_c)	Diffusion (D_I)	Diffusion (D_C)	Diffusion (D_I)
Co (II/III) bpy	2.5±0.6	2.8±0.4	2.7±0.5	6.5±0.5
Co (II/III) 4-dmb	2.2±1.0	2.6±0.7	2.7±0.1	5.9±0.7
Co (II/III) 5-dmb	2.4±0.4	2.6±0.7	2.6±0.5	6.5±0.6
Co (II/III) 4-eebpy	1.9±0.4	1.8±0.6	1.8±0.6	3.9±0.4
Co (II/III) 5-eebpy	1.9±0.5	1.8±0.2	2.2±0.8	4.7±0.6

Co(4-dmb) was observed somewhat slower at 5.9 x 10^{-7} cm^2/s with an average error of 0.6 x 10^{-7} cm^2/s. An increase in the diffusion coefficient was also detected as the ethyl ester substitutions were switched from the 4,4' positions to the 5,5' positions. By impedance, Co(4-eebpy) was found to have a diffusion coefficient of 3.9 x 10^{-7} cm^2/s while the Co(5-eebpy) complex had a diffusion coefficient of 4.7 x 10^{-7} cm^2/s.

Overall, the diffusion coefficients calculated from data collected by chronoamperometry were slower and more closely spaced compared to the data found by impedance spectroscopy. In acetonitrile, the difference is minor and the magnitude of the difference tracks with the error in the experiment. In γ-butyrolactone, there was a larger difference observed between the diffusion coefficients found by chronoamperometry and impedance spectroscopy. Similar trends between diffusion coefficients found by chronoamperometry and impedance spectroscopy were observed by Liberatore and co-workers.[28] Interestingly in that work it was found the difference in observed diffusion coefficients increased with higher temperature (i.e. lower viscosity) whereas the opposite is seen here where the viscosity difference is due to changing the solvent. Liberatore attributed the lower diffusion coefficients observed using chronoamperometry to the difference in applied potential between the techniques (0.5 V step for chronoamperometry versus 0.01 V step for impedance spectroscopy for this report) and the resulting IR drop.[28]

Complex stability

As mentioned, the Elliott group has previously reported the synthesis of cobalt complexes with a variety of electron-withdrawing groups substituted onto the bipyridine ligands.[1] It was found by Joel Kirner and C. Michael Elliott that as the potential of the redox couple became more positive, the stability of the complex in the presence of other coordinating species was decreased.[1] It was hypothesized that the strength of the ligand's association with the cobalt ion was diminished by the addition of electron withdrawing substituents such that the solvent (acetonitrile) or *tert*-butylpyridine (TBP), a common

DSSC additive, would be able to partially substitute itself into the complex in place of the ligand when coordinating with the metal.

UV-Vis spectroscopy was performed on all of the complexes before and after the addition of *tert*-butylpyridine. In the literature, TBP is commonly added to sandwich cells at a concentration of 0.20 M to the electrolyte solution because it has been shown to increase the open circuit voltage of the sandwich cell.[2] A concentration of 0.50 M was used here to exacerbate any effects at short times that would become more apparent at longer times. It can be seen in figure 2.6, when using the methyl substituents such as in the Co(5-dmb) complex, that there is only a slight change in the absorbance of the complex. This minute decrease in absorbance has been attributed to dilution of the solution from addition of the TBP. An analogous decrease in absorbance was also observed for the unsubstituted complex and Co(4-dmb). By comparison the change observed for the ethyl ester substituted complexes is notable. For both complexes there was a blue shift of the observed peak and decreased intensity of the shoulder normally attributed to the metal to ligand charge transfer. It is hypothesized this is due to the partial replacement of the ethyl ester substituted ligand with TBP. The added electron donating character of the TBP causes the blue shift in the same way that the unsubstituted and methyl

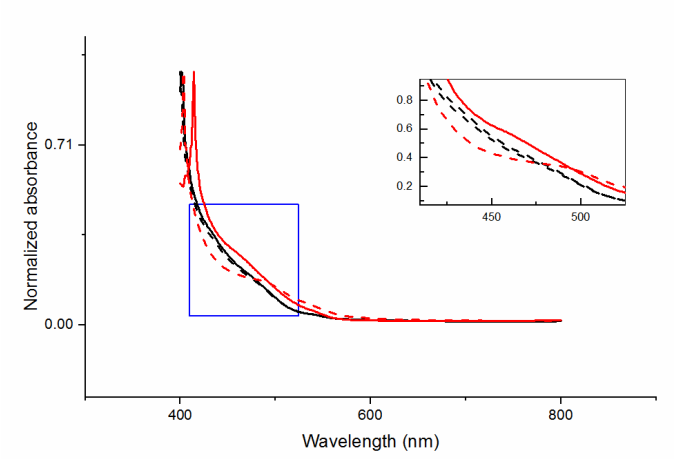

Figure 2.6: UV-Vis spectra of cobalt complexes with and without *tert*-butylpyridine (TBP). The solid black line is Co(5-dmb) while the dotted black line is after TBP addition. The solid red line is Co(5-eebpy) before TBP addition while the dotted red line is after TBP addition. Spectroscopy was performed in DCM to eliminate any solvent effects from a more coordinating solvent.

substituted complexes are blue shifted compared to the ethyl ester substituted complexes. However, the new complex could not be isolated for further characterization.

The electrochemical reversibility of complexes with di-ethyl ester substitutions, regardless of substitution position, was significantly reduced with the addition of TBP on gold electrodes. On the other hand, there appears to be very little effect on the reversibility of the cobalt complexes with dimethyl substituents or with no substituents at all within 24 hours of sample preparation. On the unsubstituted and dimethyl substituted complexes where very little disassociation of the ligands is expected in the presence of TBP, the only observed difference between cyclic voltammograms taken before and after addition of TBP was a slight change in ΔE_p as can be seen on Co(5-dmb) in figure 2.7. Both of the 5,5' substituted complexes can be seen in figure 2.7 with the Co(5-dmb) complex shown in black and the Co(5-eebpy) complex shown in red. The cyclic voltammograms shown were performed on a glassy carbon working electrode. Cyclic voltammograms performed on gold were more complicated due to the ability of *tert*-butylpyridine to adsorb onto the surface of gold electrodes and won't be reported here.[23] On glassy carbon the problem of adsorption was considered insignificant so changes

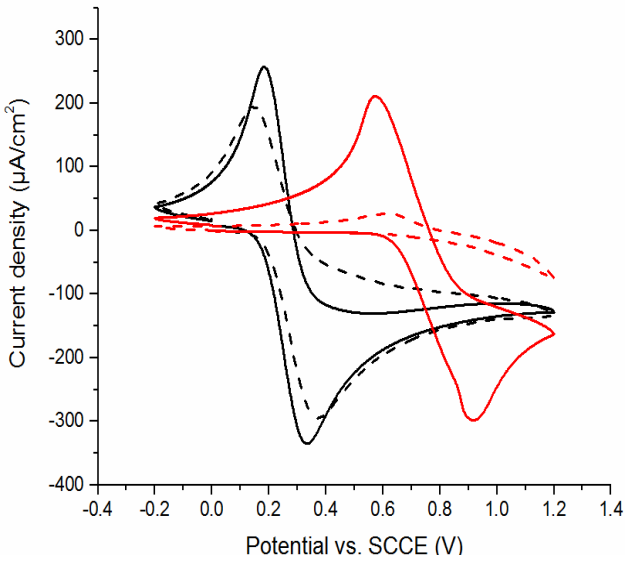

Figure 2.7: Cyclic voltammograms of Co(5-dmb) before (—) and after (---) addition of TBP and Co(5-eebpy) before (—) and after (---) addition of TBP. CVs with Co(5-dmb) were performed in ACN while CVs with Co(5-eebpy) were performed in DCM. TBP was added to solutions to a concentration of 0.50 M. Other experimental conditions are described above.

due to the addition of TBP are expected to better reflect its interaction with the mediators as opposed to the cathode.

As stated previously, the cyclic voltammetry for the di-ethyl ester complexes was performed in dichloromethane as opposed to acetonitrile. While performing multiple cycles on all the complexes in acetonitrile, it was observed that over the first couple cycles of both the Co(4-eebpy) complex and the Co(5-eebpy) complex there appeared to be something like electrode conditioning which took place as shown for Co(5-eebpy) in figure 2.S6. This conditioning was not observed for the other complexes and it was also not observed when the same experiments were performed on glassy carbon. Since some disassociation of the more electron withdrawing ligands was observed after the addition of TBP, it is hypothesized that there is also a small amount of disassociation which can be attributed to the coordinating ability of acetonitrile. This newly free ligand can then interact with the gold working electrode in such a way as to condition it. Thus, cyclic voltammetry was performed in the less coordinating dichloromethane to minimize any contributions from the dissociation or free ligand. More detailed discussion about this experimental quirk has been provided above.

2.5 Conclusions

Prior literature shows few examples of cobalt tris-2,2'-bipyridine complexes with substitutions being used in the 5,5' positions as mediators for DSSCs.[10] The results presented herein suggest that further research may be warranted as the search for mediator complexes with higher positive redox potentials continues. It has been shown that the addition of ethyl ester substituents at the 5,5' positions of the bipyridine ligands of a cobalt tris-2,2'-bipyridine based complex leads to a high $E_{1/2}$ compared to most previously reported cobalt bipyridine based complexes. The 5,5' substituted complex shows a higher redox potential ($E_{1/2}$= 0.75 V vs. SCCE) then the 4,4' substituted analogue ($E_{1/2}$= 0.67 V vs. SCCE). Further, it was found that on gold cathodes, the charge transfer resistance for the Co(5-eebpy) complex was similar to charge transfer resistance values found for Co(5-dmb) suggesting that the effect

of added steric bulk of the ethyl ester substitution can be minimized by altering its position on the structure. There was an unexpected discovery however, that the effect of changing the position of the ethyl ester substituent is reversed when performing electrochemistry on the glassy carbon electrode. It is hypothesized that the electron transfer between the ethyl ester substituted complexes on glassy carbon occurs by an inner sphere charge transfer reaction. The Co(4-eebpy) is expected to more readily adsorb to the glassy carbon surface so it's charge transfer resistance is reduced compared to the Co(5-eebpy) complex. Further testing of these complexes on an expanded library of cathode materials is recommended for optimization before use in a completed sandwich cell.

Diffusion coefficients for Co(5-eebpy) were found to be faster in γ-butyrolactone (4.7×10^{-7} cm^2/s) compared with the complex having the same substitution at the 4,4' positions (3.9×10^{-7} cm^2/s). In acetonitrile, diffusion coefficients were found to be very similar. It is suspected that the higher viscosity of the γ-butyrolactone accentuated the differences between the observed diffusion coefficients. It was found that the diffusion coefficients of the ester substituted complexes were still slower in all solvents than those observed for the dimethyl and unsubstituted complexes.

As has been the case with other high potential cobalt bipyridine based mediator complexes, the long-term stability of the complex is questionable. There is no clear evidence to suggest the position of the substituents on the bipyridine has any effect on the stability of the complexes at this point as it seems the effect of the identity of the functional group trumps that of the position. It is hypothesized that one method for improving upon the stability of these complexes is by increasing the coordination number of the bipyridine ligands. The tridentate ligand synthesized by Yum and co-workers using a pyrazole substituted 'ortho' to the nitrogen was not reported to have any sign of instability when made into a coordination complex with cobalt even though very high open circuit voltages were reported.[19] While there is most certainly reason for further research into the use of 5,5' substituted cobalt bipyridine based complexes for DSSC redox mediators, there is also an importance to be placed on the

production of complexes which also will be able to maintain stability over the lifetime of a cell. Work is currently being performed to synthesize a hexadentate ligand consisting of these same ligands linked through their esters to promote stability while maintaining their high potential.

REFERENCES FOR CHAPTER 2

1. Kirner, J. T.; Elliott, C. M., Are High-Potential Cobalt Tris(bipyridyl) Complexes Sufficiently Stable to Be Efficient Mediators in Dye-Sensitized Solar Cells? Synthesis, Characterization, and Stability Tests. *The Journal of Physical Chemistry C* **2015,** *119* (31), 17502-17514.

2. Hagfeldt, A.; Boschloo, G.; Sun, L.; Kloo, L.; Pettersson, H., Dye-Sensitized Solar Cells. *Chemical Reviews* **2010,** *110* (11), 6595-6663.

3. Mathew, S.; Yella, A.; Gao, P.; Humphry-Baker, R.; CurchodBasile, F. E.; Ashari-Astani, N.; Tavernelli, I.; Rothlisberger, U.; NazeeruddinMd, K.; Grätzel, M., Dye-sensitized solar cells with 13% efficiency achieved through the molecular engineering of porphyrin sensitizers. *Nat Chem* **2014,** *6* (3), 242-247.

4. Kakiage, K.; Aoyama, Y.; Yano, T.; Oya, K.; Fujisawa, J.-i.; Hanaya, M., Highly-efficient dye-sensitized solar cells with collaborative sensitization by silyl-anchor and carboxy-anchor dyes. *Chemical Communications* **2015,** *51* (88), 15894-15897.

5. Tsao, H. N.; Burschka, J.; Yi, C.; Kessler, F.; Nazeeruddin, M. K.; Gratzel, M., Influence of the interfacial charge-transfer resistance at the counter electrode in dye-sensitized solar cells employing cobalt redox shuttles. *Energy & Environmental Science* **2011,** *4* (12), 4921-4924.

6. O'Regan, B.; Gratzel, M., A low-cost, high-efficiency solar cell based on dye-sensitized colloidal TiO2 films. *Nature* **1991,** *353* (6346), 737-740.

7. Liberatore, M.; Decker, F.; Burtone, L.; Zardetto, V.; Brown, T. M.; Reale, A.; Di Carlo, A., Using EIS for diagnosis of dye-sensitized solar cells performance. *Journal of Applied Electrochemistry* **2009,** *39* (11), 2291-2295.

8. Hamann, T. W., The end of iodide? Cobalt complex redox shuttles in DSSCs. *Dalton Transactions* **2012,** *41* (11), 3111-3115.

9. Nusbaumer, H.; Moser, J.-E.; Zakeeruddin, S. M.; Nazeeruddin, M. K.; Grätzel, M., CoII(dbbip)22+ Complex Rivals Tri-iodide/Iodide Redox Mediator in Dye-Sensitized Photovoltaic Cells. *The Journal of Physical Chemistry B* **2001,** *105* (43), 10461-10464.

10. Sapp, S. A.; Elliott, C. M.; Contado, C.; Caramori, S.; Bignozzi, C. A., Substituted Polypyridine Complexes of Cobalt(II/III) as Efficient Electron-Transfer Mediators in Dye-Sensitized Solar Cells. *Journal of the American Chemical Society* **2002,** *124* (37), 11215-11222.

11. Feldt, S. M.; Gibson, E. A.; Gabrielsson, E.; Sun, L.; Boschloo, G.; Hagfeldt, A., Design of Organic Dyes and Cobalt Polypyridine Redox Mediators for High-Efficiency Dye-Sensitized Solar Cells. *Journal of the American Chemical Society* **2010,** *132* (46), 16714-16724.

12. Klahr, B. M.; Hamann, T. W., Performance Enhancement and Limitations of Cobalt Bipyridyl Redox Shuttles in Dye-Sensitized Solar Cells. *The Journal of Physical Chemistry C* **2009,** *113* (31), 14040-14045.

13. Elliott, C. M.; Hershenhart, E. J., Electrochemical and spectral investigations of ring-substituted bipyridine complexes of ruthenium. *Journal of the American Chemical Society* **1982,** *104* (26), 7519-7526.

14. Gamba, I.; Salvadó, I.; Rama, G.; Bertazzon, M.; Sánchez, M. I.; Sánchez-Pedregal, V. M.; Martínez-Costas, J.; Brissos, R. F.; Gamez , P.; Mascareñas, J. L.; Vázquez López, M.; Vázquez, M. E., Custom-Fit Ruthenium(II) Metallopeptides: A New Twist to DNA Binding With Coordination Compounds. *Chemistry – A European Journal* **2013,** *19* (40), 13369-13375.

15. Tsierkezos, N. G.; Ritter, U., Electrochemical impedance spectroscopy and cyclic voltammetry of ferrocene in acetonitrile/acetone system. *Journal of Applied Electrochemistry* **2010,** *40* (2), 409-417.

16. Nazeeruddin, M. K.; Péchy, P.; Renouard, T.; Zakeeruddin, S. M.; Humphry-Baker, R.; Comte, P.; Liska, P.; Cevey, L.; Costa, E.; Shklover, V.; Spiccia, L.; Deacon, G. B.; Bignozzi, C. A.; Grätzel, M., Engineering of Efficient Panchromatic Sensitizers for Nanocrystalline TiO2-Based Solar Cells. *Journal of the American Chemical Society* **2001,** *123* (8), 1613-1624.

17. Grätzel, M., Recent Advances in Sensitized Mesoscopic Solar Cells. *Accounts of Chemical Research* **2009,** *42* (11), 1788-1798.

18. Hagberg, D. P.; Marinado, T.; Karlsson, K. M.; Nonomura, K.; Qin, P.; Boschloo, G.; Brinck, T.; Hagfeldt, A.; Sun, L., Tuning the HOMO and LUMO Energy Levels of Organic Chromophores for Dye Sensitized Solar Cells. *The Journal of Organic Chemistry* **2007,** *72* (25), 9550-9556.

19. Yum, J. H.; Baranoff, E.; Kessler, F.; Moehl, T.; Ahmad, S.; Bessho, T.; Marchioro, A.; Ghadiri, E.; Moser, J. E.; Yi, C.; Nazeeruddin, M. K.; Gratzel, M., A cobalt complex redox shuttle for dye-sensitized solar cells with high open-circuit potentials. *Nat Commun* **2012,** *3*, 631.

20. Tsao , H. N.; Yi , C.; Moehl, T.; Yum, J.-H.; Zakeeruddin, S. M.; Nazeeruddin, M. K.; Grätzel, M., Cyclopentadithiophene Bridged Donor–Acceptor Dyes Achieve High Power Conversion Efficiencies in Dye-Sensitized Solar Cells Based on the tris-Cobalt Bipyridine Redox Couple. *ChemSusChem* **2011,** *4* (5), 591-594.

21. Fabregat-Santiago, F.; Bisquert, J.; Garcia-Belmonte, G.; Boschloo, G.; Hagfeldt, A., Influence of electrolyte in transport and recombination in dye-sensitized solar cells studied by impedance spectroscopy. *Solar Energy Materials and Solar Cells* **2005,** *87* (1–4), 117-131.

22. Kavan, L.; Yum, J.-H.; Nazeeruddin, M. K.; Grätzel, M., Graphene Nanoplatelet Cathode for Co(III)/(II) Mediated Dye-Sensitized Solar Cells. *ACS Nano* **2011,** *5* (11), 9171-9178.

23. Ashbrook, L. N.; Elliott, C. M., Sulfide Modification of Dye-Sensitized Solar Cell Gold Cathodes for Use with Cobalt Polypyridyl Mediators. *The Journal of Physical Chemistry C* **2014,** *118* (30), 16643-16650.

24. Nelson, J. J.; Amick, T. J.; Elliott, C. M., Mass Transport of Polypyridyl Cobalt Complexes in Dye-Sensitized Solar Cells with Mesoporous TiO2 Photoanodes. *The Journal of Physical Chemistry C* **2008,** *112* (46), 18255-18263.

25. Aribia, K. B.; Moehl, T.; Zakeeruddin, S. M.; Gratzel, M., Tridentate cobalt complexes as alternative redox couples for high-efficiency dye-sensitized solar cells. *Chemical Science* **2013,** *4* (1), 454-459.

26. Feldt, S. M.; Lohse, P. W.; Kessler, F.; Nazeeruddin, M. K.; Gratzel, M.; Boschloo, G.; Hagfeldt, A., Regeneration and recombination kinetics in cobalt polypyridine based dye-sensitized solar cells, explained using Marcus theory. *Physical Chemistry Chemical Physics* **2013,** *15* (19), 7087-7097.

27. Tsao, H. N.; Comte, P.; Yi, C.; Grätzel, M., Avoiding Diffusion Limitations in Cobalt(III/II)-Tris(2,2'-Bipyridine)-Based Dye-Sensitized Solar Cells by Tuning the Mesoporous TiO2 Film Properties. *ChemPhysChem* **2012,** *13* (12), 2976-2981.

28. Liberatore, M.; Petrocco, A.; Caprioli, F.; La Mesa, C.; Decker, F.; Bignozzi, C. A., Mass transport and charge transfer rates for Co-(III)/Co-(II) redox couple in a thin-layer cell. *Electrochim. Acta* **2010,** *55* (12), 4025-4029.

29. Brisig, B.; Constable, E. C.; Housecroft, C. E., Metal-directed assembly of combinatorial libraries-principles and establishment of equilibrated libraries with oligopyridine ligands. *New Journal of Chemistry* **2007,** *31* (8), 1437-1447.

CHAPTER 3: SYNTHESIS OF HEXADENTATE TRIS-BIPYRIDINE LIGAND FOR IMPROVED STABILITY OF COBALT (II/III) TRIS-2,2'-BIPYRIDINE REDOX MEDIATORS

3.1 Introduction

Dye sensitized solar cells (DSSCs) as a competing photovoltaic technology fall short in two key areas which have thus far limited their utility in various applications. The first is the efficiency, which cannot yet match more ubiquitous technologies such as silicon photovoltaics. The second is related to concerns about the long-term stability of some of the device components. Much of the early research for DSSCs has focused on understanding the processes influencing the efficiency of devices without much concern about stability of devices outside of the laboratory.[1] Of the studies concerning stability which have been performed, many of them utilize the iodide/tri-iodide (I^-/I_3^-) redox mediator due to its literature precedence.[2, 3]

One means to improve the efficiency of DSSCs has turned out to be replacement of the historically omnipresent iodide/tri-iodide redox couple as a charge mediator. Iodide/tri-iodide, due to its negative redox potential compared to the ground state of the sensitizer, limits the open circuit voltage (V_{oc}) of the DSSC, which then limits the efficiency of the cell.[4] There is close to 700 mV of driving force between the redox potential of I^-/I_3^- and the ground state of the most commonly used dyes. This large amount of driving force promotes fast regeneration of the dye, which is necessary for a highly efficient DSSC. However, the open circuit voltage is determined by the difference in potential between the position of the conduction band of the titanium dioxide and the redox potential of the mediator couple. Therefore, in order in improve the V_{oc}, either the position of the conduction band must be shifted more negative or the redox potential of the mediator must be driven more positive. Some research has already been conducted modifying TiO_2 or using alternative photoanode materials to move

the conduction band more negative. [5-7] However, these approaches have never yielded efficiencies matching DSSCs resulting from the use of titanium dioxide in the anatase form.

For most commonly used sensitizers, there is in excess of 700 mV of overpotential between I^-/I_3^- and the ground state of the sensitizer that the oxidized tri-iodide is looking to regenerate.[3] Changing or modifying the mediator in order to drive the redox potential of the couple more positive is another tactic to improve the open circuit voltage. Since the publication of O'Regan and Gratzel's seminal work in 1991, a large variety of different redox mediators have been used in an attempt to improve upon the initial success of the I^-/I_3^- mediator.[8-10] Of those different mediators, cobalt coordination complexes, such as cobalt (II/III) tris-2,2'-bipyridine [$Co(bpy)^{2+/3+}$] and cobalt (II/III) bis-1,10-phenanthroline, are one of the only categories of mediators to outperform the best efficiencies from iodide/tri-iodide thus far.[11, 12] These mediators typically have redox potentials which are significantly more positive than I^-/I_3^- resulting in increased V_{oc}. However, these complexes have their own problems, which are currently being addressed.

One significant disadvantage compared to I^-/I_3^- is that the rate of recombination between the oxidized form of $Co(bpy)^{2+/3+}$ and the photoanode is much higher. Some modifications to components in DSSCs using $Co(bpy)^{2+/3+}$ are currently being studied and have led to significant improvements related to charge recombination. Additives such as *tert*-butylpyridine have been shown to improve the efficiencies of both I^-/I_3^- and $Co(bpy)^{2+/3+}$ through manipulation of the conduction band and by reducing rates of recombination.[13, 14] It has also been shown that synthetic modification of $Co(bpy)^{2+/3+}$ can reduce the rate of recombination through the addition of bulky alkyl groups to the 4,4' positions of the bipyridine ligands.[15, 16] Unlike coordination complexes, I^-/I_3^- has no prospect for synthetic modification, limiting its potential for improvement. The bulky alkyl additions to the bipyridine ligands result in a negative shift in the redox potential which reduces the attainable open circuit voltage as compared to $Co(bpy)^{2+/3+}$. Though it should be noted the redox potential of cobalt (II/III) tris-4,4'di-tert-butyl-2,2'-biypridine

[$Co(dtb)^{2+/3+}$] is still more positive than the iodide/tri-iodide couple. Synthetic modification of coordination complexes can also be utilized in order to target more positive redox potentials. The addition of functional groups which are more electron withdrawing in nature has been shown to drive the redox potential more positive relative to the unmodified $Co(bpy)^{2+/3+}$ mediator.[15, 17]

The case of synthetically modifying $Co(bpy)^{2+/3+}$ to drive its potential more positive and increase the attainable open circuit voltage has been shown to decrease the long-term stability of the complexes.[17, 18] This was shown first by Kirner and co-workers who noted that the cause of the instability of these complexes was likely the addition of electron withdrawing groups, which could make the ligands more labile, thereby allowing additives such as *tert*-butylpyridine to compete for coordination with the cobalt metal center.[17] In chapter 2, I demonstrated that the use of other substitution positions besides the positions 'para' to the nitrogen on bipyridine could further shift the redox potential of the resulting complexes. However, no clear trend could be established as to whether the movement of those substitutions could also improve the stability of the complexes.

One approach that could show promise towards improving the stability of these complexes over time would be to make increased use of the chelating effect when designing new ligands. Increasing the denticity of the ligands attached to the complex should theoretically improve the stability of the complex, as it will be more difficult for ligands to spatially separate themselves from the metal center. Yum and co-workers synthesized a complex with a highly positive redox potential by synthetically modifying 2,2'-bipyridine to include a pyrazole functional group at the 6-position.[19] The added pyrazole can also coordinate to the metal center making the ligand tridentate; which should improve the stability relative to similarly high potential but bidentate bipyridine based coordination complexes. The study clarifies that stability studies are ongoing but makes no mention of any initial anecdotal evidence about lowered stability of their assembled complex which is shown below in figure 3.1. Another approach to increasing the denticity of the resulting mediator complexes is to link together 3 bipyridines using a

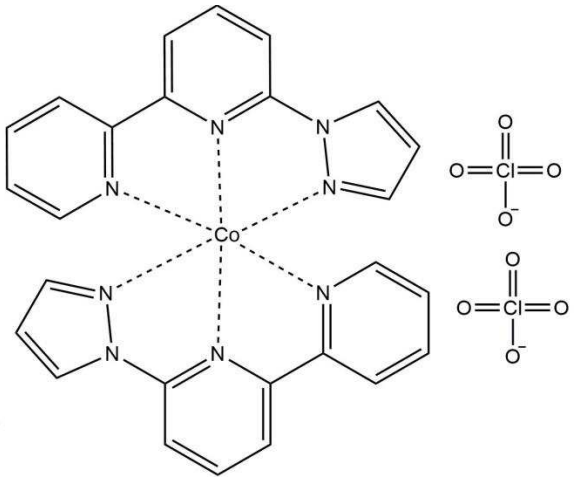

Figure 3.1: Pyrazole substituted cobalt (II) bipyridine based redox mediator for DSSCs. It was synthesized by Yum and co-workers in order to obtain high open circuit voltage.

single linker moiety. For use in DSSCs, there is currently only one reported case in the literature where this type of methodology is utilized. Freitag and co-workers reported the synthesis and subsequent use of the compound shown in figure 3.2. In this case, the addition of the linker led to a negative shift of the redox potential due to being more donating in nature. In DSSCs assembled using that novel mediator complex, efficiency was slightly lower relative to cells tested using unmodified $Co(bpy)^{2+/3+}$. As expected, the observed current for the linked complex was lower than for $Co(bpy)^{2+/3+}$ due to a slower diffusion coefficient of the mediator through the electrolyte. More surprisingly, the open circuit voltage for both complexes was nearly the same suggesting the presence of another factor helping to determine the open circuit voltage since the redox potential of the linked complex is 100 mV more negative than $Co(bpy)^{2+/3+}$. While it was shown that the stability was significantly improved, there could be added benefit in the generation of similar structures with electron withdrawing groups incorporated into the structure to provide higher redox potentials and ideally higher open circuit voltages.

As just mentioned, another disadvantage to coordination complex type mediators like $Co(bpy)^{2+/3+}$ is actually exacerbated in these synthetically modified complexes. The slower diffusion coefficient of the redox mediator through the liquid electrolyte relative to I^-/I_3^- reduces the observed

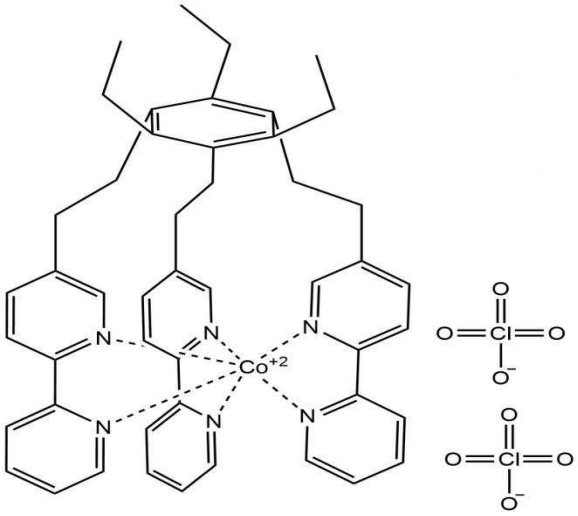

Figure 3.2: Tris-2,2'-bipyridine cobalt (II) complex linked by a substituted phenyl ring. It was synthesized by Freitag and co-workers in order to improve long term mediator stability in DSSCs.

current for assembled DSSCs. It was shown by Nelson and co-workers that when using large coordination complexes such as $Co(dtb)^{2+/3+}$, there is a substantial difference between the peak attainable current when the DSSC is first exposed to light and the steady state current during device function. This is based on mass transport limitations both through bulk solution and through the pore structure of the photoanode. The especially slow diffusion coefficient within the mesoporous film (shown to be up to 6 times slower depending on pore size) can be alleviated somewhat through careful tailoring of the porosity of the film but there is little that can be done about the slower diffusion through the bulk solution.[20] It was found that the larger the substituents used were, the slower the subsequent diffusion coefficient was.[18] Interestingly, it was found that the position of substituents was also a factor in how slow the diffusion coefficient was. This is instead of being solely determined by the size of the substituents.[18] It was found that diffusion was faster for substituents at the 5,5' positions when ethyl ester functional groups were used as substituents compared to the analogous complexes with substitutions at the 4,4' positions.

Herein, the synthesis of a high potential, bipyridine based hexadentate cobalt redox mediator was attempted. The ligand and proposed complex are shown below in figure 3.3. The synthesis was

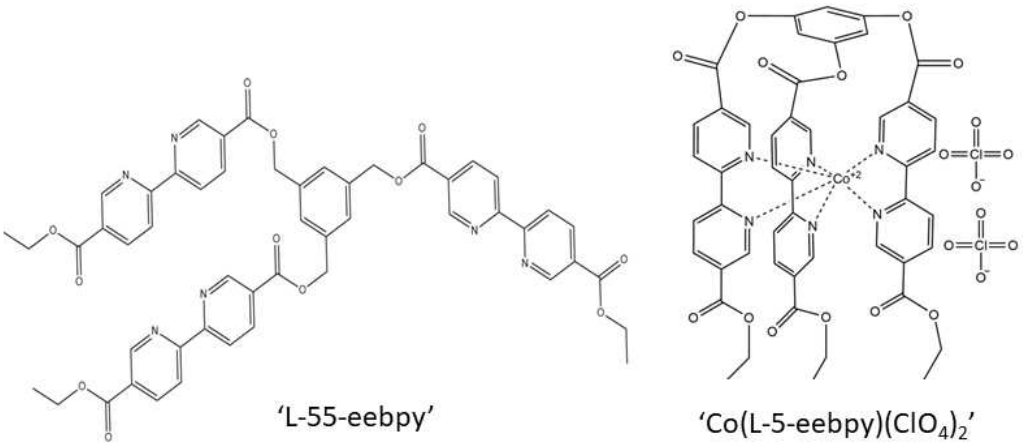

Figure 3.3: The proposed ligand and cobalt (II) complex to be synthesized. Compared to other structures, the ethyl ester moieties yield higher redox potentials than electron donating type groups.

ultimately not completed, as connecting the modified bipyridines via esterification proved to be more difficult synthetically than anticipated. The synthetic scheme as it was performed is shown below in figure 3.4 with the uncompleted reaction step shown in red. Products were characterized by ^{1}H-NMR and mass spectrometry, though for some products melting point could be used for swifter determination of known products. It is hypothesized that the failure in the final step of the scheme is in part caused by steric blocking of the third bipyridine slowing the reaction with the linker. Another possibility is that an unknown side reaction is prematurely using up one of the starting materials. Evidence is shown herein to suggest that this ligand can be synthesized but there must be further optimization of the reaction conditions in order to maximize yield of the completed product. Specifically, the use of higher boiling point solvents to increase reaction temperature may promote a faster rate of reaction with the third bipyridine. Also the use of a larger excess of the 5-ethyl ester-5'-acyl chloride-2,2'-bipyridine reagent may promote higher yields of the desired product and minimize the influence of an unknown side reaction.

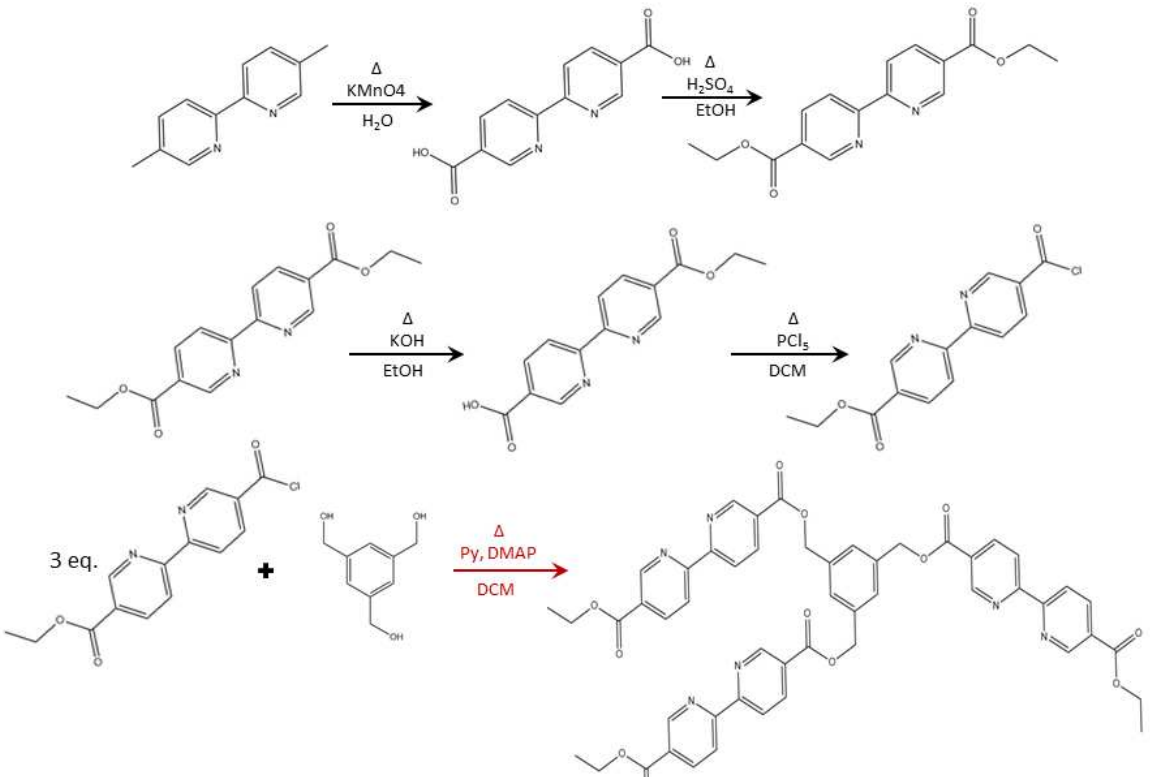

Figure 3.4: Synthetic scheme used for the synthesis of the ligand L-55-eebpy. The reaction step shown in red is indicative of the reaction not yet yielding the formation of isolatable product. Further details about each reaction step are included in the experimental section.

3.2 Experimental

Materials used

The following chemicals were used as received and are ACS grade unless otherwise noted: absolute ethanol (Pharmco-Aaper), dichloromethane (Sigma-Aldrich, reagent grade), tetrahydrofuran (EMD Millipore), potassium permanganate (Fisher Scientific), sulfuric acid (Acros Organic, reagent grade), potassium hydroxide (Fisher Scientific), phosphorus pentachloride (EMD Millipore, 99.0 %), 1,3,5-benzenetrimethanol (Synthonix, 95.0+ %), pyridine (Fisher Scientific), 4-dimethylaminopyridine (Oakwood Chemical), sodium chloride (Fisher Scientific), and distilled water purified by reverse osmosis and acquired from a department-owned tap. ^{1}H-NMR spectroscopy was performed using solvents acquired from Cambridge Isotope Laboratories. Deuterated dichloromethane, methanol, water, and dimethyl sulfoxide were all of 99.8 % purity.

Synthesis of 5,5'-di-carboxylic acid-2,2'-bipyridine (5-dcb)

5,5'-di-methyl-2,2'-bipyridine (5-dmb) was prepared previously according to the literature.[21] To a 500 mL round-bottom flask, 7.05 g of 5-dmb was suspended in 250 mL of distilled water with 39 g of potassium permanganate. This mixture was refluxed for 3 hours, during which time the pink solution, from the potassium permanganate transitioned to a clear solution with a black solid suspended within the water. The solution was allowed to cool to room temperature before being filtered to remove the black manganese dioxide. The solution was then acidified using concentrated sulfuric acid resulting in a flocculent white product precipitating out of solution. The product was removed from the water by filtration and dried in a vacuum oven at 60 °C overnight. ^{1}H-NMR spectroscopy was performed in D_2O with a small amount of homemade NaOD in order to characterize the compound. Percent yield and characterization data are provided in table 3.1 as shown below.

Synthesis of 5,5'-di-ethyl ester-2,2'-bipyridine(5-eebpy)

To a 250 mL round bottom flask, 3.00 g of 5,5'-dicarboxylic acid-2,2'-bipyridine (5-dcb) was suspended in 85 mL of absolute ethanol (EtOH). ~5 mL of concentrated sulfuric acid was added and the solution was refluxed for 36 hours during which time the suspended white solid slowly dissolved into the solution leaving a clear if very slightly yellowed solution. The solution was allowed to cool to room temperature and was reduced in volume by ~80 % by rotary evaporation. After the reduction in volume, ~120 mL of distilled water was added, crashing out the white product. The product was filtered and allowed to dry overnight on the benchtop. The next day, the product was dissolved in absolute ethanol and recrystallized to form a colorless to white needle-like crystals which were characterized by mass spectrometry, melting point, and ^{1}H-NMR after being dissolved in deuterated ethanol.

Synthesis of 5-carboxylic acid-5'-ethyl ester-2,2'-bipyridine (55-CEB)

To a 250 mL 3-neck round bottom flask, 1.50 g of 5,5'-ethyl ester-2,2'-bipyridine (5-eebpy) was dissolved in 75.0 mL of absolute ethanol. Separately, a solution of 0.35 g of potassium hydroxide was

prepared with 25.0 mL of additional absolute ethanol. After the 5-eebpy was dissolved and the reaction had reached reflux temperatures, the potassium hydroxide solution was slowly added by addition funnel over a 10 minute period of time. As the solution was added, the solution slowly became cloudy with a white precipitate. After the addition was complete, the solution was refluxed for an additional 6 hours to ensure complete formation of the product. After the reaction flask was allowed to come to room temperature, the white precipitate was removed from the solution by filtration. The white solid was dried for 3 hours at room temperature before being re-dissolved in distilled water. The solution was acidified using sulfuric acid allowing the final product to precipitate from the solution as another white solid. This product was filtered and dried in the vacuum oven at 60 °C overnight. The product was characterized by mass spectrometry and ^{1}H-NMR after being dissolved in deuterated dimethyl sulfoxide.

Synthesis of 5-acyl chloride-5'-ethyl ester-2,2'-bipyridine (55-AEB)

To a 250 mL round-bottom flask, 0.50 g of 5-carboxylic acid-5'-ethyl ester-2,2'-bipyridine was suspended in 100 mL of dichloromethane (DCM). An excess of phosphorus pentachloride (0.45 g) was added to the flask before being brought up to reflux temperatures. The solution was refluxed for 3 hours, during which time the solid slowly dissolved into the solution leaving a slightly yellowed but clear solution when the reaction was complete. After completion, the reaction was allowed to come back to room temperature and then chilled in a freezer for half an hour. The solution was worked up in a 125 mL separatory funnel with 2 additions of 40 mL of 1.0 M sodium hydroxide solution and 1 addition of 50 mL of 2.0 M sodium chloride solution. After the dichloromethane was separated, 4A molecular sieves were added to remove any remaining water. The dichloromethane was removed by rotary evaporation and the product was kept in the freezer until use. The ^{1}H-NMR was found to be no different then 55-ceb but the combination of its ^{1}H-NMR matching 55-ceb and its solubility in dichloromethane was considered evidence for its identity.

Synthesis of linked compound

Prior to the reaction, dichloromethane and pyridine were both allowed to sit on 4A molecular sieves for a minimum of 20 minutes. To a 250 mL three-necked round-bottom flask was added 1.2 g of the 5-acyl chloride-5'-ethyl ester-2,2'-bipyridine (55-AEB) after being dissolved in 100 mL of dichloromethane. A separate solution was prepared in 30 mL of dichloromethane with 0.217 g of 1,3,5-benzenetrimethanol, 0.025 g 4-dimethylaminopyridine (DMAP), and 2.0 mL of pyridine to act as a proton acceptor. After the first solution was brought to reflux temperatures in the three-necked round bottom flask, the second solution was slowly added by addition funnel over the course of 15 minutes. After the addition, the solution was refluxed for 36 hours and did not undergo any specific changes visibly during that time. After 36 hours, the heat was removed and the reaction was allowed to fall back to room temperature. The reaction was worked up by separatory funnel through consecutive additions of 50 mL of 1.0 M sulfuric acid and 50 mL of 1.0 M potassium hydroxide. The dichloromethane was then removed by rotary evaporation leaving a solid white residue. The residue was characterized by mass spectrometry and ^{1}H-NMR after being dissolved in deuterated acetonitrile.

Characterization of synthesized compounds

Synthesized compounds were all characterized by ^{1}H-NMR spectroscopy, which was performed on an Agilent Innova 300 MHz spectrometer, and mass spectrometry was performed on an Agilent G6220A TOF LC/MS using ESI/APCI ionization mode and positive ion mode. For earlier reaction steps, some products identities could be confirmed more quickly using a Mel-Temp II melting point apparatus from Laboratory Devices Incorporated. Characterization data and percent yields for the synthesized compounds are provided in table 3.1.

Table 3.1: Percent yield and 1H-NMR data for starting materials and products for various reaction steps for the scheme shown in figure 3.4. No percent yield was included for 5-dmb because it was synthesized previously and re-characterized before use. No yield was included for L-55-eebpy because it has not yet been isolated. The ^{1}H-NMR spectra for L-55-eebpy is considered crude product with some side products present, therefore instead of the number of protons, the integration intensity relative to the peak at 8.57 ppm is used. This was the peak that was used to normalize the integration in other steps as well. *The peak at 4.74 is the only peak which the side products linked-1 and linked-2 have that L-55-eebpy does not have.

Starting material/Product	Percent yield (%)	^{1}H-NMR (measured) [ppm (mult, #, group)]
5-dmb	N/A	2.12 (s, 6H, CH_3), 7.57 (d, 2H, CH), 8.20 (d, 2H, CH), 8.43 (s, 2H, CH)
5-dcb	83	7.98 (d, 2H, CH), 8.23 (d, 2H, CH), 8.92 (s, 2H, CH)
5-eebpy	73	1.44 (t, 6H, CH3), 4.42 (q, 4H, CH2), 8.45 (d, 2H, CH), 8.63 (d, 2H, CH), 9.30 (s, 2H, CH)
55-ceb	71	1.33 (t, 3H, CH3), 4.35 (q, 2H, CH2), 8.38 (dd, 2H, CH), 8.50 (dd, 2H, CH), 9.14 (dd, 2H, CH)
55-aeb	85	1.33 (t, 3H, CH3), 4.35 (q, 2H, CH2), 8.38 (dd, 2H, CH), 8.50 (dd, 2H, CH), 9.14 (dd, 2H, CH)
L-55-eebpy	N/A (inc.)	1.41 (t, 10.79, CH3),3.40 (s, 2.24, unk), 4.40 (q, 7.15, CH2), 4.74 (s, 2.44 , CH2*), 5.45 (s, 5.69, CH2), 7.49 (d, 3.78, CH), 8.42 (dd, 6.36, CH), 8.57 (t, 6.00, CH), 9.26 (dd, 4.83, CH)

3.3 Results and discussion

Synthesis of the ligand

The reaction steps as they were performed are shown in the synthetic scheme in figure 3.4. In table 3.1, the percent yield of all of the completed steps of the synthesis was calculated to be at least 70 %. The final step of the synthesis involved the reaction of 3 equivalents (3.1 equivalents were used for a slight excess) of 55-AEB with 1.0 equivalent of 1,3,5-benzenetrimethanol. Results found by ^{1}H-NMR provided evidence that the desired product may have been synthesized. However the most likely side products are either regenerated 55-CEB or the partially linked compounds which are either monosubstituted or disubstituted. This makes it difficult to differentiate between the product and either of the likely side-products. Those likely side products are shown in figure 3.5, which are not

reactants in a different step, are denoted as the disubstituted and monosubstituted species for the sake of simplicity.

In order to more conclusively characterize the products, a mass spectrum was taken of the recovered white residue. The mass/charge peak locations and intensities for identified peaks are summarized in table 3.2. The most intense peak, at 677.2246 m/z corresponds to the protonated ion of the side product, linked-2. Thankfully, there is also a small peak at 931.2938 m/z which corresponds to the protonated ion of the desired linked product. But the intensity is more than 40 times less than linked-2. It is possible that this difference in intensity is a result of selective fragmentation of the desired product, however inconsistencies in the 1H-NMR do suggest that at least some of the disubstituted species is present. This suggests that for some reason the reaction was unable to reach completion during the time period of 36 hours.

One hypothesis for the reaction's inability to reach to completion is that the acyl chloride species, 55-aeb, was prematurely consumed by a side reaction. The mass spectrum revealed an unexpected result in support of this hypothesis. The mass peak at 301.1182 m/z matches to the 5-eebpy molecule, which was a starting material and product earlier in the synthesis. The intensity of this peak was actually 10 times higher than the desired product. Given the work-up procedures and

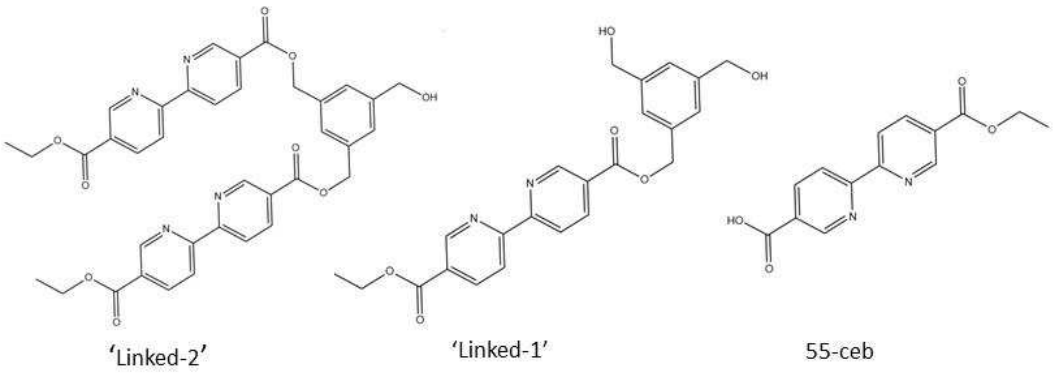

Figure 3.5: Expected side products as a result of final synthetic step. 55-ceb is soluble in basic water so (almost) any present was removed during work-up. The monosubstituted and disubstituted species ('linked-1' and 'linked-2') were both found in the mass spectrum and summarized in table 3.2.

Table 3.2: Summarized data from mass spectrometry experiments performed on crude product resulting from final synthetic step in DCM. Only peaks which could be identified as related to the desired product were included.

Identity	Calculated m/z	Experimental m/z (for H+ ion)	Peak intensity
L-55-eebpy	930.29	931.2938	7912.3
disubstituted	676.22	677.2246	359142.5
monosubstituted	422.15	423.154	6332.5
55-ceb	272.08	273.0882	604.2
5-eebpy	300.31	301.1182	76932

characterization performed in all of the reaction steps between this step and the synthesis of 5-eebpy, it is exceedingly unlikely to be a contaminant. The presence of this peak in multiple synthesis attempts suggests there is some as yet unknown rearrangement occurring amongst the substituted bipyridines to generate this species. If some of the active acyl chloride species was being deactivated through the formation of 5-eebpy, that would reduce the amount available to react and form the desired product. If this hypothesis turned out to be a primary cause for the preferred generation of the disubstituted species, there is the possibility that the creation of the product could be promoted by using larger excesses of 55-aeb. Without other means to increase the rate of formation for the desired product, it is also likely that a higher excess of the 55-aeb pre-cursor will just lead to more side product.

The other hypothesis to explain the preferred generation of the disubstituted product over the desired product is that the addition of the final bipyridine may be somewhat sterically hindered relative to the addition of the first two. The presence of the product, even in a small amount means that its synthesis is possible. The low reflux temperature of dichloromethane may have led to the exacerbation of the steric complications of the reaction. This hypothesis is considered to be the sole determining factor due to the success of Freitag and co-workers in synthesizing their complex using a reasonably analogous linker moiety.[22] It is thought that the use of a higher boiling point solvent, a larger excess of the acyl chloride reactant, and longer reaction times should eventually form high yields of the product if this hypothesis is contributing somewhat to the observed results.

Suggested procedural improvements

At this point it seems likely that the synthesis of this ligand is entirely possible. However, the optimized reaction conditions and work-up procedure for obtaining reasonable yields of isolated product have as yet proved to be difficult to find. Analysis of the mass spectrum indicates that the reaction as it has been performed cannot reach completion over the course of 36 hours. Future synthetic attempts should utilize higher-boiling point solvents such as tetrahydrofuran to increase the reflux temperature of the reaction. Allowing the reaction to proceed at a higher temperature could both increase the reaction rate for the addition of 55-aeb to the 1,3,5-benzenetrimethanol linker and possibly allow for sufficient molecular movement to reduce the effect of inconvenient steric interactions.

Another possibility may also be to treat the final step of the synthetic scheme as a 2-step reaction. It has already been shown that the disubstituted product can be generated readily given the procedure, which was already used. If that compound could be isolated, it may be possible to use the same reagents on the disubstituted product. In the presence of 'fresh' 55-aeb, the addition of the final bipyridine will possibly proceed more smoothly. This method may either be used separately or in combination with an initial larger excess of 55-aeb. The primary reason for using a second reaction step is to reduce the effect of the unknown side reaction which seems to be generating 5-eebpy. Relying on an increased excess of the acyl chloride species may increase the rate of the side reaction instead of increasing the rate of formation for the desired product.

The work-up involving the addition of both base and acid does a good job of removing both pyridine and DMAP as these were not detected in the mass spectrum or in the ^{1}H-NMR spectra. The base should also remove any 55-ceb generated over the course of performing the reaction. Thus far attempts to isolate either the small quantity of the desired product or the side products like linked-2 have proven unsuccessful. Separation of the desired product from the monosubstituted and

disubstituted species via re-crystallization has proven difficult because of their similar solubilities. A good solvent formulation has also not been found that provides clean separation via column chromatography. However, it is hoped that if the yield of the desired product can be increased, the isolation of the product should become more straight forward as well. The presence of the remaining alcohol on the side products could force them to adhere more strongly to the column in the correct mixture of polar solvents.

Hypothesized complex properties

The performance of the mediator synthesized by Freitag allows for some loose extrapolations towards the properties the completed complex may have.[22] It was found that properties such as the diffusion coefficient and redox potential for their synthesized complex was reasonably similar to $Co(bpy)^{2+/3+}$. There was a 100 mV shift negative in the redox potential of the couple as expected from the addition of the electron donating linker to the otherwise unmodified bipyridine ligand. In the case of the proposed complex in this study, the electron withdrawing character is spatially closer to the nitrogen coordinating to the metal center as shown in figure 3.3. This makes the electron withdrawing character more influential to the redox potential of the couple, suggesting there is likely to be a more positive shift in the redox potential relative to the study by Freitag.[22] The electron withdrawing character is also likely to somewhat reduce the stability of the resulting complex, but the hope is that the hexadentate nature of the ligand will lead to an overall improvement of the stability.

The diffusion coefficient was slightly lower after the ligands were adjoined, compared to the unsubstituted complex.[22] It is likely that the same would happen for the linked complex in this case relative to the analogous unlinked complex. It was shown previously that the diffusion coefficient of cobalt (II/III) tris-5,5'-ethyl ester-2,2'-bipyridine [$Co(5\text{-}eebpy)^{2+/3+}$] was significantly slower compared to $Co(bpy)^{2+/3+}$.[18] Thus, even a small change in the diffusion coefficient is likely to have noteworthy effects on the short-circuit current of the assembled DSSC.

3.4 Conclusions

There have been positive results to suggest the synthesis of this hexadentate and electron-withdrawing substituted complex is absolutely possible and simply requires the optimization of the current reaction conditions in order to be successful. To that effect several hypotheses have been made as to the most likely methods for improving the performance of the final step in the synthesis of the ligand. The results provided by mass spectrometry suggest that there is a small amount of product formed, but that the major product formed is the partially reacted disubstituted product. This is hypothesized to be a result two different factors. The first is that the starting material, 55-aeb, might be decomposing via an unknown mechanism to 5-eebpy. The other is there may be some steric influence restricting the addition of the final modified bipyridine. In order to promote the generation of larger amounts of the product within a 24-48 hour time period, it is recommended that a higher boiling point solvent such as THF be utilized. It is also recommended that a second addition of 55-aeb is performed approximately 24 hours after the beginning of the reaction. A second addition is made instead of beginning with a larger excess of 55-aeb initially to avoid the further conversion of starting material to 5-eebpy. It is unclear at this point by what mechanism 5-eebpy is formed, but it was observed by both ^{1}H-NMR and mass spectrometry as a side product of the reaction.

The use of a hexadentate ligand formed by the linking of 3 bipyridines for improved stability of metal complexes has been performed in the literature before, however there is very little precedent for their use in DSSCs.[23] Currently, the only other report found was from Freitag and co-workers creating a complex which was actually more electron donating in nature.[22] The use of electron withdrawing groups to link the bipyridines should conceivably lead to greater open circuit voltage. However, complications due to even slower diffusion of the complexes tailoring of other components have been shown to somewhat reduce the influence of the mediator diffusion coefficient.

REFERENCES FOR CHAPTER 3

1. Sauvage, F., A Review on Current Status of Stability and Knowledge on Liquid Electrolyte-Based Dye-Sensitized Solar Cells. *Advances in Chemistry* **2014,** *2014*, 23.

2. Hagfeldt, A.; Boschloo, G.; Sun, L.; Kloo, L.; Pettersson, H., Dye-Sensitized Solar Cells. *Chemical Reviews* **2010,** *110* (11), 6595-6663.

3. Boschloo, G.; Hagfeldt, A., Characteristics of the Iodide/Triiodide Redox Mediator in Dye-Sensitized Solar Cells. *Accounts of Chemical Research* **2009,** *42* (11), 1819-1826.

4. Hamann, T. W., The end of iodide? Cobalt complex redox shuttles in DSSCs. *Dalton Transactions* **2012,** *41* (11), 3111-3115.

5. Burnside, S.; Moser, J.-E.; Brooks, K.; Grätzel, M.; Cahen, D., Nanocrystalline Mesoporous Strontium Titanate as Photoelectrode Material for Photosensitized Solar Devices: Increasing Photovoltage through Flatband Potential Engineering. *The Journal of Physical Chemistry B* **1999,** *103* (43), 9328-9332.

6. Latini, A.; Cavallo, C.; Aldibaja, F. K.; Gozzi, D.; Carta, D.; Corrias, A.; Lazzarini, L.; Salviati, G., Efficiency Improvement of DSSC Photoanode by Scandium Doping of Mesoporous Titania Beads. *The Journal of Physical Chemistry C* **2013,** *117* (48), 25276-25289.

7. Lee, C.-P.; Chen, P.-W.; Li, C.-T.; Huang, Y.-J.; Li, S.-R.; Chang, L.-Y.; Chen, P.-Y.; Lin, L.-Y.; Vittal, R.; Sun, S.-S.; Lin, J.-J.; Ho, K.-C., ZnO double layer film with a novel organic sensitizer as an efficient photoelectrode for dye–sensitized solar cells. *Journal of Power Sources* **2016,** *325*, 209-219.

8. O'Regan, B.; Gratzel, M., A low-cost, high-efficiency solar cell based on dye-sensitized colloidal TiO2 films. *Nature* **1991,** *353* (6346), 737-740.

9. Daeneke, T.; Kwon, T.-H.; Holmes, A. B.; Duffy, N. W.; Bach, U.; Spiccia, L., High-efficiency dye-sensitized solar cells with ferrocene-based electrolytes. *Nat Chem* **2011,** *3* (3), 211-215.

10. Lin, R. Y.-Y.; Chu, T.-C.; Chen, P.-W.; Ni, J.-S.; Shih, P.-C.; Chen, Y.-C.; Ho, K.-C.; Lin, J. T., Phenothiazinedioxide-Conjugated Sensitizers and a Dual-TEMPO/Iodide Redox Mediator for Dye-Sensitized Solar Cells. *ChemSusChem* **2014,** *7* (8), 2221-2229.

11. Mathew, S.; Yella, A.; Gao, P.; Humphry-Baker, R.; CurchodBasile, F. E.; Ashari-Astani, N.; Tavernelli, I.; Rothlisberger, U.; NazeeruddinMd, K.; Grätzel, M., Dye-sensitized solar cells with 13% efficiency achieved through the molecular engineering of porphyrin sensitizers. *Nat Chem* **2014,** *6* (3), 242-247.

12. Kakiage, K.; Aoyama, Y.; Yano, T.; Oya, K.; Fujisawa, J.-i.; Hanaya, M., Highly-efficient dye-sensitized solar cells with collaborative sensitization by silyl-anchor and carboxy-anchor dyes. *Chemical Communications* **2015,** *51* (88), 15894-15897.

13. Koh, T. M.; Nonomura, K.; Mathews, N.; Hagfeldt, A.; Grätzel, M.; Mhaisalkar, S. G.; Grimsdale, A. C., Influence of 4-tert-Butylpyridine in DSCs with CoII/III Redox Mediator. *The Journal of Physical Chemistry C* **2013,** *117* (30), 15515-15522.

14. Boschloo, G.; Häggman, L.; Hagfeldt, A., Quantification of the Effect of 4-tert-Butylpyridine Addition to I-/I3- Redox Electrolytes in Dye-Sensitized Nanostructured TiO2 Solar Cells. *The Journal of Physical Chemistry B* **2006,** *110* (26), 13144-13150.

15. Sapp, S. A.; Elliott, C. M.; Contado, C.; Caramori, S.; Bignozzi, C. A., Substituted Polypyridine Complexes of Cobalt(II/III) as Efficient Electron-Transfer Mediators in Dye-Sensitized Solar Cells. *Journal of the American Chemical Society* **2002,** *124* (37), 11215-11222.

16. Feldt, S. M.; Wang, G.; Boschloo, G.; Hagfeldt, A., Effects of Driving Forces for Recombination and Regeneration on the Photovoltaic Performance of Dye-Sensitized Solar Cells using Cobalt Polypyridine Redox Couples. *The Journal of Physical Chemistry C* **2011,** *115* (43), 21500-21507.

17. Kirner, J. T.; Elliott, C. M., Are High-Potential Cobalt Tris(bipyridyl) Complexes Sufficiently Stable to Be Efficient Mediators in Dye-Sensitized Solar Cells? Synthesis, Characterization, and Stability Tests. *The Journal of Physical Chemistry C* **2015,** *119* (31), 17502-17514.

18. Thomas, J. D., Prieto, Amy L., Elliott, C. Michael, Utilization of 5,5’ disubstituted tris-bipyridine cobalt complexes as high potential dye sensitized solar cell electrolyte mediators. *Journal of The Electrochemical Society* **In preparation**.

19. Yum, J. H.; Baranoff, E.; Kessler, F.; Moehl, T.; Ahmad, S.; Bessho, T.; Marchioro, A.; Ghadiri, E.; Moser, J. E.; Yi, C.; Nazeeruddin, M. K.; Gratzel, M., A cobalt complex redox shuttle for dye-sensitized solar cells with high open-circuit potentials. *Nat Commun* **2012,** *3*, 631.

20. Tsao, H. N.; Comte, P.; Yi, C.; Grätzel, M., Avoiding Diffusion Limitations in Cobalt(III/II)-Tris(2,2’-Bipyridine)-Based Dye-Sensitized Solar Cells by Tuning the Mesoporous TiO2 Film Properties. *ChemPhysChem* **2012,** *13* (12), 2976-2981.

21. Elliott, C. M.; Hershenhart, E. J., Electrochemical and spectral investigations of ring-substituted bipyridine complexes of ruthenium. *Journal of the American Chemical Society* **1982,** *104* (26), 7519-7526.

22. Freitag, M.; Yang, W.; Fredin, L. A.; D'Amario, L.; Karlsson, K. M.; Hagfeldt, A.; Boschloo, G., Supramolecular Hemicage Cobalt Mediators for Dye-Sensitized Solar Cells. *ChemPhysChem* **2016,** *17* (23), 3845-3852.

23. Grammenudi, S.; Franke, M.; Vögtle, F.; Steckhan, E., The rhodium complex of a tris(bipyridine) ligand—Its electrochemical behaviour and function as mediator for the regeneration of NADH from NAD+. *Journal of inclusion phenomena* **1987,** *5* (6), 695-707.

24. Chen, X.; Xu, D.; Qiu, L.; Li, S.; Zhang, W.; Yan, F., Imidazolium functionalized TEMPO/iodide hybrid redox couple for highly efficient dye-sensitized solar cells. *Journal of Materials Chemistry A* **2013,** *1* (31), 8759-8765.

CHAPTER 4: PASSIVATION OF THE PHOTOANODE USING A HOME-BUILT ATOMIC LAYER DEPOSITION APPARATUS

4.1 Introduction

In dye sensitized solar cells (DSSCs), the redox mediator could be the component which is of the most influence to the overall efficiency of the cell. The redox mediator transfers charge between the photoanode and the cathode as a part of the electrolyte. In the literature presently, the redox mediator is typically incorporated as part of a liquid phase electrolyte.[1] As part of the electrolyte and by definition electrochemically active in the range of potentials present in the device, the redox mediator is likely to interact with any other component in the DSSC. Changes in identity or concentration of the mediator can affect mass transport through the electrolyte, charge transfer rates at several interfaces in the cell, the open circuit voltage, and the ability of the sensitizer to absorb light. This is a 'double-edged sword' in that altering the mediator can provide substantial changes to the efficiency of the cell, but those changes can be either beneficial or detrimental. Modification of other components of the DSSCs with fewer possible interactions may allow for more controlled improvement with fewer unintended or undesired consequences.

Currently, cobalt coordination complexes as redox mediators provide the highest efficiencies for liquid electrolyte based DSSCs.[2-4] However, it is often suggested that high rates of recombination with the anode material limit the attainable efficiency relative to the historically used Iodide/tri-iodide (I^-/I_3^-) redox mediator.[5, 6] As a large coordination complex, it has also been shown that diffusion of the redox mediator can also limit the efficiency. Slow mass transport can be at least somewhat alleviated by manipulating the depth and porosity of the photoanode, typically a mesoporous TiO_2 film. On the other hand, a variety of methods have been examined in an attempt to reduce the rate of recombination.[7] In the past, the Elliott group has shown that synthetic modification of cobalt (II/III) tris-2,2'-bipyridine

($Co(bpy)^{2+/3+}$) by the addition of bulky alkyl groups can reduce the recombination between the mediator and the anode.[8] However, there is a further reduction in the diffusion coefficient of the complex resulting due to the increased size.

A contrasting approach for inhibiting charge transfer between the mediator and photoanode would be to modify the photoanode. This tactic has been examined previously through the addition of organic additives to the liquid electrolyte as well as the use of particularly bulky dyes to make the surface less accessible to the oxidized form of the mediator.[9, 10] In the case of additives, *tert*-butylpyridine is the most common and has been added with the understanding it adsorbs to the TiO_2 surface and is able to block some interaction between the surface and oxidized mediator. It has also been shown to have a similar effect on a gold electrode being used as a cathode.[11] Due to the fact that the additives are present in the electrolyte they may also interact with other components in the cell leading to undesirable interactions as well. It has been shown that *tert*-butylpyridine when added as an electrolyte additive can negatively affect $Co(bpy)^{2+/3+}$ type mediators.[12]

A third approach is direct modification of the photoanode before device assembly by means of the deposition of an ultra-thin layer of a non-conducting oxide. It is hypothesized this layer must be pinhole-free, at least to the point that it is impermeable to the oxidized form of the mediator, thus inhibiting charge transfer from the photoanode. A couple of deposition methods have already been utilized in order to apply this layer in the literature. The sol-gel method has been performed to some success.[13] It has been suggested the resulting layer is thicker than would be optimal and does not provide even coverage. The technique which offers the best mixture of uniform coverage and precise depth control is atomic layer deposition (ALD). ALD allows for the depth of the deposited film to be controlled to monolayer level precision. This level of control is possible due to the self-limiting reactions taking place at each step of the ALD process.

Unlike chemical vapor deposition where the precursors are added simultaneously, during ALD each of the precursors is added separately and the excess is completely purged before the next precursor is added. Each precursor is chosen such that it can readily react with the substrate surface but not with itself making the reaction self-limiting. Each of the steps will be described in detail below however they are also summarized in figure 4.1. Atomic layer deposition is a well-established technique where many precursors and reactions have been developed, but all references here will be to the reaction of trimethylaluminum and water vapor to form aluminum oxide (Al_2O_3).

For DSSCs, a mesoporous titanium dioxide film is used as the substrate. Trimethylaluminum (TMA) is added as the first precursor and is passed over the surface at low pressure with nitrogen as a carrier gas. Methane is released as the trimethylaluminum binds to the surface at hydroxide terminated sites. After excess TMA and methane as a byproduct are purged from the system, the second step

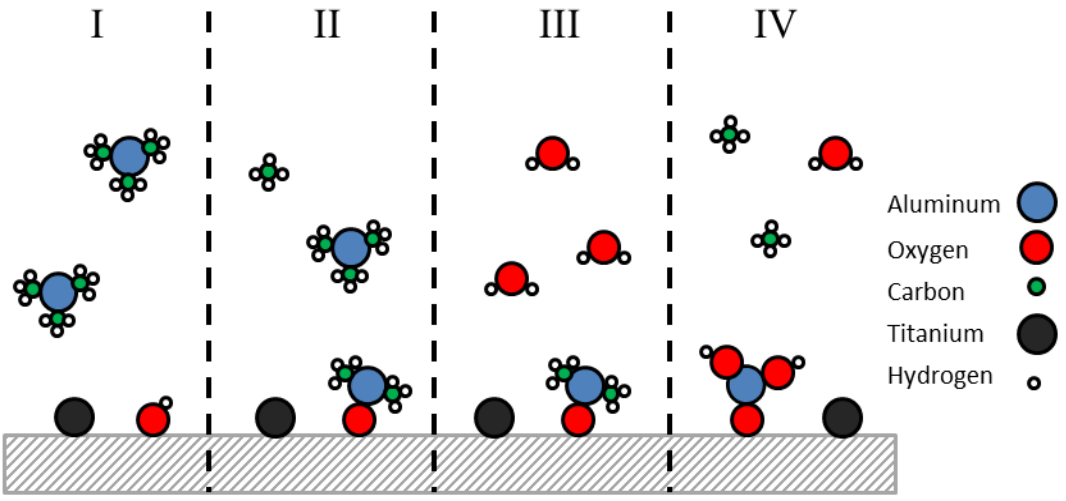

$$Al(CH_3)_3 + Ti - OH \rightarrow Ti - O - Al(CH_3)_2 + CH_4$$

Step I → Step II

$$2H_2O + Ti - O - Al(CH_3)_2 \rightarrow Ti - O - Al(OH)_2 + 2CH_4$$

Step III → Step IV

Figure 4.1: Diagram summarizing the 4 steps performed during each ALD cycle for the reaction of tri-methylaluminum and water with a titanium dioxide surface. The diagram specifically represents the pumping in of precursors and purging of excess reactants and products which are both controlled by the user. The reactions underneath represent the reactions occurring while each cycle is performed.

involves passing water vapor over the previously reacted surface. Two equivalents of methane are again evolved as a result of the removal of the remaining methyl groups in step IV of figure 4.1. This final step generates new hydroxyl sites on the surface of the substrate allowing for more cycles to be deposited. In the case of DSSCs, it has been shown that the greatest enhancement in the efficiency comes from performing just that first cycle.[14, 15]

It was shown by Klahr and co-workers that when using $Co(bpy)^{2+/3+}$ as a redox mediator, improvements to both the open circuit voltage (V_{oc}) and short circuit current (J_{sc}) were evident after a single cycle was performed to deposit Al_2O_3 onto the TiO_2 surface.[15] When more cycles were deposited after the first, the V_{oc} of the cell continued to increase but the J_{sc} began to decrease. It is suspected that the increase in V_{oc} and J_{sc} observed after the first cycle is due to a negative shift in the potential of the conduction band and decreased recombination from the oxidized mediator. The electron diffusion length is a measure of how far the injected electron can traverse the mesoporous film before recombining with either the oxidized dye or oxidized mediator. It is a related measurement to the electron lifetime and is indirectly correlated with the rate of recombination. It was shown using both cobalt based mediators and ferrocene based mediators that the electron diffusion length was increased given the ultra-thin alumina layer.[14, 15] In DSSCs using cobalt based mediators, such as $Co(bpy)^{2+/3+}$ and cobalt (III) tris-(4,4'-di-tert-butyl-2,2'-bipyridine) [$Co(dtb)^{2+/3+}$], injected electrons were shown to have lifetimes which were 6 times longer with alumina relative to without the layer.[15] Due to fast mass transport of the oxidized form away from the anode and lower rates of recombination to begin with, it was found that the ultra-thin alumina layer had no effect on the diffusion length of the iodide/tri-iodide redox mediator.

One of the downsides to atomic layer deposition as a technique is the low pressure and air-free environment that the highly reactive precursors require, meaning that the apparatus designed to perform the technique ends up being exceedingly expensive.[16] Commercial systems are able to deposit

materials for hundreds to thousands of cycles using a wide variety of pre-cursors with well controlled conditions that are easily programmed by the system. However, the requirements needed for improvement of the efficiency of DSSCs do not require nearly as many cycles as for other applications. Since the greatest improvement is achieved after only one cycle, the system requirements can be reduced relative to a commercial system. Thus, it may be possible to design a low-cost system specifically for the deposition of Al_2O_3 onto the mesoporous TiO_2 films for DSSCs. Other systems have already been designed as low cost alternatives to the commercial systems for other applications.[16, 17] Lubitz and co-workers estimated the cost of their reactor designs to be close to $10,000 which is an order of magnitude cheaper than is typical of the commercial systems.[16] The design which was used as a basis for the low-cost apparatus built and utilized here is shown in figure 4.2 and was adapted from the work performed by Elam and co-workers.[17]

After construction, the apparatus was used to coat mesoporous TiO_2 films used as anodes in DSSCs with alumina films of varying thickness. Deposition was also performed on silicon substrates as a

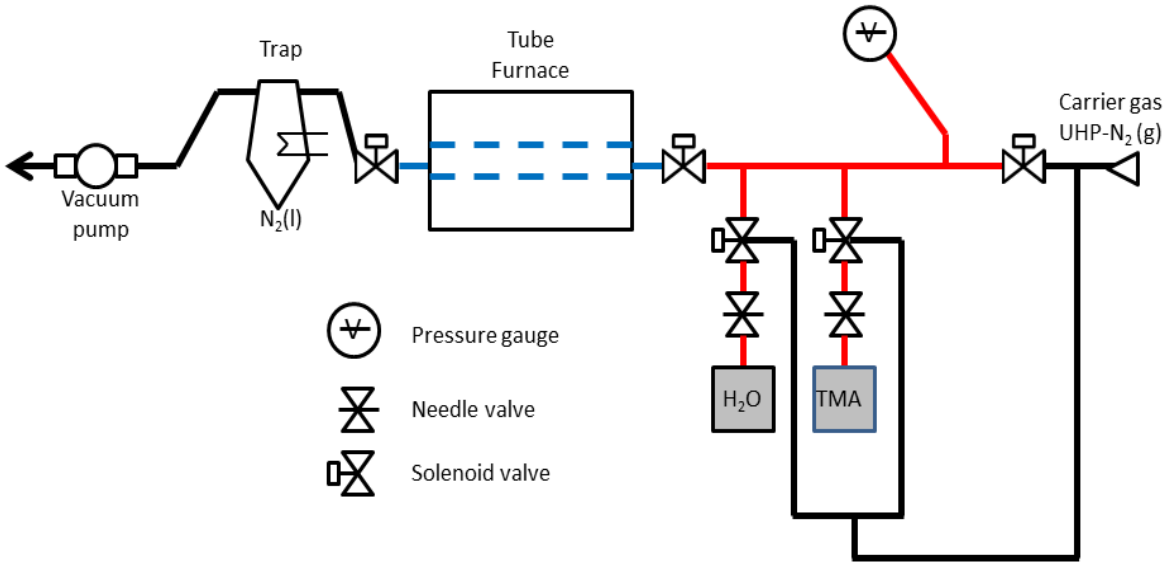

Figure 4.2: Schematic diagram of the as assembled atomic layer deposition apparatus. Lines in red indicate the material is stainless steel. Lines in blue indicate parts are made of glass. And lines in black indicate Tygon® tubing. Parts other than the flow line such as solenoid valves and the trap are all in black but are not made of Tygon® tubing.

means to characterize the deposition process on a more consistent and predictable surface. Films were prepared by cycling the apparatus between 1 and 200 times and characterized on both substrates by angle resolved x-ray photoelectron spectroscopy (XPS) and x-ray diffraction (XRD). The photoanodes, both modified and un-modified, were then used in assembled DSSCs with the cobalt based redox mediator, $Co(dtb)^{2+/3+}$, and the ruthenium based N3 [cis-dithiocyanatobis(2,2′-bipyridyl-4,4′-dicarboxylic acid)ruthenium(II)] sensitizer. The amount of dye adsorbed onto treated and untreated photoanodes was characterized by UV-Vis absorbance before the cells were assembled. Cells were characterized using current-voltage curves (JV curves) with and without light, voltage and current transient experiments, and incident photon to current efficiency (IPCE) measurements. JV curves allowed for evaluation of the V_{oc} and J_{sc} while the other measurement techniques were used to evaluate specific interactions between the photoanode and the redox mediator. It was observed that the V_{oc} did increase with the addition of the alumina layer to the photoanode, however the increase in J_{sc} could not be consistently reproduced the way it was observed in the literature. One reason for this might be inconsistency in the surface area of the photoanode films. However, it was also difficult to determine the presence of an individual monolayer of Al_2O_3 after 1 cycle was performed on the photoanode (as opposed to patchy growth or thicker growth). So other techniques which may be utilized if this project were to be re-visited are also considered throughout.

4.2 Experimental section

Materials used

Precursors used for the deposition of alumina were trimethylaluminum (Sigma-Aldrich, 97%) and high purity water from a Millipore system with ultra-high purity (99.999%) nitrogen from Airgas as the carrier gas. The sol-gel for the dense layer was synthesized using titanium isopropoxide (Strem, 98 %), absolute ethanol (Pharmco-Aaper, ACS grade), nitric acid (EMD, ACS grade), and deionized water. A commercial TiO_2 nanoparticle (T37) paste from Solaronix was used for the mesoporous layer. The

photoanodes were dyed from a solution of absolute ethanol with the ruthenium based sensitizer N3 which was synthesized from previously reported procedures.[18] The electrolyte solution used both cobalt (II) and cobalt (III) tris-(4,4'-di-tert-butyl-2,2'-bipyridine) perchlorate of which both the ligands and complexes were synthesized from previously reported procedures.[8] Also present in the electrolyte was lithium trifluoromethylsulfonate (Fluka, ≥99.0 %) and tert-butylpyridine (Sigma-Aldrich, 99%) γ-butyrolactone (Sigma-Aldrich, 99.0 %).

ALD apparatus construction

The design of the apparatus is shown in figure 4.2 and was adapted from the design of Elam and co-workers.[17] The vacuum was achieved through the use of a Welch Duo-seal 1402 vacuum pump and could reach a low-end pressure of approximately 10^{-3} torr while pulling on the system without flow of the carrier gas and was monitored by an incorporated Omega DVG64 digital vacuum gauge. Nitrogen was used as a carrier gas and was run through the system normalizing the pressure at approximately 1.0 torr. Swagelok SS-4BMG series bellows sealed metering valves were used to control the flow of each precursor gas to a partial pressure of 0.1 torr. Clippard Maximatic series solenoid valves were used to control the timing of pulses for each pre-cursor gas and to isolate the reaction chamber in later experiments. The solenoid valves were electronically controlled by a custom made BASIC Stamp board. The reactant delivery half of the apparatus is constructed of stainless steel while the reaction chamber itself is made of glass. The Lindberg 55035-DP tube furnace was controlled by an Omega CNi32 temperature and process controller attached to a K-type thermocouple set on the outside center of the reaction chamber.

ALD of Al_2O_3 films and characterization

The number of cycles deposited was varied between 0 and 200 cycles. Each cycle started with a purge by flowing the carrier gas through the system for 60 seconds. After that, trimethylaluminum was pulsed for 1-5 seconds as the first precursor. Following the pulse of the reactant gas, any methane

produced as a product or excess trimethylaluminum was purged for 60 seconds. Next, water vapor was pulsed for the same 1-5 seconds as the first precursor. As the final step, any methane or excess precursor was purged from the system for another 60 seconds. At that point, the next cycle would begin when all of the prior steps had been completed. The reactant pulses used here are much longer than those typically used in the literature. This is an attempt to ensure complete penetration of the reactants into the depths of the film. In later experiments, solenoid valves on either side of the reaction chamber were closed before the end of the pulse trapping the reactant gas in the chamber for up to 60 seconds. This was meant as a way to ensure the reactant gases had sufficient time to percolate through the mesoporous film. The ideal temperature for the reaction was previously determined in the literature to be 177 °C so depositions were typically run between 170-180 °C with some small variation likely if samples weren't quite at the center of the chamber.[19]

The elemental composition of the photoanodes was characterized by angle resolved XPS using a Physical Electronic Instruments (PHI) 5800 series multi-technique ESCA system w/ an Al Kα monochromatic source. Spectra were analyzed using the PHI Multipak software package. Adventitious carbon (284.8 eV) was present on every sample from handling between the reactor and the instrument so it was used as a calibration peak to account for sample charging. Crystal structures were analyzed by XRD using a Scintag X2 powder diffractometer with Cu Kα radiation (λ=1.54 Å).

Photoanode assembly

The substrate for all photoanodes is TEC-15 fluorine doped tin oxide (FTO) glass from the Hartford Glass Company. All of the substrates were cleaned by sonication in a solution of Alconox and water for 40 minutes. Following that substrates were rinsed sequentially in deionized (DI) water, acetone, and isopropanol and dried in an oven at 150 °C for at least 1 hour.

A dense passivation layer of titanium dioxide was deposited on all substrates to block any recombination with the transparent conducting oxide substrate. This dense layer was deposited by

spin-coating a sol-gel solution onto the substrates at 1600 rpm. The solution was prepared by first chilling 10 mL of absolute ethanol in a 20 mL scintillation vial in an ice bath. Separately, 250 µL of DI water is brought to a pH between 1 and 2 by the addition of nitric acid. After that, the DI water with adjusted pH was added to the ethanol and mixed for 5 minutes while continuing to chill. After mixing, 750 µL of titanium isopropoxide was added slowly over 3 minutes by syringe while stirring the ethanol water mixture. After the addition, the scintillation vial containing the solution stirred for an hour and then refrigerated overnight. The next day films were spin-coated and allowed to dry for 2 hours. After that, samples were annealed by slowly heating to 500 °C and staying there for 1 hour.

After annealing, the mesoporous layer was added to the films by doctor-blading 250 µL of the commercial T37 TiO_2 nanoparticle paste from Solaronix. The films were allowed to air-dry for 2 hours before being annealed by slow heating to 500 °C and maintaining the temperature for 1 hour.

DSSC assembly

Photoanodes were heated to 150 °C in a glass drying oven prior to dyeing in order to remove adsorbed water from the films. Anodes were immersed in an absolute ethanol solution containing a high concentration of the N3 dye for 24 hours. After immersion, the anodes were rinsed in absolute ethanol to remove excess dye and allowed to air dry in the dark for an hour. Before cell assembly, the visible light absorption of the anodes was characterized by UV-Vis spectroscopy on an Agilent 8453 UV-Visible spectroscopy system.

The electrolyte solution was prepared using γ-butyrolactone as the solvent in order to limit the risk of solvent evaporation during testing. Tert-butylpyridine was added to a concentration of 0.2 M, lithium trifluoromethylsulfonate was also at a concentration of 0.2 M, and the Co(II) and Co(III) species were added at concentrations of 0.135 M and 0.015 M respectively. The cathode was prepared by depositing 50 nm of chromium by evaporation onto FTO glass which had been cleaned in the same manner as the photoanodes. This was followed by deposition of 200 nm of gold on top of the

chromium, also by evaporation. The chromium was deposited first as a whetting layer in order to better adhere the gold to the surface. The anode and cathode were separated by a 25.1 µm Kapton® film spacer and the electrolyte was wicked in after the assembled cell was clipped into a custom made holder. The active area of the cell was set as 0.38 cm^2 standardized by a hole in the holder where the light was allowed to pass through.

Electrochemical testing

Several tests were performed in order to effectively evaluate the influence of the alumina layer on properties of assembled solar cells. All of these tests were performed sequentially on each sample progressing in the following order: JV curve for dark current, JV curve in light, current transient, voltage transient, and IPCE measurements. In some cases, a final JV curve in the light was employed after the other experiments to see if performance had changed over the course of the experiments. For the JV curves, the potential of the working electrode (photoanode) was scanned from -0.8 V to +0.1 V versus the auxiliary electrode as part of a two electrode set-up. The light pulse for the current and voltage transient experiments were 5 seconds and 1 second respectively and measurements were taken until the current or potential reached background levels again. For the IPCE measurements, the wavelengths were varied between 400 nm and 800 nm by the Oriel 1/8 m Cornerstone monochromator.

The testing apparatus used to run these experiments was run from a Keithley 2400 source meter controlled by a Labview virtual instrument connected to the cell in a two-electrode configuration. The virtual instrument was programmed by Dr. Jeremy Nelson, a former graduate student and group member. The light source was a 100 W Oriel xenon arc lamp calibrated to 100 $mW \cdot cm^{-2}$. Light was passed through an Oriel 1/8 m Cornerstone monochromator and subsequently through a 400 nm high-pass cutoff filter before reaching the cell holder and passing through a 0.38 cm^2 aperture to reach the sample.

4.3 Results and discussion

Deposition of alumina on substrates

The deposition apparatus underwent several rearrangements in order to maximize the ability to deposit aluminum oxide precisely and consistently over and throughout the entire mesoporous film. For the most part, the alterations to the system were not found to provide significantly different results related to the electrochemical performance of the devices. Considering the results presented herein, revisiting the design and optimization of the apparatus is likely required. The most significant changes to the system are described below along with their proposed improvements to the quality of film deposition. Possible changes to the system for further refinement are discussed below.

We demonstrate that the constructed apparatus is capable of depositing aluminum oxide onto the surface of a silicon wafer and the titanium dioxide mesoporous film. The deposited films were found to be amorphous in nature as determined by powder XRD which matches what is previously

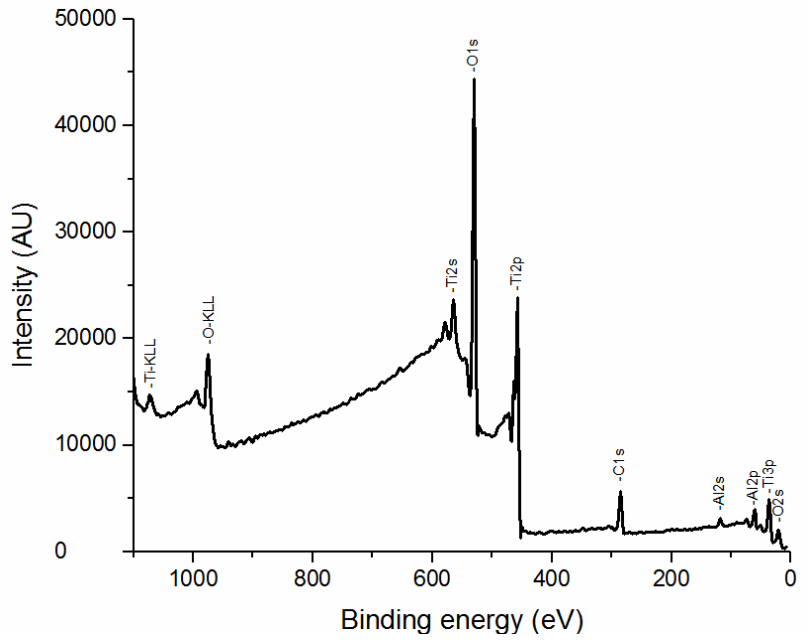

Figure 4.3: Survey scan of a DSSC samples with 1 cycle of Al_2O_3 deposited onto it by ALD. The elements that are present are aluminum, carbon, titanium, and oxygen. High resolution spectra were also taken in order to pinpoint and characterize different binding environments in the samples. Charging of the samples was accounted for by matching the peak for adventitious carbon to 284.8 eV.

reported in the literature.[20] A sample XRD pattern of a mesoporous TiO_2 film with 100 cycles of ALD performed upon it is shown in figure S4.1. The elemental composition was extensively examined through the use of x-ray photoelectron spectroscopy (XPS). In figure 4.3, the survey scan detected only titanium, aluminum, oxygen, and carbon species. The carbon species were attributed to sample handling and not to anything related to the reaction performed. It was also shown using high-resolution spectroscopy that as the number of cycles of deposited Al_2O_3 was increased, the intensity of signal from both the Al_{2p} peak and a corresponding O_{1s} peak also increased as shown in figure 4.4 which of course would be expected. The atomic percentages, even in high resolution scans, were found to vary somewhat and were not quantitative in nature due to the mesoporous nature of films leading to rough, uneven surfaces. However, this rough surface was also of benefit for detection of Al_2O_3 in that it led to higher signal the case of most samples even after just 1 cycle. For samples with lower roughness such as the FTO glass substrate on its own or the silicon wafers, several cycles were needed before Al_2O_3 could be detected.

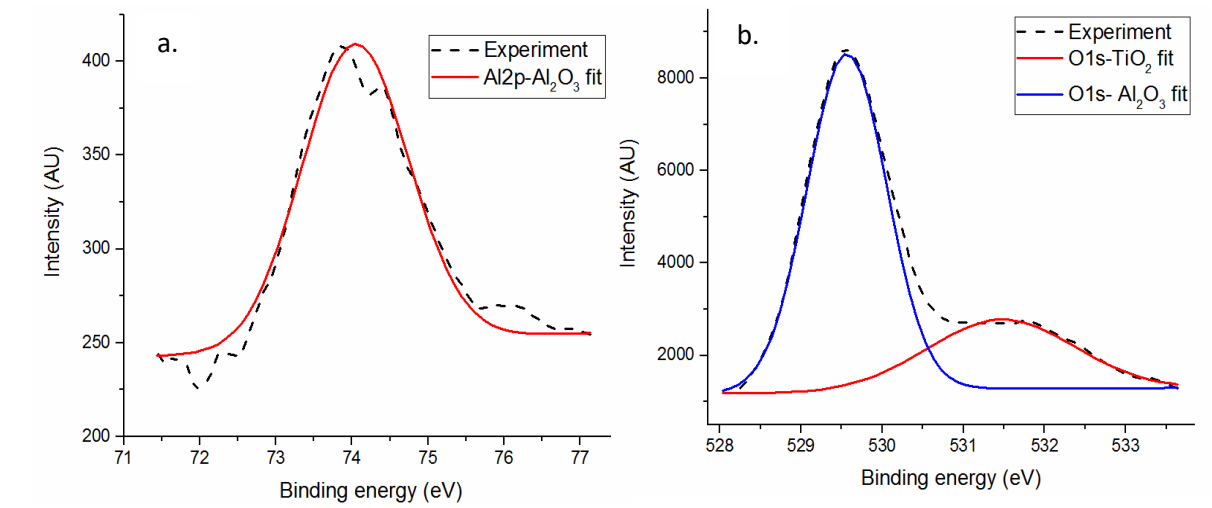

Figure 4.4a and b. High resolution spectra of aluminum peak (a) and oxygen peaks (b) from x-ray photoelectron spectroscopy. Spectrum was obtained from a sample of mesoporous TiO_2 film with 1 cycles of Al_2O_3 deposited on it. Spectrum was fit using PHI Multipak software and the binding energy axis was calibrated by matching to adventitious carbon to 284.8 eV.

In the literature, the per cycle deposition rate has been estimated at between 0.1 and 0.2 nm per cycle.[17, 21] Typically these growth rates are calculated from the precise surface area and mass from electrochemical quartz crystal microbalance (QCM) measurements. It was decided for this study that integration of the apparatus with a QCM device in the low pressure reaction chamber shouldn't be necessary for the deposition of a monolayer. It is said that the film grows via islands on the film so complete pinhole-free coverage is not estimated to be achieved before at least 10 cycles have been deposited. Multiple hypotheses have been suggested for the improvement in performance of DSSCs utilizing a single cycle of ALD compared to multiple cycles. But since film coverage is likely to be 25 % or less after the first cycle deposited, a tunneling barrier to electron transfer from the redox mediator is unlikely to serve as a complete explanation. It is more likely that as was suggested by Hamman, the deposition by atomic layer deposition is primarily reactive to surface states which are lower in energy and could act as trap states for the injected electron.

More recently, as data was re-examined, it was found there was a small shift in the Ti $2p_{3/2}$ peak after the deposition of a single cycle of Al_2O_3. It was found here that samples when 3 cycles had been

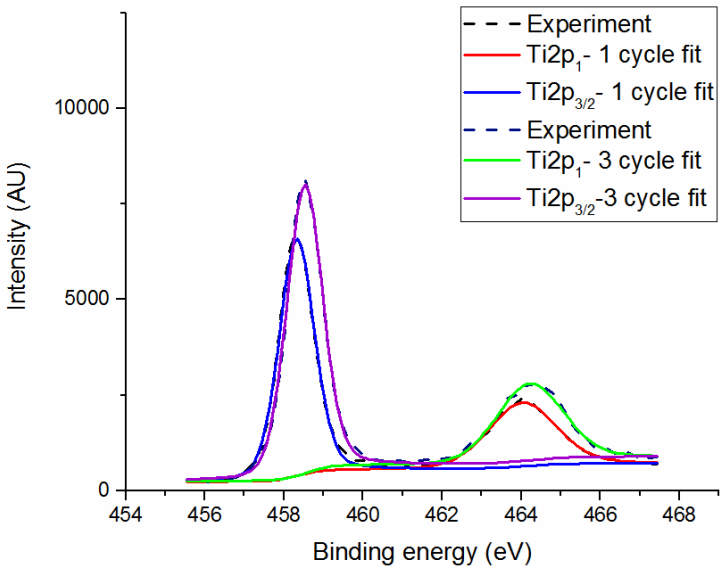

Figure 4.5: High resolution XPS spectrum for the Ti2p peaks on photoanodes with between 1 cycles or 3 cycles of Al_2O_3 deposited by ALD. Literature suggests the $Ti2p_{3/2}$ peak is shifted to lower binding energy when 1 cycle of Al_2O_3 is deposited and shifts negative when more cycles are deposited after that.

Table 4.1: Summary of the effect different numbers of deposited cycles of Al_2O_3 on the binding energy of peaks found in XPS spectra. The carbon species found on the film's surface are attributed to handling of the samples and the binding energy is independent of the number of cycles performed. *Binding energies were calibrated by anchoring the adventitious carbon peak to 284.8. There is a shift of the titanium peak when a single layer of Al_2O_3 is deposited that shifts back when more cycles are added.

Elements	Number of cycles	Position (eV)
Carbon (Adv)	N/A	284.8*
Carbon (C=O)	N/A	289.0
Titanium	0 or > 1	458.5
Titanium	1	458.3
Aluminum	> 0	74.1
Oxygen-TiO_2	1	529.8
Oxygen-Al_2O_3	> 0	531.4

deposited, a peak at 458.5 eV was observed. But that peak appeared at 458.3 eV when 1 cycle had been deposited as seen in figure 4.5 and summarized in table 4.1. Tien and co-workers observed a similar phenomenon, however they observed a slightly larger shift from 458.9 to 458.4 eV between 30 cycles deposited and 1 cycle deposited respectively.[21] It was found that the unmodified $Ti2p_{3/2}$ peak was at 458.9 eV, but it didn't seem like that peak made it quite all the way back even after exceeding 100 cycles deposited.

Design of ALD apparatus

The requirements of the apparatus are described in detail in the work by Elam and co-workers, however some important details will be reiterated here in order establish the base conditions to be used herein.[17] This system was also designed as a "viscous flow" or continuous flow ALD system. By allowing the flow to remain continuous, the goal is for the pulses of reactant gas to also remain continuous and evenly distributed to obtain precise control over the flow of gas interacting with the substrates. The pressure in the system was held between 1.5 and 2 torr according to the Omega DVG64 digital vacuum gauge and was controlled by the flow of the N_2 carrier gas. In order to provide appropriate partial

pressures of the reactant gases through the system without needing to heat the pre-cursor vessels, the total pressure in the system was recommended to be between 0.2 torr and 5.8 torr.[17] Reactant pulses were held at approximately 0.1 torr to minimize the perturbation caused by its addition. A schematic of the system as it was built is displayed in figure 4.2. Within the figure, the components added at later stages, such as solenoid valves encapsulating the reaction chamber, are shown in green. Unless otherwise noted, samples discussed herein were fabricated using the ultra-high purity nitrogen flow gas and with the added valves at either end of the reaction chamber.

One hypothesis for why the behavior of the cells from the literature could not be replicated was that continuous flow could not be maintained as precursors were forced into the pore structure of the film, meaning there may be some of the interior of the film which the precursors cannot reach. The system was altered in order to improve the consistency of the deposition process through the addition of solenoid valves on either side of the reaction chamber. The purpose of these valves was to entrap the precursor pulses within the reaction chamber to theoretically allow for completion penetration of the gases into the mesoporous film. Allowing the precursors to percolate within the chamber should maximize any reaction taking place. As will be detailed below, this change to the system did not show the expected improvements in the short-circuit current that presumably would be the result of complete coverage of the substrate. This suggests that coverage of the film is not the sole factor contributing to our inability to reproduce the results from the literature. One concern to the efficacy of this experiment is that by enclosing the reactant pulses within the reaction chamber, there may be competing reactions taking place on the chamber walls reducing the amount of precursor available to react with the film. Some form of surface treatment on the interior of the reaction chamber should decrease its reactivity in future experiments allowing for more precise use of the reactants.

The presence of oxygen or water in the apparatus during depositions was also a constant concern. The entire system, including the samples, was purged for more than 10 minutes prior to

beginning experiments with the carrier gas and at the reaction temperature in order to remove adsorbed water. Later experiments utilized ultra-high purity nitrogen as the carrier gas rather than a medical grade nitrogen gas. However, slight variations in base pressure as the vacuum was pulling on the system without carrier gas flow may indicate the apparatus was still not fully leak-free. There is also the possibility that there is still some adsorbed water on the surface of the mesoporous films when the deposition process begins which could also detract from the self-limiting nature of the process, especially during the first cycle. Even minute quantities of water during the TMA pulses may affect the self-limiting nature of the reaction. As will be shown below, large amounts of variability in the electrochemical performance of the assembled DSSCs with modified photoanodes seems to indicate a lack of precision with the apparatus used.

Electrochemical characterization of DSSCs

A number of electrochemical experiments were performed on assembled DSSCs in an attempt to compare to several studies in the literature.[5, 13, 15] Since it is expected that reduced recombination between the injected electrons in the TiO_2 and the oxidized version of the redox mediator is one of the causes for improved performance after deposition of the Al_2O_3 film, JV curves were performed in the dark where the only process occurring is charge transfer between the mediator and the anode and cathode. At beginning of the experiment, at a potential of -0.8 V, the reduction of the oxidized mediator is already occurring. In order to find the overpotential required for this reduction, the potential is scanned in the positive direction until that reduction is no longer occurring. As the number of cycles of Al_2O_3 deposited on the anode was increased, it was expected that the rate of recombination would decrease making the overpotential required increase meaning the reduction of oxidized mediator would stop sooner during the scan in the positive direction. Interestingly, the onset of dark current occurred at less negative potentials with 2 cycles deposited than with 0 cycles suggesting that the rate of recombination was higher with 2 cycles as is shown in figure 4.6. It is unclear at this point why that was

the case, though high rates of recombination could explain the lackluster performance of samples with 2 cycles in other electrochemical tests as well. This was not the case for DSSCs when 1 or 3 cycles were deposited. The onset of dark current occurred at higher negative potentials in the case of samples with both 1 and 3 cycles.

When the same photoanodes were exposed to light and the JV curve experiments were performed again, the performances were relatively analogous to the performance of the cells in the dark. In figure 4.7, samples utilizing 2 cycles of deposited Al_2O_3 exhibited the lowest values in terms of both the open circuit voltage (V_{oc}) and the short circuit current density (J_{sc}). The lower open circuit voltage was especially unexpected because the literature suggests any deposition of Al_2O_3 on the anode surface should increase the V_{oc}. The short-circuit current density can be effected by a lot of subtle factors such as temperature of the electrolyte (to be discussed later), the thickness of the photoanode, and the amount of dye adsorbed which all can vary somewhat from sample to sample. The V_{oc} is determined by the position of the quasi-Fermi level in the TiO2 and the redox potential of the mediator couple which should not change. The quasi-Fermi level should be mostly independent of factors that are normally highly variable such as the film thickness and amount of dye adsorbed. There could be

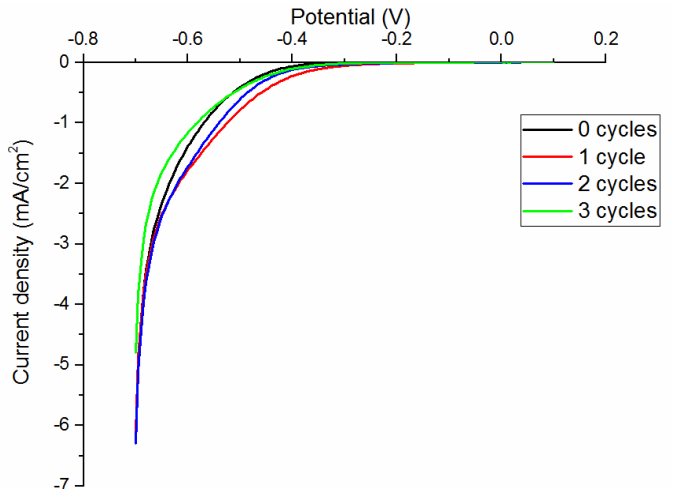

Figure 4.6: Current density-potential plot of assembled DSSCs before being exposed to light. The photoanodes have been treated with between 0 and 3 cycles of Al_2O_3 by ALD prior to dyeing and assembly.

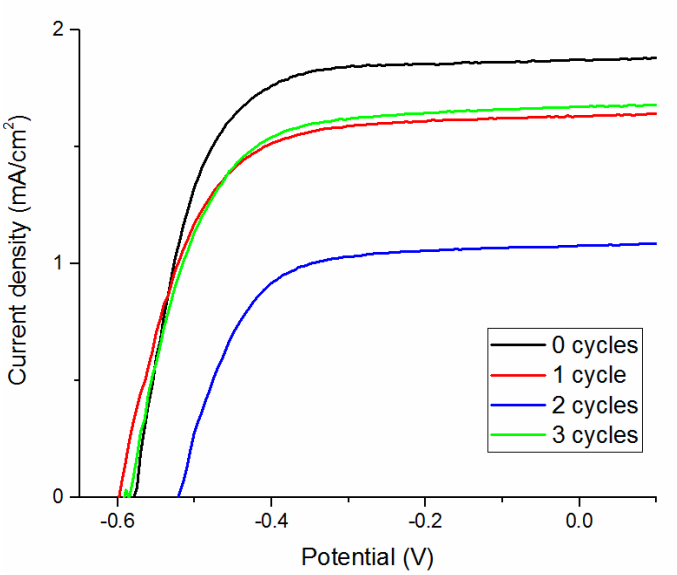

Figure 4.7: Current density-potential plot of assembled DSSCs while being exposed to light. The photoanodes have been treated with between 0 and 3 cycles of Al_2O_3 by ALD prior to dyeing and assembly. From these plots, open circuit voltage and short circuit current can be determined.

some unknown surface effect occurring to cause a lower Fermi level but it has not been mentioned previously in the literature. On the other hand samples utilizing 1 or 3 cycles acted more as would be predicted; with a V_{oc} which slightly surpassed that of the unmodified photoanodes and J_{sc} which was less then observed by the unmodified anodes. Interestingly, the V_{oc} and J_{sc} of samples with both 1 and 3 cycles performed on them were almost identical. This may suggest that the reaction during the first cycle is not as self-limited as would be required to get the desired effect. The V_{oc}, J_{sc}, and fill factor (FF) for 0 to 3 deposited cycles of Al_2O_3 are reported in table 4.2. The fill factor did not seem to be effected by the presence of the alumina layer with any number of cycles which is interested because it might be affected to decrease if injection of the excited electron was slowed by the presence of the Al_2O_3.

During the voltage transient experiment, a short light pulse is used to excite the dye and force the excited electrons to be injected into the conduction band of the TiO_2. No current is allowed to pass during the experiment so the only mechanism for alleviating the build-up of potential is either through recombination with either the oxidized dye or the oxidized redox mediator. Since the deposition of

Table 4.2: Data collected from the current density-potential curves is summarized. Short circuit current density, open circuit voltage, and fill factor (as a ratio of max power generated vs. ideal power generation) were reported. Efficiencies were found collectively to be low and were not reported here.

# of cycles	0	1	2	3
J_{sc} (mA/cm^2)	1.85	1.61	1.06	1.58
V_{oc} (mV)	581	603	520	590
Fill factor	0.69	0.67	0.67	0.67

Al_2O_3 is intended to reduce the recombination at the photoanode surface, it would be expected that the voltage transient would show slower decay of the signal back to a ground state for samples with thicker layers of Al_2O_3. This was not observed for the modified anodes when 2 or 3 cycles were deposited onto the films as can be seen in figure 4.8 along with the transients for other numbers of cycles as well. The signal decay of photo-excited samples with 2 and 3 cycles was actually faster than was seen with unmodified DSSCs suggesting that recombination was occurring more quickly. The samples with 1 deposited cycle decayed at very close to the same rate as the modified samples. However, the addition of that 1 cycle did seem to yield a slightly higher peak potential related to the position of the conduction band right after the photo-excitation which would be expected.

Overall, the results reported herein showed unfortunate sample-to-sample variability, which decreases the reliability of the results shown. While the increase in the open circuit voltage was consistent with the literature, the short circuit current was higher with the controls, before Al_2O_3 was deposited onto the films. It was hoped that the current would be higher after the first cycle was deposited and begin to trail off as more Al_2O_3 was deposited. Other electrochemical characterization techniques, such as the voltage transients showed faster decay of injected electrons with 2 and 3 deposited cycles, which does not match the expectation of reduced mediator recombination as the amount of deposited Al_2O_3 is increased. This could suggest that the apparatus is not doing its job of

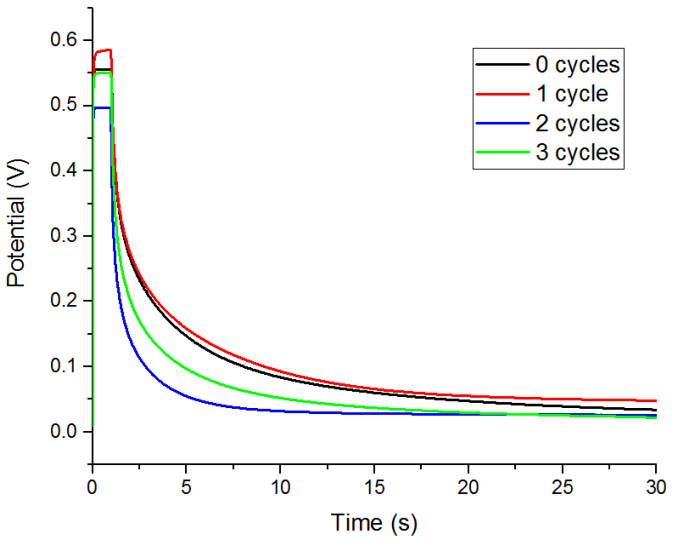

Figure 4.8: Voltage transient experiments were performed on assembled DSSCs with between 0 and 3 cycles of Al_2O_3 deposited by ALD present on the photoanodes.

precisely controlling the amount of Al_2O_3 deposited onto the surface of the films. These results may suggest there are both some areas of the film remaining unmodified and some areas of the film where excess material is deposited due to the reaction not acting self-limited. Also contributing to some of the variability could be the inherent complexity in the preparation mesoporous films such as slight differences in film thickness. It was found that by profilometry, the photoanodes as prepared here varied typically between 2.5 µm and 3 µm, which also effects the amount of dye that can adsorb. Since there is little that can be done to further organize the randomness of depositing a mesoporous film all other facets of the experiment must be precisely controlled in order to minimize sample to sample variability.

The testing procedure itself may also require the control of more variables then was originally understood. It was found after this study by Lance Ashbrook that exposure to light over time increased the current observed from the cell. It was determined this was due to an increase in the temperature of the electrolyte which decreased the viscosity of the solvent and decreased the limitations due to mass transport. Thus, even small variation in the testing procedure could have allowed some samples more light exposure and thus artificially higher currents relative to other samples.

Future directions

There are a myriad of issues which have complicated the refinement of this benchtop atomic layer deposition apparatus for use in curbing the recombination of the oxidized redox mediator and improving the device's efficiency. The difficulty starts in the analysis of the deposited ultra-thin films and their even coverage over a complex surface such as a mesoporous film. Clever sample preparation could allow for analysis of different numbers of cycles via high resolution transmission electron microscopy (HR-TEM) which was unavailable when this project was first performed.[22]

Impedance spectroscopy was a technique which was also not utilized during the initial steps of this project and could have proved valuable. Electrochemical impedance spectroscopy (EIS) is often used to gather information about the transfer of charge across interfaces in an electrochemical cell. EIS has actually become a common technique for the evaluation of several of the complex charge transfer events inherent to DSSCs.[23, 24] If the deposition of Al_2O_3 stifles recombination by passivation of low energy trap states, there is very likely to be a change in a spectrum from EIS either by reduction of the signal related to recombination or a shift in the frequency it occurs at. EIS can also serve as a secondary method for evaluating some of the differences between the numbers of ALD cycles deposited on the film. Some work has previously been done to evaluate the change in the lifetime of injected electrons as the number of cycles performed on samples has been increased.[14]

While work must first be done to allow for better characterization of the films, there is already evidence to suggest the apparatus itself must be refined as well. The inability to reproduce the electrochemical performance from the literature while using modified photoanodes suggest that we have not obtained the desired precision to be considered atomic layer deposition. Contamination of samples and the system with errant oxygen and water vapor could result in a loss of the self-limiting nature of the desired reaction. Leaks throughout the system are likely to result in the reduction in the amount of TMA pre-cursor gas which reaches the substrate which could lead to less than full coverage.

It has been suggested that adsorbed water on the intricate surface of mesoporous TiO_2 films is a problem in some fully assembled DSSCs.[25, 26] If the purging step at the deposition temperature currently used was insufficient at desorbing water from the TiO_2 surface, it would likely reduce the self-limiting nature of the desired reaction. Thus, performing the initial purging step at a higher temperature may prove more efficient at complete desorption of water on the film's surface.

4.4 Conclusions

Atomic layer deposition as a surface passivation technique has been shown in the literature to be an effective means to reduce the rate of recombination and improve the efficiency of DSSCs, especially when using redox mediators like $Co(bpy)^{2+/3+}$ and $Co(dtb)^{2+/3+}$.[5, 27] The cost of the apparatus typically responsible for the deposition is can exceed $100,000 and is not likely to be cost-effective upon scale up using commercially available systems.[16] The greatest benefit of DSSCs at this point as a third generation photovoltaic is their low cost relative to other technologies such as silicon based photovoltaics. Therefore, if surface passivation by the deposition of an ultra-thin layer of another metal oxide is to be undertaken, the apparatus must be cheaper and with some ability to scale the technology to meet demands.

It is unclear at this point if the apparatus constructed herein provides the precision necessary to be considered atomic layer deposition. X-ray photoelectron spectroscopy is able to detect Al_2O_3 after just a single cycle of ALD is performed on the mesoporous TiO_2 film. However, when these photoanodes are tested in assembled DSSCs, the increase in performance that was observed in the literature cannot be replicated. While the expected increase in V_{oc} was observed, the increase in J_{sc} as a result of the first cycle was not present. There was significant sample to sample variability in the performance of both unmodified control samples and samples with modified anodes with deposited Al_2O_3. However, it was interesting that 2 deposited cycles appeared to be an outlier electrochemically as it appeared to suffer from higher rates of recombination and lower open circuit potentials relative to all other samples.

There is no current hypothesis which sufficiently explains this observation because of the difficulty of fully characterizing the subtle differences in the film surface between 1 to 3 cycles of deposited Al_2O_3.

Unlike when this study was first conducted, there is now a high resolution transmission electron microscope present in the department. This may allow for more precise characterization of the deposited film surface on a cycle by cycle basis. This could occur either by performing ALD directly on a TEM grid or by preparing ultra-thin mesoporous films on the grids themselves to deposit Al_2O_3 on. Due to the method of sample preparation, HR-TEM won't be helpful in the characterization of thicker films and probing the ability of the precursors to completely penetrate the film's pore structure.

Electrochemical impedance spectroscopy (EIS) is a useful technique for elucidating kinetic information about processes occurring at interfaces of an electrochemical cell. If there is uneven coverage through the pore structure of the photoanode recombination with the oxidized mediator may occur by multiple processes that may be detectable by EIS at different frequencies. Even if the same process is occurring, the frequency at which it occurs is likely to shift as Al_2O_3 is deposited onto the mesoporous surface.

Finally, there may also be approaches to pre-emptively modify aspects of the apparatus and the deposition procedure to improve its function. An extra-long purging step at higher than deposition temperatures may be necessary in order to fully desorb water from the complex and porous TiO_2 film used as a substrate. Samples with 1 cycle were difficult to differentiate from samples with 3 deposited cycles in their performance suggesting that the reaction occurring during that first cycle may not be self-limiting. While some care was taken to purge water from the film prior to the deposition process it may not have been accomplished as completely as was thought. Chemical treatment of the surface of the reaction chamber surface may also improve the consistency of the deposition process. The reaction chamber is currently a quartz glass tube, which may allow for reaction of some precursor gases along its surface. The previous approach was to provide such a large excess of the pre-cursors that reaction with

the chamber was unimportant. But now it seems that any method which may improve the consistency of the process should be considered to improve the overall performance.

REFERENCES FOR CHAPTER 4

1. Hagfeldt, A.; Boschloo, G.; Sun, L.; Kloo, L.; Pettersson, H., Dye-Sensitized Solar Cells. *Chemical Reviews* **2010,** *110* (11), 6595-6663.

2. Kakiage, K.; Aoyama, Y.; Yano, T.; Oya, K.; Fujisawa, J.-i.; Hanaya, M., Highly-efficient dye-sensitized solar cells with collaborative sensitization by silyl-anchor and carboxy-anchor dyes. *Chemical Communications* **2015,** *51* (88), 15894-15897.

3. Mathew, S.; Yella, A.; Gao, P.; Humphry-Baker, R.; CurchodBasile, F. E.; Ashari-Astani, N.; Tavernelli, I.; Rothlisberger, U.; NazeeruddinMd, K.; Grätzel, M., Dye-sensitized solar cells with 13% efficiency achieved through the molecular engineering of porphyrin sensitizers. *Nat Chem* **2014,** *6* (3), 242-247.

4. Yella, A.; Lee, H.-W.; Tsao, H. N.; Yi, C.; Chandiran, A. K.; Nazeeruddin, M. K.; Diau, E. W.-G.; Yeh, C.-Y.; Zakeeruddin, S. M.; Grätzel, M., Porphyrin-Sensitized Solar Cells with Cobalt (II/III)–Based Redox Electrolyte Exceed 12 Percent Efficiency. *Science* **2011,** *334* (6056), 629.

5. Ondersma, J. W.; Hamann, T. W., Impedance Investigation of Dye-Sensitized Solar Cells Employing Outer-Sphere Redox Shuttles. *The Journal of Physical Chemistry C* **2010,** *114* (1), 638-645.

6. Nelson, J. J.; Amick, T. J.; Elliott, C. M., Mass Transport of Polypyridyl Cobalt Complexes in Dye-Sensitized Solar Cells with Mesoporous TiO2 Photoanodes. *The Journal of Physical Chemistry C* **2008,** *112* (46), 18255-18263.

7. Tsao, H. N.; Comte, P.; Yi, C.; Grätzel, M., Avoiding Diffusion Limitations in Cobalt(III/II)-Tris(2,2'-Bipyridine)-Based Dye-Sensitized Solar Cells by Tuning the Mesoporous TiO2 Film Properties. *ChemPhysChem* **2012,** *13* (12), 2976-2981.

8. Sapp, S. A.; Elliott, C. M.; Contado, C.; Caramori, S.; Bignozzi, C. A., Substituted Polypyridine Complexes of Cobalt(II/III) as Efficient Electron-Transfer Mediators in Dye-Sensitized Solar Cells. *Journal of the American Chemical Society* **2002,** *124* (37), 11215-11222.

9. Koh, T. M.; Nonomura, K.; Mathews, N.; Hagfeldt, A.; Grätzel, M.; Mhaisalkar, S. G.; Grimsdale, A. C., Influence of 4-tert-Butylpyridine in DSCs with CoII/III Redox Mediator. *The Journal of Physical Chemistry C* **2013,** *117* (30), 15515-15522.

10. Feldt, S. M.; Gibson, E. A.; Gabrielsson, E.; Sun, L.; Boschloo, G.; Hagfeldt, A., Design of Organic Dyes and Cobalt Polypyridine Redox Mediators for High-Efficiency Dye-Sensitized Solar Cells. *Journal of the American Chemical Society* **2010,** *132* (46), 16714-16724.

11. Ashbrook, L. N.; Elliott, C. M., Sulfide Modification of Dye-Sensitized Solar Cell Gold Cathodes for Use with Cobalt Polypyridyl Mediators. *The Journal of Physical Chemistry C* **2014,** *118* (30), 16643-16650.

12. Kirner, J. T.; Elliott, C. M., Are High-Potential Cobalt Tris(bipyridyl) Complexes Sufficiently Stable to Be Efficient Mediators in Dye-Sensitized Solar Cells? Synthesis, Characterization, and Stability Tests.

The Journal of Physical Chemistry C **2015,** *119* (31), 17502-17514.
13. Liberatore, M.; Burtone, L.; Brown, T. M.; Reale, A.; Carlo, A. D.; Decker, F.; Caramori, S.; Bignozzi, C. A., On the effect of Al2O3 blocking layer on the performance of dye solar cells with cobalt based electrolytes. *Applied Physics Letters* **2009,** *94* (17), 173113.

14. Hamann, T. W.; Farha, O. K.; Hupp, J. T., Outer-Sphere Redox Couples as Shuttles in Dye-Sensitized Solar Cells. Performance Enhancement Based on Photoelectrode Modification via Atomic Layer Deposition. *The Journal of Physical Chemistry C* **2008,** *112* (49), 19756-19764.

15. Klahr, B. M.; Hamann, T. W., Performance Enhancement and Limitations of Cobalt Bipyridyl Redox Shuttles in Dye-Sensitized Solar Cells. *The Journal of Physical Chemistry C* **2009,** *113* (31), 14040-14045.

16. Lubitz, M.; Medina, P. A.; Antic, A.; Rosin, J. T.; Fahlman, B. D., Cost-Effective Systems for Atomic Layer Deposition. *Journal of Chemical Education* **2014,** *91* (7), 1022-1027.

17. Elam, J. W.; Groner, M. D.; George, S. M., Viscous flow reactor with quartz crystal microbalance for thin film growth by atomic layer deposition. *Review of Scientific Instruments* **2002,** *73* (8), 2981-2987.

18. Grätzel, M., Conversion of sunlight to electric power by nanocrystalline dye-sensitized solar cells. *Journal of Photochemistry and Photobiology A: Chemistry* **2004,** *164* (1–3), 3-14.

19. Ott, A. W.; Klaus, J. W.; Johnson, J. M.; George, S. M., Al3O3 thin film growth on Si(100) using binary reaction sequence chemistry. *Thin Solid Films* **1997,** *292* (1), 135-144.

20. Hanson, K.; Losego, M. D.; Kalanyan, B.; Ashford, D. L.; Parsons, G. N.; Meyer, T. J., Stabilization of [Ru(bpy)2(4,4'-(PO3H2)bpy)]2+ on Mesoporous TiO2 with Atomic Layer Deposition of Al2O3. *Chemistry of Materials* **2013,** *25* (1), 3-5.

21. Tien, T.-C.; Pan, F.-M.; Wang, L.-P.; Tsai, F.-Y.; Lin, C., Coverage Analysis for the Core/Shell Electrode of Dye-Sensitized Solar Cells. *The Journal of Physical Chemistry C* **2010,** *114* (21), 10048-10053.

22. Ganapathy, V.; Karunagaran, B.; Rhee, S.-W., Improved performance of dye-sensitized solar cells with TiO2/alumina core–shell formation using atomic layer deposition. *Journal of Power Sources* **2010,** *195* (15), 5138-5143.

23. Liberatore, M.; Decker, F.; Burtone, L.; Zardetto, V.; Brown, T. M.; Reale, A.; Di Carlo, A., Using EIS for diagnosis of dye-sensitized solar cells performance. *Journal of Applied Electrochemistry* **2009,** *39* (11), 2291-2295.

24. Liu, Y.; Jennings, J. R.; Zakeeruddin, S. M.; Grätzel, M.; Wang, Q., Heterogeneous Electron Transfer from Dye-Sensitized Nanocrystalline TiO2 to [Co(bpy)3]3+: Insights Gained from Impedance Spectroscopy. *Journal of the American Chemical Society* **2013,** *135* (10), 3939-3952.

25. Bella, F.; Gerbaldi, C.; Barolo, C.; Gratzel, M., Aqueous dye-sensitized solar cells. *Chemical Society Reviews* **2015,** *44* (11), 3431-3473.

26. Lu, H.-L.; Shen, T. F. R.; Huang, S.-T.; Tung, Y.-L.; Yang, T. C. K., The degradation of dye sensitized solar cell in the presence of water isotopes. *Solar Energy Materials and Solar Cells* **2011,** *95* (7), 1624-1629.

27. Katz, M. J.; DeVries Vermeer, M. J.; Farha, O. K.; Pellin, M. J.; Hupp, J. T., Dynamics of Back Electron Transfer in Dye-Sensitized Solar Cells Featuring 4-tert-Butyl-Pyridine and Atomic-Layer-Deposited Alumina as Surface Modifiers. *The Journal of Physical Chemistry B* **2015,** *119* (24), 7162-7169.

CHAPTER 5: FUTURE OPPORTUNITIES FOR IMPROVEMENT AND RESEARCH OF DYE SENSITIZED SOLAR CELLS

5.1 Looking toward commercialization of DSSCs

The fundamental understanding of dye sensitized solar cells (DSSCs) has reached a point where it is important to consider where the future for this technology is going to lie. The complexity and multitude of processes involved in the determination of efficiency for DSSCs is both a blessing and a curse when optimizing devices for real use. The modification of individual components can have a cascading effect on other components and processes, severely reducing the efficiency of the device.[2] And as new dyes, solvents, additives, mediators, and electrodes are developed it has been difficult to predict behavior of each component as they interact leading to hampered device performance.

An example of this complexity would be the task of optimizing the depth of the mesoporous TiO_2 film. The film must be thin in order to avoid mass transport limitations but thick enough to still maximize light absorption from an appropriate amount of adsorbed dye.[3] Even though the optimization of that parameter could be considered a task left for device engineering at late stages of development, it is absolutely vital to proper device function. Optimization of film thickness requires balancing several other components and processes. Altering any of the following could change what the optimum thickness would be. Possibilities to alleviate issues related to mass transport might include using titanium tetrachloride ($TiCl_4$) to tailor film porosity, switching dyes for one with a higher extinction coefficient to allow for thinner films, and altering the redox mediator to reduce the diffusion coefficient through the electrolyte. Post-deposition treatment of the mesoporous film with $TiCl_4$ may also affect the presence of surface trap states which are suspected to increase rates of undesired recombination.[3] Using higher extinction coefficient dyes would allow for thinner films and reduce the time that oxidized mediator must spend diffusing back to the cathode to be regenerated. This would also affect the

maximum distance electrons must travel through the TiO_2 film after being injected.[4] Altering the identity of the redox mediator can affect the kinetics of both desirable electron transfer processes such as regeneration of the dye, regeneration of the mediator at the cathode, and undesirable electron transfer processes such as recombination with the mesoporous film or the transparent conducting oxide.[2, 5] The advantages and potential solutions to disadvantages of different film thicknesses are summarized below in table 5.1.

As mentioned above, there are a great number of interconnected components to a DSSC which must all be able to interact cohesively to achieve even a moderate efficiency relative to other technologies. Every time a perceived improvement is made to one of the components of a DSSC, that improvement must also be able to not negatively affect or be affected by the other components. It has become evident as more research has gone into DSSCs as a technology that even though their biggest advantage is affordability that should not be confused with simplicity.

It is my belief that while DSSCs have become moderately efficient and remain reasonably cost-effective, the future of commercialization for the technology lies in consumer goods. In this area, use of DSSCs over other photovoltaic technologies can be advantageous because of their low cost, literal and

Table 5.1: Summary of advantages to both thick and thin photoanode films used in DSSCs as well as possible solutions to minimize disadvantages of each.

Thick films: > 4 µm Advantages	Thin films: < 4 µm Advantages
-High absorption from dye -Larger prospective current	-Shorter diffusion length -Lower rates of recombination
Potential solutions	
-Larger pore size could still allow diffusion -Diffusion can be somewhat controlled by solvent viscosity	-Higher extinction coefficient dyes still allow for strong absorption -Removes limitations on obtainable current based on mass transport

figurative flexibility, and the potential for non-toxic components. There have already been several examples of consumer goods where DSSCs have been uniquely qualified. The semi-transparency of traditional DSSCs allow for applications such as the stained glass window DSSCs at École Polytechnique Fédérale de Lausanne in Switzerland. And the fact that DSSCs exhibit higher efficiencies at low light intensities such as indoors allow for a keyboard to be powered by DSSCs such as the model from Logitech for the iPad.[6] Further research may begin to home in on those attributes which will best match the possible future applications of DSSCs.

5.2 Organic molecular redox mediators for DSSCs

Maintaining and further decreasing the low cost of DSSCs will mean continuing to avoid precious metal catalysts on the cathode side of the DSSC and the use of rare earth metals in sensitizers and mediators. Organic triphenylamine based sensitizers have become popular options for use in DSSCs instead of the historically used ruthenium sensitizers.[7-8] These organic sensitizers are known to have high absorption coefficients, long excited state lifetimes, and bulkiness that can somewhat shield the TiO_2 surface from unwanted recombination.[9] Organic sensitizers have seen a lot of success when combined with cobalt tris-2,2-biypridine [$Co(bpy)^{2+/3+}$] as a redox mediator instead of the iodide/tri-iodide couple.[4] $Co(bpy)^{2+/3+}$ or similar complexes such as cobalt tris-1,10-phenanthroline ($Co(phen)^{2+/3+}$) are currently used in several of the highest efficiency liquid electrolyte based DSSCs.[10-11] The redox potential of these mediators is one of the primary modes of comparison between different candidates. Figure 5.1 shows a comparison of several of the most widely used redox mediators in terms of their redox potential and driving force for regeneration with the high potential organic sensitizer, D35. Recent studies have also shown promising small molecular organic redox mediators which have several properties which may be advantageous for future improvements in DSSCs.[12-14] The use of a nitroxide radical as part of (2,2,6,6-Tetramethylpiperidin-1-yl)oxyl or $TEMPO^{0/1+}$ has been studied as an alternative mediator which combines the high positive redox potential and synthetic tunability of

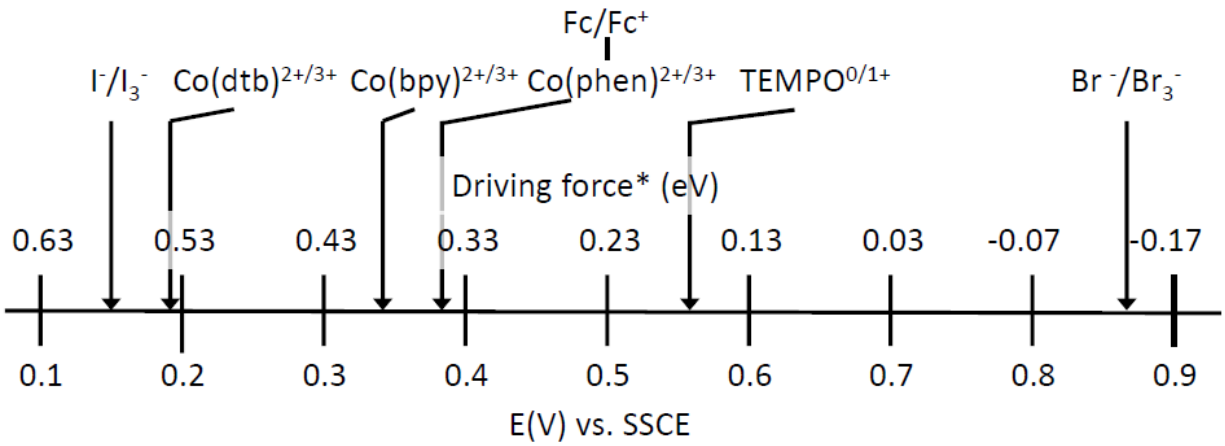

Figure 5.1: Diagram relating the redox potential of various redox mediators utilized in the literature to the driving force afforded to regeneration of the ground state of the organic dye, D35* (0.73 V vs. SCCE). The potential vs. saturated sodium calomel electrode is reported in volts while the driving force is reported in electron volts. It should be noted there is negative driving force for the regeneration of the dye with the bromide/tri-bromide couple due to its redox potential being too positive.

$Co(bpy)^{2+/3+}$ with the small size of iodide/tri-iodide (I^-/I_3^-).[12] Relative to I^-/I_3^- the redox potential of $TEMPO^{0/1+}$ was found to be more than 400 mV more positive. But its diffusion coefficient under similar concentrations and conditions was found to be very similar to the I^-/I_3^- redox couple or close to 50 times faster than $Co(bpy)^{2+/3+}$. $TEMPO^{0/1+}$ or other modified systems utilizing a nitroxide radical have become a popular topic of research related to electrochemical processes. Recently, it has been studied as an electrocatalyst for other systems such as the oxidation of hydrogen peroxide.[15]

5.3 Approaches targeting reduction of recombination rates while using TEMPO

While there are a growing number of studies using this redox mediator, the efficiency is still much lower then what is observed using other redox couples (less than 10 %). While there are a lot of promising aspects about this mediator, there are also several disadvantages which have not been thoroughly explored. The mediator system of I^-/I_3^- saw so much early success in part because it has very poor charge transfer kinetics related to its electron transfer between itself and titanium dioxide. This allows for slow rates of recombination with the titanium dioxide. For the $TEMPO^{0/1+}$ mediator system, recombination of the injected electron from the TiO_2 has been shown to occur much faster.[1] Higher

rates of recombination lead to a reduction of the attainable short circuit current and maximum efficiency that the cell can obtain. The $Co(bpy)^{2+/3+}$ mediator also suffers from faster rates of recombination between the oxidized version of the mediator and the mesoporous film.[5, 9, 16] However, it was shown that recombination rates could be decreased by the use of bulky organic sensitizers that have been able to somewhat block off the oxidized form of the $Co(bpy)^{2+/3+}$ from being able to reach the surface of the film.[4] Due to the smaller size of the molecular $TEMPO^{0/1+}$ mediator, it is not as sterically hindered by the presence of the organic sensitizer and recombination rates were not improved to the same degree.[1] One approach that has already been taken to minimize the impact of recombination to the $TEMPO^{0/1+}$ mediator is the use of additives to the electrolyte solution such as different benzimidazole derivatives.[1] It is suggested that benzimidazole is able to form a barrier layer similar to *tert*-butylpyridine which blocks the oxidized mediator from being able to access the TiO_2 surface, both of which are shown in figure 5.2.[17] Different derivatives were synthesized in order to improve binding of the benzimidazole to the film's surface. It was shown that using these additives could increase the short circuit current substantially suggesting that recombination rates were reduced.[1]

An approach which has not been taken in the literature, to the best of my knowledge, is to couple the use of the TEMPO redox mediator with the use of atomic layer deposition (ALD) in order to

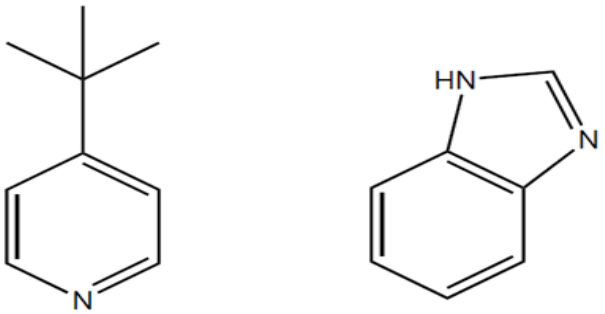

4-*tert*-butylpyridine (TBP) Benzimidazole (BIZ)

Figure 5.2: Common electrolyte additives for DSSCs. It is suggested that they improve cell function by limiting recombination at the anode and raising conduction band of the anode. It has also been shown that benzimidazole can be functionalized further.[1]

make an ultra-thin coating of some sort of non-conducting oxide on the surface of the anode. While it has been shown previously to reduce the rate of recombination and improve electron lifetime in the mesoporous film for other redox mediators like $Co(bpy)^{2+/3+}$, it has not been used in conjunction with $TEMPO^{0/1+}$.[18-19] It would seem that the notion of depositing an ultra-thin layer of a non-conductive oxide such as aluminum oxide could be especially suitable for reducing recombination from the oxidized form of $TEMPO^{0/1+}$. Aluminum oxide deposited by ALD will be more strongly bound to the surface of the TiO_2 relative to the molecular additives such as benzimidazole, bound by intermolecular forces, and it would be expected that the film would show excellent long term stability. It would also not rely on sterically bulky organic sensitizers in order to discourage interaction of the TiO_2 film and mediator. The first cycle of atomic layer deposition is expected to react mainly with surface trap states as discussed in chapter 4, which are more likely to act as sites for recombination with the mobile oxidized mediator species. The deposition of the first cycle results in an increase of the open circuit voltage as well as a small increase in the short circuit current.[18, 20] Continued cycles still improve the reported open circuit voltage, while the short circuit current and fill factor both steadily decrease after the first cycle. This is likely due to slower electron injection from the excited dye which also is influenced by the non-conducting oxide layer. There is no reason to expect multiple cycles will be of any more advantage with $TEMPO^{0/1+}$ then with $Co(bpy)^{2+/3+}$ as the decrease in efficiency seems to be more a result of interaction between the sensitizer and anode.[18] A summary of the potential effects of each recombination reduction strategy is provided in table 5.2. The cost of each technique is determined by how much more performing the technique is likely to cost in addition to manufacture of the cell. Even though there will be added cost in design of new dyes and mediators, the added cost to the manufacture of cells is considered to be low relative to the addition of entirely new additives or processing techniques.

Table 5.2: Summary of benefits related to various methods for surface passivation of the photoanode film. Methods were evaluated based on the effect on diffusion of the redox mediator and relative cost of implementation on a commercial scale. Several or all of these methods could potentially be used in conjunction in order to further decrease recombination rates.

Method for passivation	Location in DSSC	Effect on diffusion	Relative cost
Bulky organic dyes	Fixed to anode	Low	Low
Mediator modification	Electrolyte	High	Low
Electrolyte additives	Electrolyte/ adsorbed to anode	Low	Medium
Atomic layer deposition	Fixed to anode	None	High

5.4 Synthetic modification of the TEMPO redox mediator

Another approach to reduce recombination as well as 'fine-tune' the redox potential was originally shown by Sapp and co-workers in that synthetic modification of the $Co(bpy)^{2+/3+}$ redox mediator through the addition of sterically bulky substituents can reduce the rate of recombination exhibited by the $Co(bpy)^{2+/3+}$ type mediator.[21] This result has since been replicated in the literature by other groups.[5, 19] However, it was also shown that the diffusion coefficient is significantly reduced as a result of the substitutions on these redox mediators.[22] Nelson and co-workers showed that the mass transport limitations were exacerbated even more while in the porous photoanode film.[22] And in the case of electron donating groups as the substituents, the redox potential was driven more negative reducing the attainable open circuit voltage.[21]

In the case of both the initial diffusion coefficient and the redox potential of the unsubstituted mediator, $TEMPO^{0/1+}$ has the advantage over $Co(bpy)^{2+/3+}$ by way of much faster diffusion and a more highly positive redox potential under typical electrolyte conditions. The diffusion coefficient for TEMPO is close to 2×10^{-5} cm^2s^{-1} while the diffusion coefficient for $Co(bpy)^{2+/3+}$ is typically reported as a full order of magnitude slower at $2\text{-}4 \times 10^{-6}$ cm^2s^{-1}.[23-24] The reported potential for the unmodified $TEMPO^{0/1+}$ redox couple is 0.56 V vs. SCCE while the redox couple for $Co(bpy)^{2+/3+}$ is found at 0.34 V vs. SCCE.[12, 21] The optimal redox potential for the mediator will be partially determined by the identity and properties of

the sensitizer that the mediator is required to regenerate but if recombination can be reduced significantly through the use of electron donating moieties substituted onto the TEMPO$^{0/1+}$ species, it would be worth a small loss in redox potential due to its potential. The reduction in recombination caused by blocking layers as discussed above also results in an increase in the open circuit voltage of the assembled cells due to negative shift in the potential of the conduction band.[25] So in some cases it might be observed that the reduction in recombination offsets the negative shift in potential of the redox mediator. It may even be worthwhile to choose a sensitizer which will best match the mediator instead of the other way around. The diffusion coefficient is fast enough for TEMPO$^{0/1+}$ that its utilization as a redox mediator is unlikely to lead to limitations from mass transport even if the diffusion coefficient were to decrease substantially, due to substitutions, as is reported when Co(bpy)$^{2+/3+}$ is synthetically modified to include tert-butyl groups on each of the bipyridine ligands.[22, 24]

Unlike iodide/tri-iodide, an organic redox mediator such as TEMPO$^{0/1+}$ allows for a number of avenues of synthetic modification resulting in advantageous control over different properties. Several analogues related to TEMPO$^{0/1+}$ have already been synthesized in the literature, associated by the presence of the nitroxide radical, several of which are shown in figure 5.3.[14, 23, 26] In fact, a number of derivatives are available for purchase from vendors such as Sigma-Aldrich and TCI Chemicals. TEMPO$^{0/1+}$ and its derivatives are also used in catalysis for various organic reactions such as the oxidation of alcohols to aldehydes and so are easily available. The primary motivation for synthetic modification of

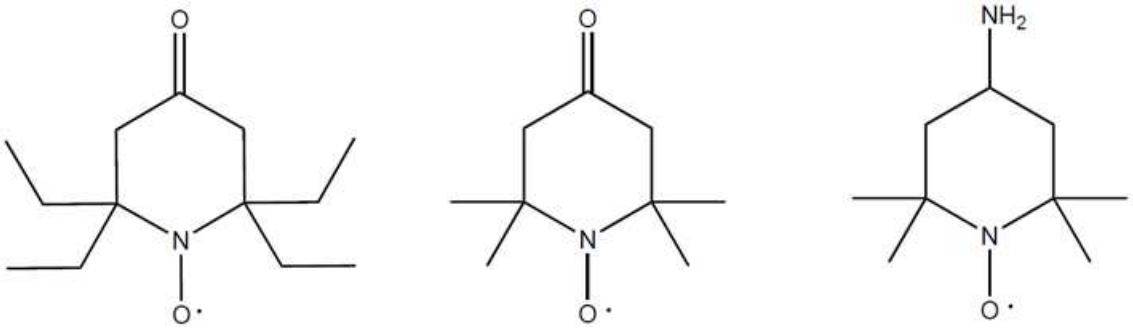

Figure 5.3: Several examples of modifed TEMPO redox mediators which have been used in the literature for DSSCs. Relevant characteristics of these redox mediators are shown in table 5.2.

TEMPO$^{0/1+}$ in the literature, as it relates to DSSCs, has been optimization of the redox potential of the couple. Several electron withdrawing groups such as cyanide, carbonyl, and amine groups have been added 'para' to the nitroxide radical.[23] As expected, the addition of the electron withdrawing group led to a positive shift in the potential of the couple. However all of the groups were shifted from the original couple by nearly the same amount (within ~20 mV of each other). This is unlike when using Co(bpy)$^{2+/3+}$ where Kirner and co-workers reported much larger differences between the use of amide, ester, and cyanide based substituents.[27] So one might expect similarly reduced changes in redox potential with the addition of electron donating groups to the 4-position leading to smaller losses in open circuit voltage relative to those observed with Co(bpy)$^{2+/3+}$. However, since the substitutions are added opposite of the nitroxide radical where the charge transfer process occurs on TEMPO$^{0/+1}$, the effect on the recombination at least as would be caused by steric hindrance would be minimal. There has been much less work dedicated to synthetic modification of positions on TEMPO$^{0/1+}$ closer to the nitroxide radical (positions 1, 2, and 6 as shown in figure 5.4) and its effect on DSSCs. In work unrelated to DSSCs, studies have focused on decreasing the steric bulk at those positions around the nitroxide radical in order to improve the rate of electron transfer to the reactant in several molecular catalytic systems.[28] But it has also been shown that reducing the steric bulk around the nitroxide radical leads to greatly decreased stability.[29]

Unlike other applications of the TEMPO$^{0/1+}$ redox couple, the redox mediator in a DSSC must paradoxically exhibit fast electron transfer with the sensitizer while having slow electron transfer during interactions with the semi-conductor film. Reducing the rate of charge transfer between the mediator and the semi-conductor could involve either modification of the photoanode surface or synthetic modification of the mediator itself. Modification of the semi-conductor surface has already been discussed in chapter 4 as well as above so the benefits of synthetic modification will be discussed further here.

When designing alternative mediators based off of the TEMPO$^{0/1+}$ template, larger alkyl substitutions at the 2 and 6 positions may increase the stability of the molecule as well as slow the electron transfer.[30] It was shown by Yamasaki and co-workers that the stability of the complexes are related to the redox potential caused by the identity of substituents placed at the 2 and 6 positions. That is to say the substituents which are slightly more electron-donating in nature should stabilize the nitroxide. On the other hand, it has been suggested that increased decomposition of 4-oxo-TEMPO was caused in part due to the electron withdrawing characteristics of the carbonyl group at the 4-position.[31] Zhang and co-workers suggested that the reduction in performance of their TEMPO$^{0/1+}$ based DSSCs was partially due to decomposition of the oxidized, presumably oxoammonium, form of the mediator.[12] At reasonably low temperatures and mild pH, TEMPO$^{0/1+}$ in its reduced form was found to be fairly stable.[32] In table 5.3, relevant properties concerning several modified TEMPO-based mediators found in the literature are summarized. As previously discussed, the redox potential of the couple has been a primary motivator for much of the research into synthetically modifying TEMPO$^{0/1+}$ for DSSCs. However, the function of devices will also be heavily dependent on both the diffusion coefficient and the stability

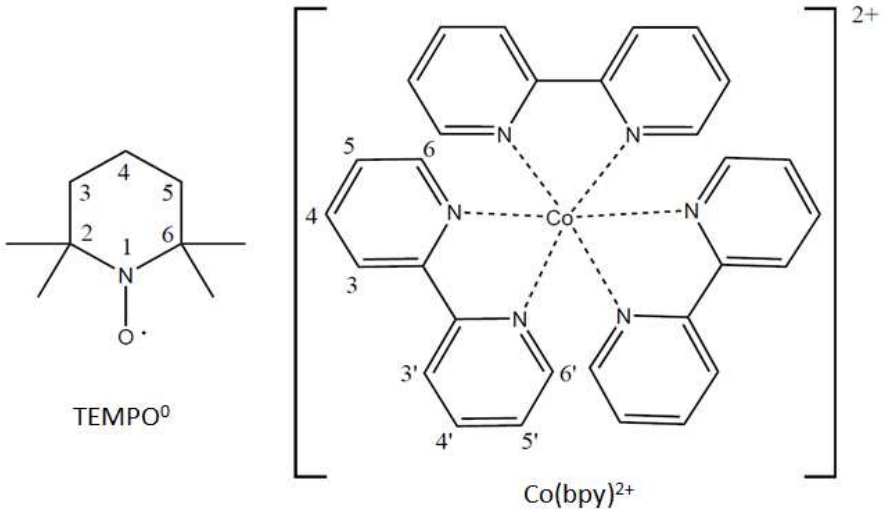

Figure 5.4: Examples of the reduced forms of unmodified Co(bpy) and TEMPO. Sites for possible substitution are labelled by numerical position. Substitutions performed on Co(bpy) are typically performed on both pyridine rings simultaneously (ex. 4 and 4').

Table 5.3: The relevant characteristics related to modified TEMPO derivatives is reported. It should be kept in mind that reported values in the literature, especially for diffusion coefficients, are dependent on the composition of the electrolyte used. AZA* is the molecule 2-azaadamantan-N-oxyl as reported by Kato and co-

Mediator	Redox potential (V vs. SCCE)	Diffusion coefficient (cm^2/s)	Notes on stability	[Ref]
TEMPO	0.65	1.2×10^{-5}	Seemingly unstable as oxidized form	[26], [11]
4-oxo-TEMPO	0.86	8.02×10^{-6}	Less stable than 4-oxo-TEEPO	[30], [23]
4-oxo-TEEPO	0.72	Not reported	More stable than 4-oxo-TEMPO	[30]
4-amino-TEMPO	0.83	1.98×10^{-5}	Exhibits 2nd irreversible peak in slow scan CVs	[23]
AZA*	0.59	1.2×10^{-6}	Both oxidized and reduced are stable	[26]

of the compounds in the electrolyte. Though table 5.3 shows that the diffusion coefficient for almost any of the modified TEMPO-based mediators (with the exception of 2-azaadamantan-N-oxyl or AZA) seem to be higher than those observed for $Co(bpy)^{2+/3+}$.[24]

When considering the possibility of using substitutions on $TEMPO^{0/1+}$ for DSSC applications as mentioned above, substituents which are more electron donating in nature are more likely to contribute to high stability of the nitroxide radical. Substituents closer to the nitroxide, such as at the 2 or 6 position, are more likely to affect the rate of electron transfer while substituents at the 4 position would be considered mainly for to optimize the redox potential and contribute to improved stability. Though it is important to keep in mind these two factors may act to oppose each other. As bulkier and bulkier substituents are placed at the 2 and 6 positions, an optimum size may be discovered, after which the ability of the mediator to regenerate the sensitizer is sacrificed. Another consideration is the solubility of the mediator in the chosen electrolyte solvent. Using water as an electrolyte solvent has a number of advantages which will be expounded upon in great detail below; but the solubility of $TEMPO^{0/1+}$ in water is likely to be reduced as larger alkyl substituents are utilized.

5.5 Use of water as an electrolyte solvent in DSSCs

The use of organic solvents has been the standard for liquid electrolyte DSSCs since O'Regan and Grätzel's seminal paper in 1991.[33] Some of the most common solvents used are acetonitrile, 3-methoxypropionitrile, γ-butyrolactone, and propylene carbonate.[2] Ideally the solvent will have low viscosity so as to not limit diffusion, no reactivity with the other components of the cell, and provide good solubility for the other components in the electrolyte. Relevant properties of the above mentioned solvents are summarized in table 5.4. Solvents like γ-butyrolactone and propylene carbonate are typically utilized for coordination complex type mediators due to being less coordinating with the metal center, but far more viscous then acetonitrile.[34] More coordinating solvents such as acetonitrile may force coordination with the metal center, replacing the initial ligand and decomposing the mediator over time. Another solvent, 3-methoxypropionitrile has been used in solvent mixtures with acetonitrile because it is less coordinating but more viscous.[35] This allows for improved stability of the coordination complex mediators as well as attempts to keep the mass transport limitations to a minimum. In the case of $TEMPO^{0/1+}$ in acetonitrile it has been reported, that after irradiation with ultraviolet light, the nitroxide radical has the ability to abstract a proton from the solvent which then allows the formation of a TEMPO-acetonitrile adduct as shown in figure 5.5.[36]

Table 5.4: Table comparing properties of commonly used organic solvents for DSSCs and water. Viscosity relates to mediator diffusion, toxicity is important to potential commercialization, the vapor pressure is in regards to possibility of the electrolyte evaporating over time, and the donor number is a reference to the ability of the solvent to destabilize a coordination complex based mediator.

Solvent	Viscosity (mPa s)	Toxicity (LD 50 as mg/kg)	Vapor Pressure (kPa)	Donor number (kcal/mol)
Acetonitrile	0.369	1320-6690	11.9	14.1
γ-butyrolactone	1.7	1540	0.20	18
3-methoxypropionitrile	1.1	4390	0.23	15.4
Propylene carbonate	2.5	>5000	0.05	15.1
Water	0.89	>90000	3.17	18

When considering the applications likely to utilize DSSCs, there are other characteristics to the solvent which must be considered. The toxicity and the vapor pressure at room temperature of the solvent are both important for the commercialization of devices but typically are less of a focus for fundamental studies. There are other approaches which will not be covered here and strive to meet the unique demands resulting from commercialization. The use of solid state electrolytes is one tactic for minimizing concerns of vapor pressure. Though like other alternative approaches, there are both benefits and detriments to this approach. Diffusion of charge carriers across the cell through a solid electrolyte is generally slower than in common liquid electrolyte cells and results in lower observable current. Many of the hole conductor type materials used, like polypyrrole, also reduce the transparency of the overall device and lead to competition for absorption within the pores of the photoanode.[2]

A simple way to alleviate concerns of toxicity, at least as it pertains to the solvent, is to remove the organic solvent and replace it with water, making an aqueous dye sensitized solar cell. Interestingly, early research into dye sensitized solar cells suggested that just a small amount of water, as a result of device manufacturing, was a nuisance and detriment to the stability of the device.[37] It was found the mesoporous network of titanium dioxide used as the anode made it impossible to keep the cell air-free. Even if cells were manufactured utilizing a glovebox or other inert environment leaching of water through the sealants was observed over long-term studies.[37] Instead of attempting to make DSSCs which are entirely water-free, the use of aqueous DSSCs could be embraced and optimized in regards to

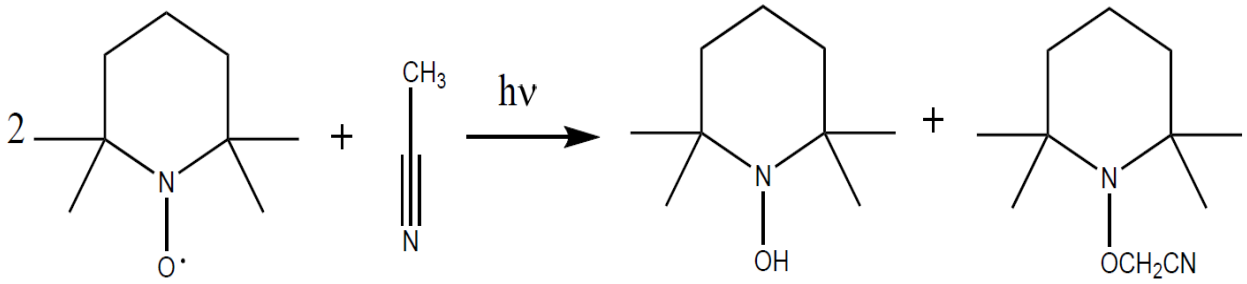

Figure 5.5: Reaction scheme detailing the formation of an adduct between acetonitrile as a solvent and TEMPO as a mediator (adapted from Johnston et al.)[36]

the most effective sensitizers, redox mediators, and electrolyte additives. Understanding the processes occurring at the various interfaces and what affect water has can lead to the rational design of more efficient aqueous DSSCs.

It has been suggested in multiple reports that the introduction of water increases the open circuit voltage of the cell while decreasing the short circuit current.[38-39] Due to water's ability to strongly adsorb onto the TiO_2 surface, it was proposed that the improvement in the open circuit voltage was caused by a reduction in the rate of recombination. In the case of iodide/tri-iodide, the water acted as a sort of blocking layer which limited the ability of the oxidized form of the mediator to interact with the surface.[38] It was proposed the decrease in the short circuit current was due to an interaction with the dye while using ruthenium sensitizers which led to inefficient charge injection into the conduction band of the anode. When the electrolyte that was contaminated with water was replaced with a water-free version it was found that the decrease in current was reversible. Interestingly, the increase in voltage remained while the current returned to that observed before water was added.[38]

It was shown in later work that some ligand switching between the thiocyanate ligand on the ruthenium based sensitizers and water may contribute to the observed decrease in efficiency of DSSCs over time after having been contaminated with water.[40] The different ligand environments were observed by changes in spectra from Fourier transform infrared (FTIR) spectroscopy and ultraviolet-visible (UV-VIS) spectroscopy. Water was added to the electrolyte of assembled DSSCs between 0 % and 5 % by volume, and diffuse reflectance FTIR spectra were taken after the cells were allowed to age for 8 days. It was found that as the percentage of water added increased the signal from the peak at 2100 cm^{-1}, which is representative of thiocyanate (SCN^-), decreased. There was also a small decrease in signal just from aging the DSSC for 8 days with electrolyte without added water, suggesting there may be some water even when care is taken not to include it. As an alternative to the ruthenium sensitizers, the use of organic dyes such as MK-2 removes the possibility of loss of thiocyanate.[41] The likelihood of

complete desorption of the dye would also be reduced as water would be partially blocked from the surface of the film by the bulkiness of the organic dye. It has been found that surfactants such as Triton X100 and chenodeoxycholic acid (CDCA) can be used in conjunction with these sensitizers in order to more completely block off the TiO_2 film.[42-43] The graphic found in figure 5.6 shows how the surfactant is expected to interact with the film surface in order to fill in the gaps between adsorbed dye molecules. In the case of the hydrophobic organic dyes, the use of a surfactant also allows for better whetting between the hydrophobic dye and the oxidized form of the mediator as it traverses the aqueous electrolyte. A study performed by Zhang and co-workers showed that cells prepared with N-719 as the sensitizer (a ruthenium based sensitizer but with long aliphatic chains on the bipyridines) and an aqueous electrolyte with any one of several added surfactants was more efficient.[44] The addition of surfactants led to almost no change in the open circuit voltage or the fill factor of the cell but instead led only to an increase in the short circuit current. The authors attribute this increase in current to improved interaction between the sensitizer and mediator leading to more efficient regeneration but there is likely some decreased recombination as well due to surfactant impeding the path of the oxidized mediator species to the TiO_2 surface. The authors also noted that stability of the cells with the

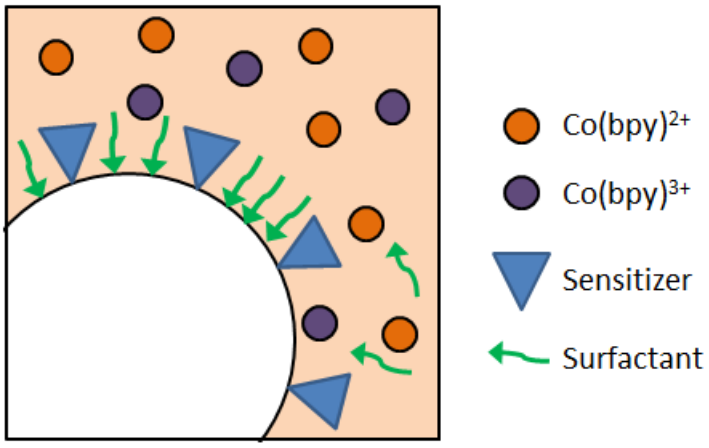

Figure 5.6: Diagram representing a simplified version of the hypothesized interaction of surfactant with the surface of titanium dioxide. The TiO_2 nanoparticle is shown in white while the liquid electrolyte is shown in a pale orange. The surfactant, represented by an arrow, adsorbs to the surface by its hydrophilic head (represented by the arrow's head), blending into the space next to the organic sensitizers.

added surfactant was improved; however a solid mechanism for the improved stability was not provided.

Another early study suggested one pathway for degradation of iodide-based DSSCs was through the reaction of the redox mediator with water that has leached into the cell in order to form iodate (IO_3^-) in solution.[45] Other classes of redox mediators are unlikely to follow the same pathways for decomposition and many have been shown in organic solvent based electrolyte systems to maintain several other advantages as well. Replacement of the iodide/tri-iodide mediator with $Co(bpy)^{2+/3+}$ has already been performed in the case of aqueous dye sensitized solar cells.[46] One study using the $Co(bpy)^{2+/3+}$ redox mediator led to an efficiency greater than 5 %, the highest achieved for a fully aqueous DSSC.[46] For this study, in order to minimize phase separation between the hydrophobic sensitizer and the electrolyte, the amount of poly-ethylene glycol added as a surfactant was varied between 0 – 12.5 % by weight. It was found that a 1 % addition maximized interaction of the phases without overly limiting the mediator. The use of water as a solvent may allow for improvement in stability for the $Co(bpy)^{2+/3+}$ mediator as well.[46] Unlike the commonly used acetonitrile as a solvent, water is unlikely to have the binding strength to compete with the bipyridine ligands and thus one of the most commonly theorized pathways for coordination complex mediator degradation could be significantly reduced. However, water's viscosity is significantly higher than the viscosity of acetonitrile which is likely to exacerbate problems related to slow diffusion of the redox mediator, especially in the mesoporous film.

Note that $TEMPO^{0/1+}$ has also been used as a redox mediator for aqueous DSSCs both on its own and in combination with other mediators.[47-48] Water will strongly adsorb onto the TiO_2 film surface, which allows for decreased recombination between the oxidized mediator and the film's surface relative to when organic solvents are used. This is particularly useful for $TEMPO^{0/1+}$ which is known to have high rates of recombination with the anode compared to other commonly used redox mediators.

Interestingly, the redox potential of the couple was found to be almost 200 mV more negative in water compared to in acetonitrile (0.71 V vs. NHE in water to 0.88 V vs. NHE in acetonitrile).[47] Thankfully, it has also been shown that the conduction band of the TiO_2 is brought more negative in the presence of water meaning that the open circuit voltage of the cell remains high (~940 mV).[37, 47] The viscosity of water will likely still slow diffusion of the oxidized mediator out of the mesoporous film. But due to $TEMPO^{0/1+}$ beginning with a diffusion coefficient in acetonitrile which is around 100 times faster than $Co(bpy)^{2+/3+}$, the limitations are not expected to be as severe.

Understanding the components of a DSSC which are sensitive to contamination by water and the pathways by which water historically has negatively affected cells allows for the opportunity to alter the paradigm and make the inclusion of water beneficial. Historically, research into the incorporation of water into DSSCs has focused mainly on the negative effects at small concentrations.[37] However, it has also been shown that there are a number of characteristics inherent to aqueous DSSCs which show promise such as the improvement of open circuit voltage while using water as an electrolyte solvent relative to acetonitrile in some systems.[37, 49-50] Many of the suggested complications causing decreased stability by means of water involve the decomposition of either the sensitizer or mediator. In both cases, there are already large numbers of alternative species, many of which have shown promise. Organic sensitizers in many cases have replaced the thiocyanate containing ruthenium sensitizers and $TEMPO^{0/1+}$ and $Co(bpy)^{2+/3+}$ have shown promise as alternative mediators with and without the presence of water. Overall efficiencies for aqueous DSSCs are still much lower than traditional cells utilizing the same components but with organic electrolytes. However, the renewed interest in aqueous DSSCs is provides hope that in the near future the efficiency of these devices will begin to catch up to their non-aqueous counterparts.

5.6 The future of DSSCs

Dye sensitized solar cells will continue to be a target of further fundamental research, as it has been shown to be a promising low cost alternative to other photovoltaic technologies. Device efficiency continues to increase, though at sluggish rate relative to other technologies like perovskite based photovoltaics.[51] Much of the literature has focused solely on improvement of initial device performance and many reports have left off discussion of long-term device stability entirely. Long term device stability will be one of the next fundamental obstacles researchers will attempt to understand more completely. Existing literature on device stability has shown that many of the pathways towards decreased efficiency over time are caused by the deposition of commonly used sensitizers and mediators in contact with inadvertent water contamination in the cell from either the manufacturing process or from leaching through the sealant.[52] Two conceivable solutions to that problem have been addressed here, both of which also offer other advantages past improving stability and masking contamination. First, further development of sensitizers and mediators which are not sensitive to the presence of water is essential. It has been suggested that the cost required to manufacture water-free DSSCs is excessive for any large scale effort at commercialization and it is still likely that over time water will leach into the cells.[37] Organic molecular sensitizers containing triphenylamine moieties are now commonly used in some of the most efficient DSSCs and are less affected by the presence of water then the ruthenium sensitizers.[7-8, 11] Both $Co(bpy)^{2+/3+}$ and $TEMPO^{0/1+}$ have been utilized as mediators in DSSCs with either added water or water as the electrolyte solvent and stability problems have not been mentioned.[46-47] Also, with both mediators there is ample opportunity for synthetic modification. Varying substituents at different positions on the redox mediators could be used to further improve both stability and interaction between itself and the sensitizer.

Second, adjusting the focus of fundamental research to the investigation of aqueous DSSCs, where the electrolyte solvent is water, could also help to minimize the negative effects of water

contamination. Cells that were designed using water as a solvent would obviously suffer no additional ill effects from further contamination of water. The use of water could also be beneficial for commercial applications where normally used organic solvents would exhibit higher toxicity and vapor pressure. It has been shown that water in DSSCs can have some positive effects on the function of the cell when stability of the components is not at risk.[37] Current research suggests that the presence of a surfactant of some kind allows for improved interaction between the organic sensitizer and the electrolyte for dye regeneration and can help block recombination with the titanium dioxide film.[42, 44] Interestingly, it was also found that efficiencies were improved in one study with a mixed solvent using both ethanol and water.[53] However, the overall efficiencies for the cells still only reached 2.2 % so there is a lot of work to be done.

Overall, the future of dye sensitized solar cells is reliant on their ability to fit into a niche for potential commercialization. Paradoxically, the idea that DSSCs are reasonably cheap to manufacture while providing middle-of-the-road efficiencies, especially in low light conditions, is incredibly valuable. The improvement of open circuit voltage and short circuit current as it relates to improving the efficiency has been the focus of research in the field thus far. But the next metaphorical frontier for research on dye sensitized solar cells relates to the improved stability of the various cell components, specifically how while interacting with one another. Some recent examples of high efficiency devices report some stability measurements suggesting between 10 and 25 % decrease in efficiency over 500 hours of testing.[10, 54] In these cases, both examples suggest improvement of sensitizer anchoring in order to improve stability. Lifetime of the devices may not maintain efficiency for 20+ years as is necessary for photovoltaic cells used in large scale power generation retain efficiency well enough for typical consumer good applications.

REFERENCES FOR CHAPTER 5

1. Min, J.; Won, J.; Kang, Y. S.; Nagase, S., Benzimidazole derivatives in the electrolyte of new-generation organic dye-sensitized solar cells with an iodine-free redox mediator. *Journal of Photochemistry and Photobiology A: Chemistry* **2011,** *219* (1), 148-153.

2. Hagfeldt, A.; Boschloo, G.; Sun, L.; Kloo, L.; Pettersson, H., Dye-Sensitized Solar Cells. *Chemical Reviews* **2010,** *110* (11), 6595-6663.

3. Tsao, H. N.; Comte, P.; Yi, C.; Grätzel, M., Avoiding Diffusion Limitations in Cobalt(III/II)-Tris(2,2'-Bipyridine)-Based Dye-Sensitized Solar Cells by Tuning the Mesoporous TiO2 Film Properties. *ChemPhysChem* **2012,** *13* (12), 2976-2981.

4. Feldt, S. M.; Gibson, E. A.; Gabrielsson, E.; Sun, L.; Boschloo, G.; Hagfeldt, A., Design of Organic Dyes and Cobalt Polypyridine Redox Mediators for High-Efficiency Dye-Sensitized Solar Cells. *Journal of the American Chemical Society* **2010,** *132* (46), 16714-16724.

5. Feldt, S. M.; Wang, G.; Boschloo, G.; Hagfeldt, A., Effects of Driving Forces for Recombination and Regeneration on the Photovoltaic Performance of Dye-Sensitized Solar Cells using Cobalt Polypyridine Redox Couples. *The Journal of Physical Chemistry C* **2011,** *115* (43), 21500-21507.

6. Mastroianni, S.; Lanuti, A.; Penna, S.; Reale, A.; Brown, T. M.; Di Carlo, A.; Decker, F., Physical and Electrochemical Analysis of an Indoor–Outdoor Ageing Test of Large-Area Dye Solar Cell Devices. *ChemPhysChem* **2012,** *13* (12), 2925-2936.

7. Hagberg, D. P.; Marinado, T.; Karlsson, K. M.; Nonomura, K.; Qin, P.; Boschloo, G.; Brinck, T.; Hagfeldt, A.; Sun, L., Tuning the HOMO and LUMO Energy Levels of Organic Chromophores for Dye Sensitized Solar Cells. *The Journal of Organic Chemistry* **2007,** *72* (25), 9550-9556.

8. Gabrielsson, E.; Ellis, H.; Feldt, S.; Tian, H.; Boschloo, G.; Hagfeldt, A.; Sun, L., Convergent/Divergent Synthesis of a Linker-Varied Series of Dyes for Dye-Sensitized Solar Cells Based on the D35 Donor. *Advanced Energy Materials* **2013,** *3* (12), 1647-1656.

9. Feldt, S. M.; Lohse, P. W.; Kessler, F.; Nazeeruddin, M. K.; Gratzel, M.; Boschloo, G.; Hagfeldt, A., Regeneration and recombination kinetics in cobalt polypyridine based dye-sensitized solar cells, explained using Marcus theory. *Physical Chemistry Chemical Physics* **2013,** *15* (19), 7087-7097.

10. Mathew, S.; Yella, A.; Gao, P.; Humphry-Baker, R.; CurchodBasile, F. E.; Ashari-Astani, N.; Tavernelli, I.; Rothlisberger, U.; NazeeruddinMd, K.; Grätzel, M., Dye-sensitized solar cells with 13% efficiency achieved through the molecular engineering of porphyrin sensitizers. *Nat Chem* **2014,** *6* (3), 242-247.

11. Kakiage, K.; Aoyama, Y.; Yano, T.; Oya, K.; Fujisawa, J.-i.; Hanaya, M., Highly-efficient dye-sensitized solar cells with collaborative sensitization by silyl-anchor and carboxy-anchor dyes. *Chemical Communications* **2015,** *51* (88), 15894-15897.

12. Zhang, Z.; Chen, P.; Murakami, T. N.; Zakeeruddin, S. M.; Grätzel, M., The 2,2,6,6-Tetramethyl-1-piperidinyloxy Radical: An Efficient, Iodine- Free Redox Mediator for Dye-Sensitized Solar Cells. *Advanced Functional Materials* **2008,** *18* (2), 341-346.

13. Yang, W.; Vlachopoulos, N.; Hao, Y.; Hagfeldt, A.; Boschloo, G., Efficient dye regeneration at low driving force achieved in triphenylamine dye LEG4 and TEMPO redox mediator based dye-sensitized solar cells. *Physical Chemistry Chemical Physics* **2015,** *17* (24), 15868-15875.

14. Chen, X.; Xu, D.; Qiu, L.; Li, S.; Zhang, W.; Yan, F., Imidazolium functionalized TEMPO/iodide hybrid redox couple for highly efficient dye-sensitized solar cells. *Journal of Materials Chemistry A* **2013,** *1* (31), 8759-8765.

15. Abdellaoui, S.; Knoche, K. L.; Lim, K.; Hickey, D. P.; Minteer, S. D., TEMPO as a Promising Electrocatalyst for the Electrochemical Oxidation of Hydrogen Peroxide in Bioelectronic Applications. *Journal of The Electrochemical Society* **2016,** *163* (4), H3001-H3005.

16. Nakade, S.; Makimoto, Y.; Kubo, W.; Kitamura, T.; Wada, Y.; Yanagida, S., Roles of Electrolytes on Charge Recombination in Dye-Sensitized TiO2 Solar Cells (2): The Case of Solar Cells Using Cobalt Complex Redox Couples. *The Journal of Physical Chemistry B* **2005,** *109* (8), 3488-3493.

17. Koh, T. M.; Nonomura, K.; Mathews, N.; Hagfeldt, A.; Grätzel, M.; Mhaisalkar, S. G.; Grimsdale, A. C., Influence of 4-tert-Butylpyridine in DSCs with CoII/III Redox Mediator. *The Journal of Physical Chemistry C* **2013,** *117* (30), 15515-15522.

18. Hamann, T. W.; Farha, O. K.; Hupp, J. T., Outer-Sphere Redox Couples as Shuttles in Dye-Sensitized Solar Cells. Performance Enhancement Based on Photoelectrode Modification via Atomic Layer Deposition. *The Journal of Physical Chemistry C* **2008,** *112* (49), 19756-19764.

19. Klahr, B. M.; Hamann, T. W., Performance Enhancement and Limitations of Cobalt Bipyridyl Redox Shuttles in Dye-Sensitized Solar Cells. *The Journal of Physical Chemistry C* **2009,** *113* (31), 14040-14045.

20. Nepal, J.; Mottaghian, S. S.; Iefanova, A. V.; Mallam, V.; Biesecker, M.; Baroughi, M. F. In *Modeling trap assisted recombination in Dye Sensitized Solar Cells*, 2013 IEEE 39th Photovoltaic Specialists Conference (PVSC), 16-21 June 2013; 2013; pp 2734-2737.

21. Sapp, S. A.; Elliott, C. M.; Contado, C.; Caramori, S.; Bignozzi, C. A., Substituted Polypyridine Complexes of Cobalt(II/III) as Efficient Electron-Transfer Mediators in Dye-Sensitized Solar Cells. *Journal of the American Chemical Society* **2002,** *124* (37), 11215-11222.

22. Nelson, J. J.; Amick, T. J.; Elliott, C. M., Mass Transport of Polypyridyl Cobalt Complexes in Dye-Sensitized Solar Cells with Mesoporous TiO2 Photoanodes. *The Journal of Physical Chemistry C* **2008,** *112* (46), 18255-18263.

23. Lee, J. Y.; Lee, C.; Lee, Y. M.; Cho, K. Y.; Choi, J. W.; Park, J.-K., Thiophene–nitroxide radical as a novel combination of sensitizer–redox mediator for dye-sensitized solar cells. *Journal of Solid State Electrochemistry* **2012,** *16* (2), 657-663.

24. Kavan, L.; Yum, J.-H.; Nazeeruddin, M. K.; Grätzel, M., Graphene Nanoplatelet Cathode for Co(III)/(II) Mediated Dye-Sensitized Solar Cells. *ACS Nano* **2011,** *5* (11), 9171-9178.

25. Ondersma, J. W.; Hamann, T. W., Impedance Investigation of Dye-Sensitized Solar Cells Employing Outer-Sphere Redox Shuttles. *The Journal of Physical Chemistry C* **2010,** *114* (1), 638-645.

26. Kato, F.; Kikuchi, A.; Okuyama, T.; Oyaizu, K.; Nishide, H., Nitroxide Radicals as Highly Reactive Redox Mediators in Dye-Sensitized Solar Cells. *Angewandte Chemie International Edition* **2012,** *51* (40), 10177-10180.

27. Kirner, J. T.; Elliott, C. M., Are High-Potential Cobalt Tris(bipyridyl) Complexes Sufficiently Stable to Be Efficient Mediators in Dye-Sensitized Solar Cells? Synthesis, Characterization, and Stability Tests. *The Journal of Physical Chemistry C* **2015,** *119* (31), 17502-17514.

28. Amar, M.; Bar, S.; Iron, M. A.; Toledo, H.; Tumanskii, B.; Shimon, L. J. W.; Botoshansky, M.; Fridman, N.; Szpilman, A. M., Design concept for α-hydrogen-substituted nitroxides. *Nature Communications* **2015,** *6*, 6070.

29. Bobbitt, J. M.; BrüCkner, C.; Merbouh, N., Oxoammonium- and Nitroxide-Catalyzed Oxidations of Alcohols. In *Organic Reactions*, John Wiley & Sons, Inc.: 2004.

30. Yamasaki, T.; Mito, F.; Ito, Y.; Pandian, S.; Kinoshita, Y.; Nakano, K.; Murugesan, R.; Sakai, K.; Utsumi, H.; Yamada, K.-i., Structure−Reactivity Relationship of Piperidine Nitroxide: Electrochemical, ESR and Computational Studies. *The Journal of Organic Chemistry* **2011,** *76* (2), 435-440.

31. Ma, Y.; Loyns, C.; Price, P.; Chechik, V., Thermal decay of TEMPO in acidic media via an N-oxoammonium salt intermediate. *Organic & Biomolecular Chemistry* **2011,** *9* (15), 5573-5578.

32. Ciriano, M. V.; Korth, H.-G.; van Scheppingen, W. B.; Mulder, P., Thermal Stability of 2,2,6,6-Tetramethylpiperidine-1-oxyl (TEMPO) and Related N-Alkoxyamines. *Journal of the American Chemical Society* **1999,** *121* (27), 6375-6381.

33. O'Regan, B.; Gratzel, M., A low-cost, high-efficiency solar cell based on dye-sensitized colloidal TiO2 films. *Nature* **1991,** *353* (6346), 737-740.

34. Mahanta, S.; Matsuzaki, H.; Murakami, T. N.; Katoh, R.; Matsumoto, H.; Furube, A., Modulation of Electron Injection Dynamics of Ru-Based Dye/TiO2 System in the Presence of Three Different Organic Solvents: Role of Solvent Dipole Moment and Donor Number. *ChemPhysChem* **2015,** *16* (8), 1657-1662.

35. Venkatesan, S.; Su, S.-C.; Kao, S.-C.; Teng, H.; Lee, Y.-L., Stability improvement of gel-state dye-sensitized solar cells by utilization the co-solvent effect of propionitrile/acetonitrile and 3-methoxypropionitrile/acetonitrile with poly(acrylonitrile-co-vinyl acetate). *Journal of Power Sources* **2015,** *274*, 506-511.

36. Johnston, L. J.; Tencer, M.; Scaiano, J., Evidence for hydrogen transfer in the photochemistry of 2, 2, 6, 6-tetramethylpiperidine N-oxyl. *The Journal of Organic Chemistry* **1986,** *51* (14), 2806-2808.

37. Bella, F.; Gerbaldi, C.; Barolo, C.; Gratzel, M., Aqueous dye-sensitized solar cells. *Chemical Society Reviews* **2015,** *44* (11), 3431-3473.

38. Liu, Y.; Hagfeldt, A.; Xiao, X.-R.; Lindquist, S.-E., Investigation of influence of redox species on the interfacial energetics of a dye-sensitized nanoporous TiO2 solar cell. *Solar Energy Materials and Solar Cells* **1998,** *55* (3), 267-281.

39. Nazeeruddin, M. K.; Kay, A.; Rodicio, I.; Humphry-Baker, R.; Mueller, E.; Liska, P.; Vlachopoulos, N.; Graetzel, M., Conversion of light to electricity by cis-X2bis(2,2'-bipyridyl-4,4'-dicarboxylate)ruthenium(II) charge-transfer sensitizers (X = Cl-, Br-, I-, CN-, and SCN-) on nanocrystalline titanium dioxide electrodes. *Journal of the American Chemical Society* **1993,** *115* (14), 6382-6390.

40. Lu, H.-L.; Shen, T. F. R.; Huang, S.-T.; Tung, Y.-L.; Yang, T. C. K., The degradation of dye sensitized solar cell in the presence of water isotopes. *Solar Energy Materials and Solar Cells* **2011,** *95* (7), 1624-1629.

41. Wang, Z.-S.; Koumura, N.; Cui, Y.; Takahashi, M.; Sekiguchi, H.; Mori, A.; Kubo, T.; Furube, A.; Hara, K., Hexylthiophene-Functionalized Carbazole Dyes for Efficient Molecular Photovoltaics: Tuning of Solar-Cell Performance by Structural Modification. *Chemistry of Materials* **2008,** *20* (12), 3993-4003.

42. Jung, Y.-S.; Yoo, B.; Lim, M. K.; Lee, S. Y.; Kim, K.-J., Effect of Triton X-100 in water-added electrolytes on the performance of dye-sensitized solar cells. *Electrochim. Acta* **2009,** *54* (26), 6286-6291.

43. Law, C.; Moudam, O.; Villarroya-Lidon, S.; O'Regan, B., Managing wetting behavior and collection efficiency in photoelectrochemical devices based on water electrolytes; improvement in efficiency of water/iodide dye sensitised cells to 4%. *Journal of Materials Chemistry* **2012,** *22* (44), 23387-23394.

44. Zhang, H.; Qiu, L.; Xu, D.; Zhang, W.; Yan, F., Performance enhancement for water based dye-sensitized solar cells via addition of ionic surfactants. *Journal of Materials Chemistry A* **2014,** *2* (7), 2221-2226.

45. Macht, B.; Turrión, M.; Barkschat, A.; Salvador, P.; Ellmer, K.; Tributsch, H., Patterns of efficiency and degradation in dye sensitization solar cells measured with imaging techniques. *Solar Energy Materials and Solar Cells* **2002,** *73* (2), 163-173.

46. Xiang, W.; Huang, F.; Cheng, Y.-B.; Bach, U.; Spiccia, L., Aqueous dye-sensitized solar cell electrolytes based on the cobalt(ii)/(iii) tris(bipyridine) redox couple. *Energy & Environmental Science* **2013,** *6* (1), 121-127.

47. Yang, W.; Soderberg, M.; Eriksson, A. I. K.; Boschloo, G., Efficient aqueous dye-sensitized solar cell electrolytes based on a TEMPO/TEMPO+ redox couple. *RSC Advances* **2015,** *5* (34), 26706-26709.

48. Lin, R. Y.-Y.; Chuang, T.-M.; Wu, F.-L.; Chen, P.-Y.; Chu, T.-C.; Ni, J.-S.; Fan, M.-S.; Lo, Y.-H.; Ho, K.-C.; Lin, J. T., Anthracene/Phenothiazine π-Conjugated Sensitizers for Dye-Sensitized Solar Cells using Redox Mediator in Organic and Water-based Solvents. *ChemSusChem* **2015,** *8* (1), 105-113.

49. Kong, E.-H.; Lim, J.; Chang, Y.-J.; Yoon, Y.-H.; Park, T.; Jang, H. M., Aerosol OT/Water System Coupled with Triiodide/Iodide (I3−/I−) Redox Electrolytes for Highly Efficient Dye-Sensitized Solar Cells. *Advanced Energy Materials* **2013,** *3* (10), 1344-1350.

50. Law, C.; Pathirana, S. C.; Li, X.; Anderson, A. Y.; Barnes, P. R. F.; Listorti, A.; Ghaddar, T. H.; O'Regan, B. C., Water-Based Electrolytes for Dye-Sensitized Solar Cells. *Advanced Materials* **2010,** *22* (40), 4505-4509.

51. Nie, W.; Tsai, H.; Asadpour, R.; Blancon, J.-C.; Neukirch, A. J.; Gupta, G.; Crochet, J. J.; Chhowalla, M.; Tretiak, S.; Alam, M. A.; Wang, H.-L.; Mohite, A. D., High-efficiency solution-processed perovskite solar cells with millimeter-scale grains. *Science* **2015,** *347* (6221), 522.

52. Sauvage, F.; #xe9; #xe9; ric, A Review on Current Status of Stability and Knowledge on Liquid Electrolyte-Based Dye-Sensitized Solar Cells. *Advances in Chemistry* **2014,** *2014*, 23.

53. Saito, H.; Uegusa, S.; Murakami, T.; Kawashima, N.; Miyasaka, T., Fabrication and Efficiency Enhancement of Water-based Dye-Sensitized Solar Cells by Interfacial Activation of TiO~ 2 Mesopores (E). *ELECTROCHEMISTRY-TOKYO-* **2004,** *72* (5), 310-316.

54. Yella, A.; Lee, H.-W.; Tsao, H. N.; Yi, C.; Chandiran, A. K.; Nazeeruddin, M. K.; Diau, E. W.-G.; Yeh, C.-Y.; Zakeeruddin, S. M.; Grätzel, M., Porphyrin-Sensitized Solar Cells with Cobalt (II/III)–Based Redox Electrolyte Exceed 12 Percent Efficiency. *Science* **2011,** *334* (6056), 629.

SUPPLEMENTARY INFORMATION

Table 2.S1: Characterization for bipyridine based ligands. The ligands, 4-dmb and 5-dmb, were synthesized previously by another group member by previously published methods and re-characterized before use so no yield is provided.[13] Mass spectra were taken of both the 4-eebpy and 5-eebpy ligands after synthesis to confirm their identity.

Ligand	% Yield	^{1}H-NMR [ppm (mult, #, group)]	Mass Spectra-$[M+H]^+$ (m/z) [exp. (calc.)]	Melting Pt (°C)
$C_{12}H_{12}N_2$ 4-dmb	N/A	2.42 (s, 6H, CH_3), 7.13 (d, 2H, CH), 8.19 (s, 2H, CH), 8.54 (d, 2H, CH)	N/A	163
$C_{12}H_8O_4N_2$ 4-dcb	90	7.65 (d, 2H, CH), 8.20 (s, 2H, CH), 8.60 (d, 2H, CH)	N/A	>290
$C_{16}H_{16}O_4N_2$ 4-eebpy	76	1.44 (t, 6H, CH_3), 4.42 (q, 4H, CH_2), 7.92 (d, 2H, CH), 8.85 (d, 2H, CH), 8.95 (s, 2H, CH)	301.1188 (301.1182)	160
$C_{12}H_{12}N_2$ 5-dmb	N/A	2.12 (s, 6H, CH_3), 7.57 (d, 2H, CH), 8.20 (d, 2H, CH), 8.43 (s, 2H, CH)	N/A	110
$C_{12}H_8O_4N_2$ 5-dcb	85	7.98 (d, 2H, CH), 8.23 (d, 2H, CH), 8.92 (s, 2H, CH)	N/A	>290
$C_{16}H_{16}O_4N_2$ 5-eebpy	78	1.44 (t, 6H, CH3), 4.42 (q, 4H, CH2), 8.45 (d, 2H, CH), 8.63 (d, 2H, CH), 9.30 (s, 2H, CH)	301.1188 (301.1182)	143

Table 2.S2: Characterization for synthesized Co(II) coordination complexes. ^{1}H-NMR spectra being performed on cobalt coordination complexes has previously been reported.[1, 29] NMR spectra were performed in dichloromethane to attempt to minimize decomposition of the complexes. However, there was a small amount of uncoordinated ligand observed in both Co(II)(4-eebpy) and Co(II)(5-eebpy). It is unclear at this point if that is a result of excess ligand or deposition of the complex. Elemental analysis was performed by Galbraith Laboratories to determine percentages of Carbon, Hydrogen, and Nitrogen. Calculations were matched within 1 percent.

Complex	^{1}H-NMR [ppm (mult, #, group)]	Elemental analysis (%) [exp. (calc.)]
$Co(C_{10}H_8N_2)_3(ClO_4)_2$ Co(II)(bpy)	14.60 (s, 6H, CH), 46.34 (s, 6H, CH), 84.73 (s, 6H, CH), 88.23 (s, 6H, CH)	C [48.93(49.60)], H [3.66(3.33)], N[11.50(11.57)], Co [(8.11)], O [(17.62)], Cl[(9.76)]
$Co(C_{12}H_{12}N_2)_3(ClO_4)_2$ Co(II)(4-dmb)	0.36 (s, 18H, CH_3), 44.59 (s, 6H, CH), 81.75 (s, 6H, CH), 90.08 (s, 6H, CH)	C [52.76(53.39)], H [4.56(4.48)], N [10.32(10.38)], Co [(7.28)], O [(15.81)], Cl[(8.75)]
$Co(C_{16}H_{16}O_4N_2)_3(ClO_4)_2$ Co(II)(4-eebpy)	2.26 (t, 18H, CH_3), 5.57 (d, 12H, CH_2), 45.72 (s, 6H, CH), 83.27 (s, 6H, CH), 89.32 (s, 6H, CH)	C [48.84(49.79)], H [4.57(4.18)], N [7.31(7.26)], Co [(5.09)], O [(27.64)], Cl[(6.12)]
$Co(C_{12}H_{12}N_2)_3(ClO_4)_2$ Co(II)(5-dmb)	1.57 (s, 18H, CH_3), 13.83 (s, 6H, CH), 86.21 (s, 6H, CH), 89.16 (s, 6H, CH)	C [52.26(53.39)], H [5.03(4.48)], N [10.05(10.38)], Co [(7.28)], O [(15.81)], Cl[(8.75)]
$Co(C_{16}H_{16}O_4N_2)_3(ClO_4)_2$ Co(II)(5-eebpy)	-1.04 (t, 18H, CH_3), 1.35 (d, 12H, CH_2), 14.60 (s, 6H, CH), 82.95 (s, 6H, CH), 98.94 (s, 6H, CH)	C [49.28(49.79)], H [4.50(4.18)], N [7.28(7.26)], Co [(5.09)], O [(27.64)], Cl[(6.12)]

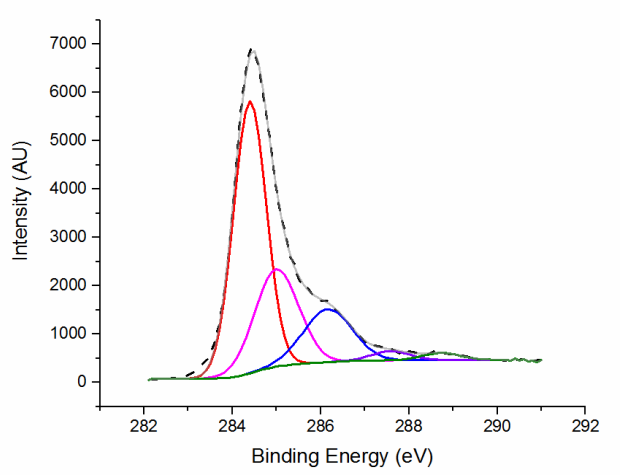

Figure 2.S1: High resolution XPS spectra of the carbon region for glassy carbon electrodes used for impedance and chronoamperometry studies. The experimental data is plotted as the dotted line while the gray line is the total fit. The individual components of the fits are broken up so that red is the sp^2 graphitic carbon, magenta is sp^3 adventitious carbon, blue is carbon bonded to 1 oxygen, purple is carbon bonded to 2 oxygens, and green is carbonate.

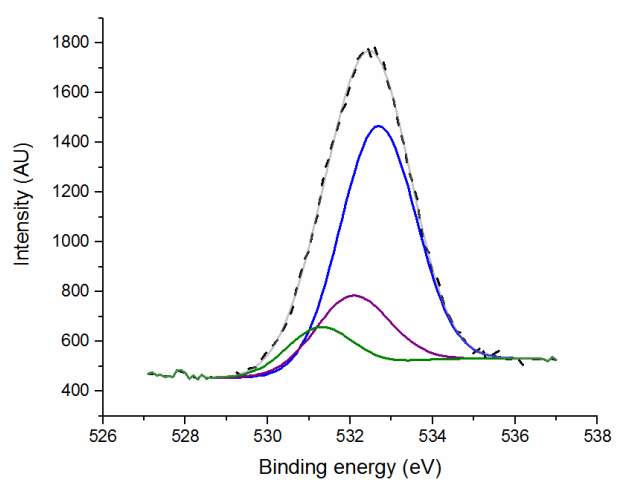

Figure 2.S2: High resolution XPS spectra of the oxygen peaks for glassy carbon electrodes used for impedance and chronoamperometry studies. The experimental data is plotted as the dotted line while the gray line is the total fit. The blue trace represents oxygen species in an alcohol type binding environment, purple is those species in a carboxylate environment and the green trace is for the species in a binding environment similar to carbonate.

Table 2.S3: Atomic percents and peak locations from fitted high resolution XPS specta for carbon on glassy carbon electrodes. Fits were performed by CasaXPS. It is expected that some amount of the sp^3 carbon is a result of sample handling between vacuums.

Carbon species	Binding energy (eV)	Atomic %
C1s sp^2	284.4	48.31
C1s sp^3	285	22.98
C1s C-O	286.16	13.82
C1s CO_2	287.59	1.84
C1s CO_3	288.72	1.43
Total % carbon	N/A	88.38

Table 2.S4: Atomic percents and peak locations from fitted high resolution XPS specta for oxygen on glassy carbon electrodes. Fits were performed by CasaXPS.

Oxygen species	Binding energy (eV)	Atomic %
O1s C-O	532.67	7.85
O1s CO_2	532.03	2.39
O1s CO_3	531.27	1.38
Total % oxygen	N/A	11.62

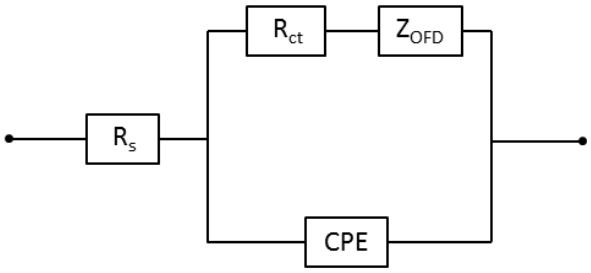

Figure 2.S3: Equivalent circuit used to fit impedance spectra using software included with CH instruments 750D bi-potentiostat. Simple resistors were used for series resistance (R_s) and charge transfer resistance (R_{ct}). A constant phase element (CPE) was used to simulate non-ideal capacitance on the electrode surfaces. And an open finite diffusion element (Z_{OFD}) was used to model diffusion between the symmetrical electrodes.

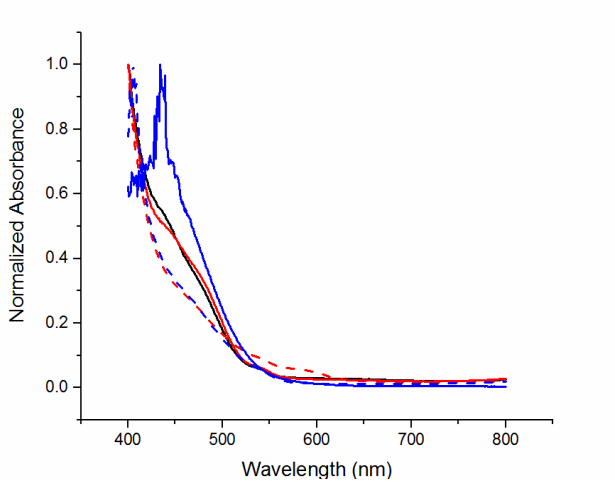

Figure 2.S4: UV-Vis spectra of Co^{2+} complexes. Concentrations were 10 mM in DCM of Co(bpy) (—), Co(4-dmb) (—), Co(5-dmb) (----), Co(4-eebpy) (—), and Co(5-eebpy) (----).

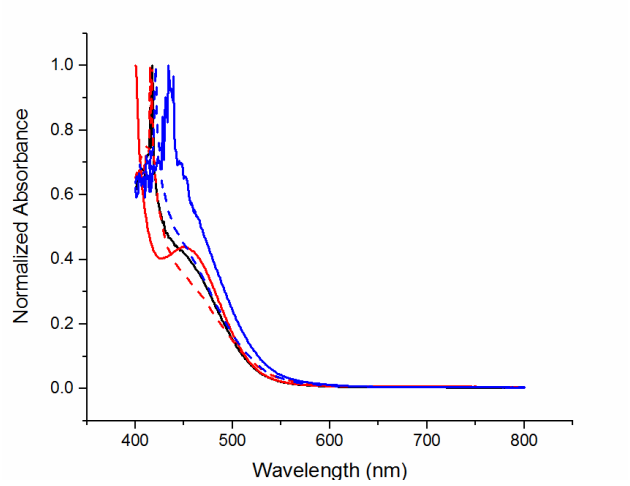

Figure 2.S5: UV-Vis spectra of Co^{3+} complexes. Concentrations were 10 mM in DCM of Co(bpy) (—), Co(4-dmb) (—), Co(5-dmb) (----), Co(4-eebpy) (—), and Co(5-eebpy) (----).

Table 2.S5: UV-Vis spectroscopy performed in dichloromethane at a concentration of 10 mM. Absorption coefficients were taken at 450 nm to compare specifically with max absorption of the ruthenium based N3 dye. Transmittance was calculated based on the reported absorption coefficients at 450 nm, common mediator concentrations for the Co(II) species of 0.150 M, and a cell pathlength of 60 µm.

Complex	Absorption coefficient ($mol^{-1}cm^{-1}L$)	λ_{max} (nm)		Transmittance w/ 60 µm spacer @450 nm (%)
		Co(II)	Co(III)	
$Co(C_{10}H_8N_2)_3(ClO_4)_2$ Co(II/III)(bpy)	105	<400	417	80.45
$Co(C_{12}H_{12}N_2)_3(ClO_4)_2$ Co(II/III)(4-dmb)	166	<400	<400	70.89
$Co(C_{16}H_{16}O_4N_2)_3(ClO_4)_2$ Co(II/III)(4-eebpy)	225	434	434	62.73
$Co(C_{12}H_{12}N_2)_3(ClO_4)_2$ Co(II/III)(5-dmb)	125	<400	415	77.18
$Co(C_{16}H_{16}O_4N_2)_3(ClO_4)_2$ Co(II/III)(5-eebpy)	157	405	421	72.23

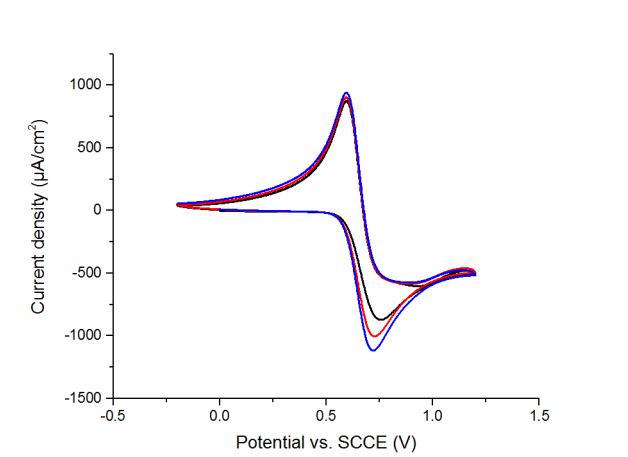

Figure 2.S6: Cyclic voltammogram of 0.010 M Co(4-eebpy) complex in acetonitrile with 0.200 M $TBAPF_6$ as a supporting electrolyte run with 3 consecutive cycles at a scan rate of 100 mV/s on gold. It is seen that the oxidative current decreases going from the 1st cycle (—) to the 2nd cycle (—) to the 3rd cycle (—).

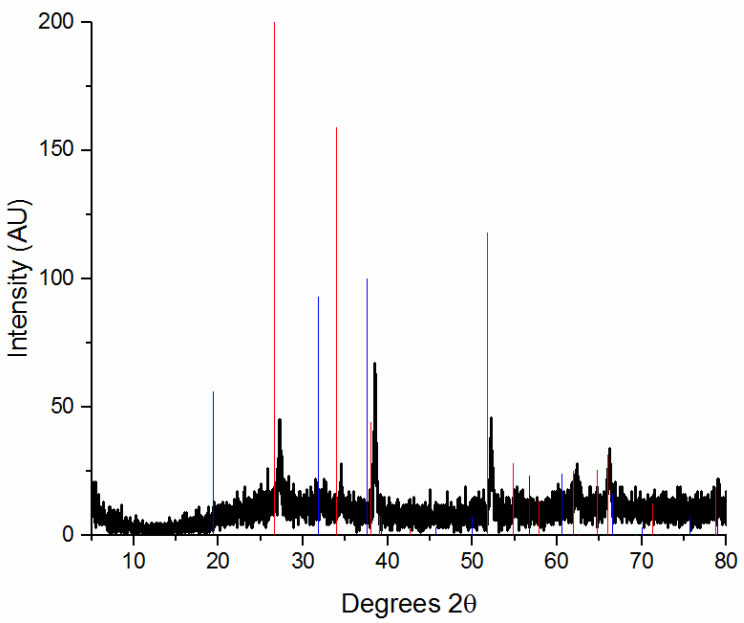

Figure 4.S1: X-ray diffraction pattern of a sample of FTO coated glass with 100 cycles of Al_2O_3 deposited on top. The peaks match closely with the pattern for tin oxide (PDF: 01-077-0447) with systematic deviation due to the doping with fluorine. There are no peaks for aluminum oxide (PDF: 00-047-1292) present due to the amorphous nature of films deposited by ALD. The red lines represent peaks corresponding to SnO_2 and blue lines represent peaks corresponding to Al_2O_3.

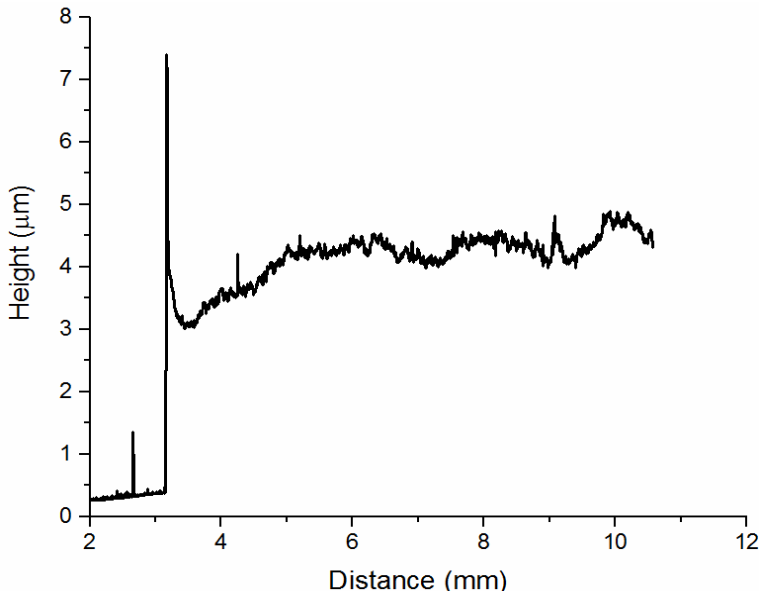

Figure 4.S2: Example profilometry image showing typical roughness and thickness of DSSC films. The film itself begins at a little after 3 microns, prior to that is the FTO substrate. It is suspected that the excessive jump at the start of the film is considered to be an artifact of the sample preparation and is not expected to affect any of the other tests.

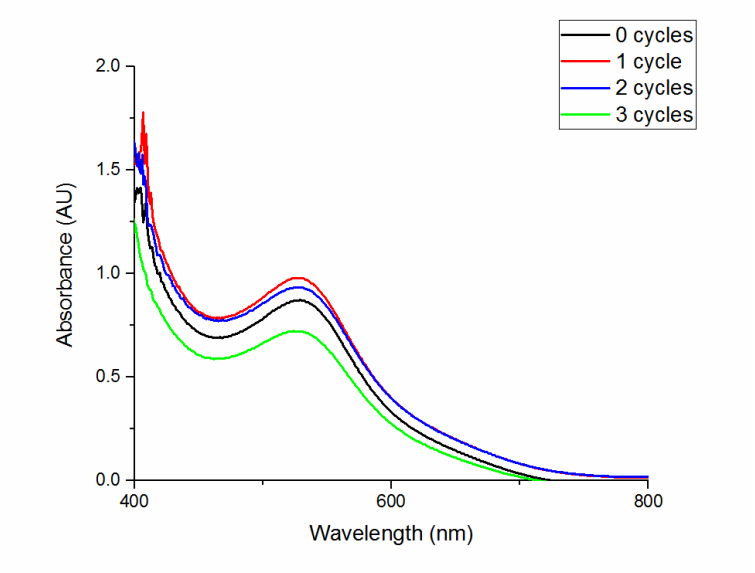

Figure 4.S3: UV-Vis spectra of DSSC films after dyeing with N3 but before any electrochemical testing is performed.